

Toric Fano varieties and Chern-Simons quivers

Cyril Closset[♣], Stefano Cremonesi[♣]

[♠] *Department of Particle Physics and Astrophysics
Weizmann Institute of Science, Rehovot 76100, Israel.*

[♣] *Theoretical Physics Group, Imperial College London,
Prince Consort Road, London, SW7 2AZ, UK*

ABSTRACT: In favourable cases the low energy dynamics of a stack of M2-branes at a toric Calabi-Yau fourfold singularity can be described by an $\mathcal{N} = 2$ supersymmetric Chern-Simons quiver theory, but there still does not exist an “inverse algorithm” going from the toric data of the CY_4 to the CS quiver. We make progress in that direction by deriving CS quiver theories for M2-branes probing cones over a large class of geometries $Y^{p,q}(B_4)$, which are S^3/\mathbb{Z}_p bundles over toric Fano varieties B_4 . We rely on the type IIA understanding of CS quivers, giving a firm string theory footing to our CS theories. In particular we give a derivation of some previously conjectured CS quivers in the case $B_4 = \mathbb{CP}^1 \times \mathbb{CP}^1$, as field theories dual to M-theory backgrounds with nontrivial torsion G_4 fluxes.

KEYWORDS: Chern-Simons Theories, AdS-CFT Correspondence, M-Theory.

Contents

1. Introduction	2
2. Toric quivers, CY_3 cones and fractional brane charges	4
2.1 Toric quiver and crepant resolutions of Y	5
2.2 GIT quotient and moduli space	9
2.3 Quiver representations, θ -stability and Kähler chambers	10
2.4 Tilting collection of line bundles from toric quiver	13
2.5 2d toric Fano varieties and brane charge dictionaries	15
2.6 Kähler moduli space and quiver locus	19
2.7 Dictionaries, monodromies and Freed-Witten anomaly	20
3. Reduction of M-theory on $\mathbb{R}^{1,2} \times CY_4$ to type IIA	22
3.1 Generalities	22
3.2 Cones over toric $Y^{p,q}(B_4)$ Sasaki-Einstein 7-folds	24
3.3 GLSM for the CY_3 fibres in type IIA	26
3.4 RR 2-form flux and D6-branes	28
3.5 Torsion G_4 and generic type IIA background	28
4. From type IIA to CS quiver gauge theories and back	29
4.1 Translating from IIA background to CS quiver	29
4.2 Semi-classical moduli space of CS quiver theories and type IIA geometry	31
4.3 Monopole operators and GIT quotient	32
5. M2-brane theories for backgrounds without torsion G_4 flux	34
5.1 $dP_0 \equiv \mathbb{C}P^2$	34
5.2 $\mathbb{F}_0 \equiv \mathbb{C}P^1 \times \mathbb{C}P^1$	36
5.2.1 Phase a of \mathbb{F}_0	37
5.2.2 Phase b of \mathbb{F}_0	39
5.3 dP_1	41
5.4 dP_2	43
5.4.1 Phase a of dP_2	43
5.4.2 Phase b of dP_2	44
5.5 dP_3	45
5.5.1 Phase d of dP_3	46
5.5.2 Phase c of dP_3	47
5.5.3 Phase b of dP_3	49
5.6 $WC\mathbb{C}P^2_{[1,1,2]}$	51
5.7 PdP_2	52

5.8	PdP_{3b}	53
5.8.1	Phase c of PdP_{3b}	53
5.9	PdP_{3c}	55
5.9.1	Phase b of PdP_{3c}	55
5.10	$WC\mathbb{P}^2_{[1,2,3]}$	56
5.11	PdP_4	57
5.11.1	Phase c of PdP_4	58
5.12	PdP_{4b}	59
5.13	PdP_5	60
5.14	PdP_{5b}	61
5.15	$WC\mathbb{P}^2_{[2,2,4]}$	62
5.16	$WC\mathbb{P}^2_{[3,3,3]}$	63
6.	Partial resolutions and Higgsing	64
6.1	Higgsings	66
7.	Adding torsion G_4 flux: The $Y^{p,q}(\mathbb{F}_0)$ case	70
7.1	Theories covering the full torsion group	72
7.1.1	Crossing the Seiberg duality walls: mutated dictionaries	74
7.2	Periodicities and Seiberg duality	76
7.3	Remark on $Y^{p,q_1,q_2}(\mathbb{F}_0)$ and quiver with equal ranks	77
8.	Conclusion and outlook	78
A.	$Y^{p,q}(B_4)$ geometry and type IIA background	79
A.1	Topology of M_6	80
A.2	Topology of $Y^{p,q}(B_4)$	83
A.3	Type IIA background and the IIA dual of torsion flux	84
A.4	D6-branes and Freed-Witten anomaly	85
A.5	Large gauge transformations and shift of the D2 Page charge	86
A.6	Fluxes and D-branes in $C(M_6)$	87

1. Introduction

The AdS_4/CFT_3 correspondence has been the object of intense study in recent years, especially in its maximally supersymmetric version ($\mathcal{N} = 6$ or 8 in three dimension) embodied in the ABJM proposal [1], where the three dimensional conformal field theory is a Chern-Simons (CS) quiver gauge theory. Many more instances of AdS_4/CFT_3 dualities can be proposed if the number of supersymmetries is lowered. A particularly interesting field of study is the 3d $\mathcal{N} = 2$ supersymmetric case, the minimal number

that allows holomorphy. The corresponding AdS/CFT duality arises from a decoupling limit [2] on N M2-branes located at a Calabi-Yau (CY) fourfold conical singularity [3].

The first thing to understand in order to study those dualities explicitly is the low energy theory on the worldvolume of N M2-branes at a CY_4 singularity. This is an interesting problem even independently from the AdS/CFT motivation. Soon after the ABJM proposal, numerous examples of $\mathcal{N} = 2$ quiver gauge theories were proposed to describe theories which might flow to the correct M2-brane theories in the infrared (IR) [4, 5, 6, 7, 8, 9, 10]. Unlike the higher supersymmetric cases where the field theories could be deduced from brane constructions, however, many of those proposals were lacking a convincing motivation, apart from their reproducing a CY_4 geometry as their classical moduli space. This state of affairs started to change with the proposal of [11]: the idea is to use the M-theory/type IIA duality mapping M2-branes on a CY fourfold to D2-branes on a Calabi-Yau threefold together with Ramond-Ramond (RR) background fluxes accounting for the non-trivial M-theory fibration. This proposal was sharpened and developed in [12, 13, 14]: from the string theory side it was understood that generically D6-branes are present in the type IIA reduction, while from the field theory side progress was made to include in the analysis of the moduli space quantum corrections due to D2-D6 open string modes.

We should note that many of the theories derived¹ that way have passed non-trivial independent checks by matching their large N partition function on S^3 [16, 17] or/and their superconformal index [18] to the expectation from supergravity [19, 20, 21, 22, 23, 15].

The type IIA framework allows to connect $\mathcal{N} = 2$ Chern-Simons quiver theories to the well studied setup of D-branes on CY_3 cones. In this work we develop this perspective in the case of *toric* Calabi-Yau threefolds, which can be studied in terms of “toric quivers”, also known as brane tilings [24, 25].

We study M2-branes on toric CY_4 cones over seven dimensional manifolds that we dub $Y^{p,q}(B_4)$. Those $Y^{p,q}$ spaces are S^3/\mathbb{Z}_p bundles over complex two dimensional Fano varieties B_4 , which generalise the $Y^{p,q}$ geometries studied in [26, 27].² The relevant type IIA dual setup corresponds to D2-branes on the CY_3

$$\tilde{Y} \cong \mathcal{O}_{B_4}(K), \tag{1.1}$$

the canonical bundle over the Fano variety B_4 . Importantly, there are also D6-branes wrapped on the compact 4-cycle B_4 in the IIA reduction. The presence of M5-branes on torsion 3-cycles in $Y^{p,q}$ (corresponding to turning on torsion G_4 flux through $Y^{p,q}$ in the $AdS_4 \times Y^{p,q}$ background) can also lead to D4-branes on 2-cycles in type IIA.

¹More precisely, some theories had been proposed before by an inspired guess, such as the equal rank C^3/\mathbb{Z}_3 quiver for $Y^{p,q}(CP^2)$ first proposed in [5] and derived from string theory in [14]. That particular theory (including some subtle corrections introduced in [14]) was nicely checked recently at the level of the S^3 partition function and of the superconformal index [15].

²We are not looking for explicit metrics on those SE_7 spaces, we only need that they exist, as guaranteed in the toric case by [28].

Such a situation has been studied in detail in the simplest case $B_4 = \mathbb{CP}^2$ [14]. In the present work we generalise the results of [14] to any toric Fano variety B_4 . There are only 16 such varieties, including the five smooth del Pezzo surfaces. Much of the corresponding CY_3 cones (1.1) were studied from the brane tiling point of view in the literature, and the corresponding brane tilings are fully classified [29].

This paper is organised as follows. In section 2, we introduce a formalism which allows an efficient study of fractional branes on any of the spaces (1.1). We review the crucial notion of θ -stability [30] and some of its applications to CY_3 quivers.

In section 3 we explain which KK reduction we perform to obtain a useful IIA background from the conical geometry $C(Y^{p,q})$ in M-theory. Several interesting details on the $Y^{p,q}$ geometry and the type IIA reduction are relegated to Appendix A.

In section 4 we explain how to translate the type IIA data into a Chern-Simons quiver gauge theory and we show that the field theory reproduces the type IIA geometry as its semiclassical moduli space by construction.³ We also briefly comment on the inclusion of monopole operators, and how they naturally fit into the language of GIT quotient for quiver moduli spaces.

In section 5 we use the type IIA approach to give a first principle derivation of $\mathcal{N} = 2$ CS quiver gauge theories dual to any of the $Y^{p,q}(B_4)$ geometries. For simplicity we focus on the case where the M-theory background contains no G_4 torsion flux.

In section 6 we study Higgsing and the resulting RG flow between the field theories of section 5, showing in numerous examples that they match with the geometric process of partial resolution.

Finally, in section 7 we consider adding G_4 discrete torsion flux to the $Y^{p,q_1,q_2}(\mathbb{F}_0)$ geometry, showing that the dual theory is a CS quiver with generic ranks and Chern-Simons levels. In particular we show that the $U(N)^4$ quiver gauge theories of [31], in the absence of Romans mass in IIA, are dual to M-theory backgrounds with specific nontrivial torsion G_4 fluxes; we generalise the duality to allow for generic torsion G_4 fluxes in $Y^{p,q}(\mathbb{F}_0)$, *i.e.* when $q_1 = q_2 = q$. An interesting ingredient in this analysis are the 3d Seiberg dualities for chiral quivers studied in [32, 33].

Most of the computations of this paper have been algorithmised using *Mathematica* [34], building on a package developed by Jurgis Pasukonis for [35].

2. Toric quivers, CY_3 cones and fractional brane charges

D-branes at conical Calabi-Yau singularities have been extensively studied in the past [36, 37, 38, 39, 40, 41, 42, 43]. At the singularity, a transverse D-brane decays into a marginal bound state of so-called fractional branes. The low energy physics on the bound state of fractional branes is described by a supersymmetric quiver gauge theory

³As explained in [14], additional Chern-Simons interactions coupling the central $U(1)$ factors of the $U(N_i)$ gauge groups are often needed to cancel a \mathbb{Z}_2 global anomaly. While their precise type IIA origin is not yet understood, it is always possible to add them without changing the result of the semiclassical analysis of the moduli space. We leave this subtlety aside in this paper.

with four supercharges. When the cone Y is a *toric* CY threefold, the quiver gauge theory has a very convenient description as a *brane tiling*: a bipartite graph on the torus which encodes the quiver and superpotential data [24, 25]. We refer to [44] for a review.

Quiver gauge theories are best known to describe D3-branes at CY_3 singularities Y in type IIB, but they arise more generally for any lower dimensional D-branes transverse to Y . In this work we are interested in D2-branes in type IIA string theory, giving rise to three dimensional $\mathcal{N} = 2$ supersymmetric gauge theories.

If there are only D2-branes transverse to the singularity, the quiver gauge theory has a gauge group $U(N)^G$ with equal ranks and G the number of quiver nodes. In this paper we will consider a more general set of D2-branes together with D4- and D6-branes wrapped on compact 2- and 4-cycles in Y , respectively, giving rise to rather generic field theories with $\prod_i U(N_i)$ gauge groups. We thus need to know the translation between the number of compactly supported D-branes and the quiver ranks. We will find matrices Q^\vee such that

$$\mathbf{N} = \mathbf{Q}_{\text{brane}}(Q^\vee)^{-1}, \quad (2.1)$$

where $\mathbf{N} = (N_i)$ are the quiver ranks, and $\mathbf{Q}_{\text{brane}}$ is a vector encoding the D-brane Page charges [45] of the supergravity background. The $G \times G$ matrix Q^\vee containing the brane charges sourced by fractional branes will be called the *dictionary*.

Although most of what follows is valid more generally, our main focus will be on Y a complex cone over a two-complex-dimensional Fano variety. In this case we have an explicit algorithm to determine Q^\vee . Along the way we will review various important results about quivers and their moduli spaces, which will be useful when we turn to M2-brane theories.

2.1 Toric quiver and crepant resolutions of Y

To any toric CY_3 Y we can associate at least one toric quiver with superpotential \mathcal{Q} . Toric quiver theories admit a description in term of a brane tiling (see Figure 1(b) for an example): each quiver node becomes a face, each arrow becomes an edge and each superpotential term becomes a white or black vertex in the brane tiling, depending on its sign. A *dimer* is a distinguished edge in a brane tiling. A *perfect matching* p_k is a configuration of dimers such that every vertex is touched exactly once. We define the perfect matching matrix \mathbf{P}_{ak} as

$$\mathbf{P}_{ak} = \begin{cases} 1 & \text{if the perfect matching } p_k \text{ contains the fields } X_a \\ 0 & \text{otherwise} \end{cases} \quad (2.2)$$

A dimer model is a brane tiling together with its perfect matchings. Efficient “inverse algorithms” exist to go from the geometry to \mathcal{Q} [46, 47].

The low energy worldvolume theory of a single D2-brane transverse to the cone Y is a 3d $\mathcal{N} = 2$ quiver gauge theory \mathcal{Q} with Abelian gauge group $\mathcal{G} = U(1)^G$. Indeed the variety Y probed by the D2-brane is reproduced as the vacuum moduli space of

the Abelian quiver. Resolving the cone Y to \tilde{Y} corresponds to turning on Fayet-Ilioupoulos (FI) terms in the quiver gauge theory. The FI parameters $\boldsymbol{\xi} = (\xi_i)$ affect D-term equations, leading to non-zero levels for the moment maps of \mathcal{G} in the Kähler quotient description of the moduli space,

$$\mathcal{M}(\mathcal{Q}; \boldsymbol{\xi})_K \equiv \{X_a \mid \partial W = 0\} //_{\boldsymbol{\xi}} \mathcal{G} . \quad (2.3)$$

We have that $\tilde{Y} \cong \mathcal{M}(\mathcal{Q}; \boldsymbol{\xi})_K$. The moment maps correspond to the D-terms

$$\mu_i \equiv \sum_{X_a=X_{ij}} |X_a|^2 - \sum_{X_a=X_{ji}} |X_a|^2 = \xi_i . \quad (2.4)$$

The great advantage of toric quiver gauge theories is that we can trade the F-term equations $\partial W = 0$ in (2.3) for D-term equations in some auxiliary gauged linear sigma model (GLSM) with no superpotential. The idea is to trivialise the relations $\partial W = 0$ by introducing new variables p_k , $k = 1, \dots, c$ [42]. The solution of the F-term equations is given explicitly in term of so-called perfect matching (p.m.) variables p_k . We have

$$X_a = \prod_k (p_k)^{P_{ak}} , \quad (2.5)$$

where \mathbf{P} is the perfect matching matrix (2.2) [25, 48]. To eliminate the redundancy in the description (2.5) one introduces a spurious $U(1)^{c-G-2}$ gauge symmetry. Let Q_D be the charge matrix of the variables p_k under the original gauge group $U(1)^G$ and Q_F the charge matrix under the spurious gauge symmetry. The GLSM is conveniently summarised by its charge matrix together with its FI parameters:

	p_1	\cdots	p_c	FI
$U(1)_F^l$	$(Q_F)_1^l$	\cdots	$(Q_F)_c^l$	0
$U(1)_D^i$	$(Q_D)_1^i$	\cdots	$(Q_D)_c^i$	ξ^i

(2.6)

Remark that one should not introduce FI parameters for the spurious gauge symmetries. This connects to the GLSM description of toric varieties. Each p_k corresponds to a point in the toric diagram Γ of Y , and moving in FI parameter space allows to describe various (complete or partial) resolutions of Y . Importantly, the GLSM (2.6) never probes non-geometric phases of Y . This is possible because any internal point in the toric diagram is associated to several variables p_k (the number of p_k 's associated to a toric point is called its *multiplicity*).⁴ For any choice of ξ_i , we can always choose a unique variable $p_{0,r}$ for each internal point w_r such that all other variables $p_{k;r}$ associated to w_r are written in term of $p_{0;r}$ for any field value, making these $p_{k;r}$ redundant. More precisely, the D-term equations of the GLSM relate the modulus according to $|p_{k;r}|^2 = |p_{0;r}|^2 + \xi_{k,0}$,

⁴A note on terminology. The toric diagram Γ of Y is a convex lattice polygon. We call a lattice point which is either inside Γ or inside some of its edges *internal*, a point inside Γ *strictly internal*, and an internal point of an external edge *internal-external*. Finally a point which is not internal (i.e. one of the vertices of Γ) is called *strictly external*.

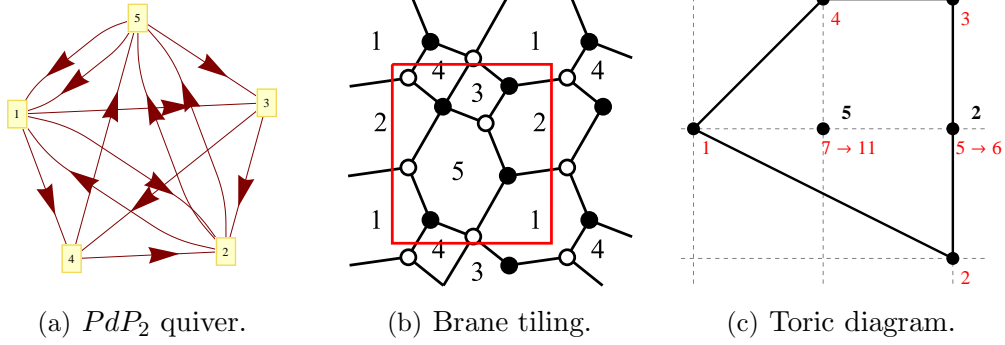


Figure 1: Quiver, brane tiling and toric diagram for the complex cone over PdP_2 . Black numbers above toric points are the multiplicities of these points (when they are larger than one), red numbers are the names of the corresponding perfect matchings. The strictly internal point conventionally has coordinates $(0, 0)$.

with $\xi_{k,0}$ some positive combination of the FI parameters; the phase of $p_{k;r}$ is fixed by the gauge symmetry.

Going the other way, any choice of a single p.m. variable per point in Γ determines an *open string Kähler chamber* in FI parameter space, denoted

$$KC = \{p_{r_1}, \dots, p_{r_{n_I}}\}, \quad (2.7)$$

where n_I denote the number of internal points in Γ . Such a choice determines a wedge in FI space by requiring that all other p.m. variables from internal points can be solved for in term of the variables (2.7) — see the example below. This leads us to a minimal GLSM for \tilde{Y} ,

$$\begin{array}{c|cc|c} CY_3 \tilde{Y} & p_s & p_r & \text{FI} \\ \hline U(1)_\alpha & Q_s^\alpha & Q_r^\alpha & \chi_\alpha(\xi) \end{array} \quad (2.8)$$

where p_s and p_r are strictly external and internal points in Γ , respectively, and the resolution parameters χ_α are the Kähler volumes of a basis of 2-cycles \mathcal{C}_α , which depend linearly on the FI parameters in such a way that (2.8) is always in a geometric phase.

Example: The PdP_2 quiver. As an example which contains all the complications of the general case, consider the quiver of Figure 1(a), with superpotential

$$\begin{aligned} W_{PdP_2} = & X_{13}X_{34}X_{45}X_{51}^2 + X_{21}X_{14}X_{42} + X_{51}^1X_{12}X_{25}^2 + X_{53}X_{32}X_{25}^1 + \\ & - X_{13}X_{32}X_{21} - X_{14}X_{45}X_{51}^1 - X_{51}^2X_{12}X_{25}^1 - X_{53}X_{34}X_{42}X_{25}^2. \end{aligned} \quad (2.9)$$

The brane tiling is shown in Fig. 1(b). It describes D-branes transverse to the complex cone over the pseudo-del Pezzo surface PdP_2 , whose toric diagram is shown in Figure

1(c). The perfect matchings, as collections of dimers in the brane tiling, are

$$\begin{aligned}
p_1 &= \{X_{21}, X_{53}, X_{12}, X_{45}\}, & p_7 &= \{X_{14}, X_{53}, X_{12}, X_{13}\}, \\
p_2 &= \{X_{14}, X_{32}, X_{25}^2, X_{51}^2\}, & p_8 &= \{X_{14}, X_{32}, X_{12}, X_{34}\}, \\
p_3 &= \{X_{42}, X_{25}^1, X_{51}^1, X_{13}\}, & p_9 &= \{X_{42}, X_{32}, X_{12}, X_{45}\}, \\
p_4 &= \{X_{21}, X_{25}^1, X_{51}^1, X_{34}\}, & p_{10} &= \{X_{21}, X_{25}^1, X_{25}^2, X_{45}\}, \\
p_5 &= \{X_{14}, X_{25}^1, X_{25}^2, X_{13}\}, & p_{11} &= \{X_{21}, X_{53}, X_{51}^1, X_{51}^2\}, \\
p_6 &= \{X_{42}, X_{32}, X_{51}^1, X_{51}^2\}
\end{aligned} \tag{2.10}$$

From this we can read the perfect matching matrix \mathbf{P} and express the 13 fields X_{ij} in term of p.m. variables p_k , according to (2.5). The GLSM (2.6) is

	p_1	p_2	p_3	p_4	p_5	p_6	p_7	p_8	p_9	p_{10}	p_{11}	FI
$U(1)_1^F$	0	-1	0	-1	1	0	-1	1	0	0	1	0
$U(1)_2^F$	-1	0	0	0	-1	0	1	0	0	1	0	0
$U(1)_3^F$	-1	0	-1	1	0	0	1	-1	1	0	0	0
$U(1)_4^F$	0	-1	-1	0	1	1	0	0	0	0	0	0
$U(1)_1^D$	0	-1	0	-1	1	0	0	1	0	0	0	ξ_1
$U(1)_2^D$	0	0	-1	1	1	0	0	-1	0	0	0	ξ_2
$U(1)_3^D$	0	0	0	0	0	0	-1	1	0	0	0	ξ_3
$U(1)_4^D$	1	0	1	-1	0	0	-1	0	0	0	0	ξ_4

(2.11)

The last line of Q_D (for the fifth gauge group) is omitted because it is redundant. There are 10 Kähler chambers, corresponding to choosing one of the 5 p.m. variables (p_7, \dots, p_{11}) for the toric point $(0, 0)$ and one of the 2 variables (p_5, p_6) for the point $(1, 0)$. Indeed, the D-term equations of the GLSM (2.11) can be massaged into

$$\begin{aligned}
|p_5|^2 - |p_6|^2 &= \xi_1 + \xi_2, & |p_7|^2 - |p_{11}|^2 &= \xi_1, & |p_8|^2 - |p_{11}|^2 &= \xi_1 + \xi_3, \\
|p_9|^2 - |p_{11}|^2 &= \xi_1 + \xi_3 + \xi_4, & |p_{10}|^2 - |p_{11}|^2 &= \xi_1 + \xi_2 + \xi_3 + \xi_4,
\end{aligned} \tag{2.12}$$

together with three more equations. Consider for instance the choice $\{p_5, p_7\}$. We can solve the D-terms (2.12) in term of p_5 as $|p_6|^2 = |p_5|^2 - \xi_1 - \xi_2$ as long as $\xi_1 + \xi_2 \leq 0$, and similarly for p_8, \dots, p_{11} in term of p_7 . Proceeding that way, we find 10 Kahler chambers $\{p_{(1,0)}, p_{(0,0)}\}$ with the conditions

$$p_{(1,0)} = \begin{cases} p_5 : & \xi_1 + \xi_2 \leq 0 \\ p_6 : & \xi_1 + \xi_2 \geq 0 \end{cases}, \tag{2.13}$$

and

$$p_{(0,0)} = \begin{cases} p_7 : & \xi_3 \geq 0, \xi_3 + \xi_4 \geq 0, \xi_2 + \xi_3 + \xi_4 \geq 0, \xi_1 \leq 0 \\ p_8 : & \xi_3 \leq 0, \xi_4 \geq 0, \xi_2 + \xi_4 \geq 0, \xi_1 + \xi_3 \leq 0 \\ p_9 : & \xi_3 + \xi_4 \leq 0, \xi_4 \leq 0, \xi_2 \geq 0, \xi_1 + \xi_3 + \xi_4 \leq 0 \\ p_{10} : & \xi_2 + \xi_3 + \xi_4 \leq 0, \xi_2 + \xi_4 \leq 0, \xi_2 \leq 0, \xi_1 + \xi_2 + \xi_3 + \xi_4 \leq 0 \\ p_{11} : & \xi_1 \geq 0, \xi_1 + \xi_3 \geq 0, \xi_1 + \xi_3 + \xi_4 \geq 0, \xi_1 + \xi_2 + \xi_3 + \xi_4 \geq 0 \end{cases} \tag{2.14}$$

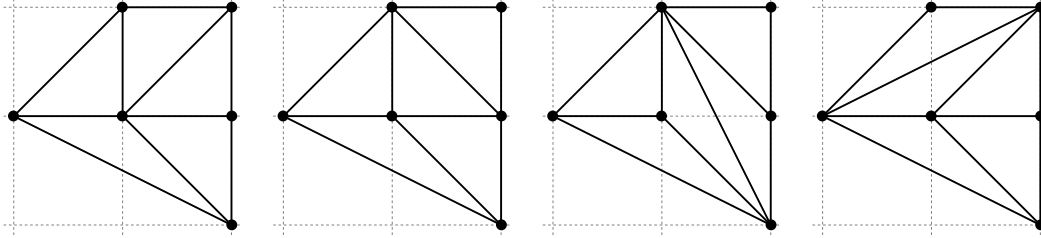


Figure 2: The four possible triangulations $T_\Gamma^{(1)}, \dots, T_\Gamma^{(4)}$ of the toric diagram of $C_{\mathbb{C}}(PdP_2)$.

These conditions subdivide the FI parameter space $\xi \cong \mathbb{R}^4$ into 10 wedges. For a generic choice of ξ , the singularity $Y = C_{\mathbb{C}}(PdP_2)$ is fully resolved, consisting of one of the four possible triangulations of the toric diagram shown in Figure 2.

We will discuss an elegant way of recovering these Kähler chambers in the following. Let us note already that this notion of Kähler chamber stems from the quiver \mathcal{Q} and is ultimately related to the complexified Kähler moduli space seen by the type II string, including α' corrections. On the other hand, given a toric CY_3 Y with toric diagram Γ , the classical geometric notion of (partial) resolution corresponds to a (partial) triangulation of the toric diagram. The space \tilde{Y} is completely smooth if it is described by a simplicial fan, corresponding to a complete triangulation of Γ such as in Fig. 2. For a given Kähler chamber (2.7) only some of the triangulations of Γ might be allowed.⁵ We will return to this point below after introducing more powerful tools.

2.2 GIT quotient and moduli space

In the absence of FI parameters, i.e. when all D-term equations give vanishing moment maps on the space of constant fields $\{X_a\}$, the moduli space can be recovered algebraically by ignoring the D-terms and quotienting the space of F-flatness solutions by the complexified gauge group. We recover the cone Y as an affine algebraic variety,

$$Y \cong \{X_a \mid \partial W = 0\} / \mathcal{G}_{\mathbb{C}}. \quad (2.15)$$

This is because whenever $\xi_i = 0$ there always exists a unique solution of (2.4) in the closure of each complexified gauge orbit [49]. Such quotient is called a GIT (Geometric Invariant Theory) quotient, and it is very intuitive from the physics point of view: we just consider the classical chiral ring of holomorphic gauge invariant operators.

There is a natural GIT generalization of (2.15) to allow for partial resolution of Y . Let $\mathcal{Z} = \{X_a \mid \partial W = 0\} = \text{Spec } \mathbb{C}[X_a] / (\partial W)$ be the set of solutions of the F-term

⁵Any internal edge (r_1, r_2) in the triangulated toric diagram corresponds to a curve $D_{r_1} \cap D_{r_2}$ of positive volume χ , where D_r is the toric divisor associated to the toric point w_r . The volume χ is a linear combination of the χ_α 's in (2.8), which in turn depend on the FI parameters in a specific way in each wedge in FI space (Kähler chamber). It might thus happen that χ is never positive in that Kähler chamber.

equations, also known as the *master space*, and z_a some affine coordinates on \mathcal{Z} . In our toric Abelian theory, this can also be described as

$$\mathcal{Z} = \text{Spec } \mathbb{C}[p_1, \dots, p_c]^{\mathcal{G}_{\mathbb{C}}^F}, \quad (2.16)$$

in term of polynomials in the p.m. variables invariant under the spurious gauge symmetry $\mathcal{G}^F = U(1)^{c-G-2}$. Consider a trivial line bundle $\mathcal{Z} \times \mathbb{C}$, with t the coordinate on \mathbb{C} , and pick some integers $(\theta_i) \equiv \boldsymbol{\theta} \in \mathbb{Z}^G$ (such that $\sum_i \theta_i = 0$). The choice of $\boldsymbol{\theta}$ determines a one-dimensional representation $\chi_{\boldsymbol{\theta}}$ of $\mathcal{G}_{\mathbb{C}} \cong (\mathbb{C}^*)^G$ on the \mathbb{C} fibre,

$$(z_a, t) \mapsto (\lambda \cdot z_a, \chi_{\boldsymbol{\theta}}(\lambda) t), \quad \text{with} \quad \chi_{\boldsymbol{\theta}} = \prod_{i=1}^G \lambda_i^{\theta_i}, \quad (2.17)$$

for $\lambda = (\lambda_1, \dots, \lambda_G) \in (\mathbb{C}^*)^G$. Let $\mathcal{G}_{\mathbb{C}}(\boldsymbol{\theta})$ denote the action of the gauge group $\mathcal{G}_{\mathbb{C}}$ on $\mathcal{Z} \times \mathbb{C}$. The GIT quotient is given by

$$\mathcal{M}(\mathcal{Q}; \boldsymbol{\theta})_{GIT} = \text{Proj } \mathbb{C}[\mathcal{Z} \times \mathbb{C}]^{\mathcal{G}_{\mathbb{C}}(\boldsymbol{\theta})}. \quad (2.18)$$

We refer to [50] for some background on this construction in the present context. A crucial result is the Kempf-Ness theorem stating the equivalence of GIT quotient and Kähler quotient,

$$\mathcal{M}(\mathcal{Q}; \boldsymbol{\theta})_{GIT} \cong \mathcal{M}(\mathcal{Q}; \boldsymbol{\xi})_K, \quad \text{with} \quad \boldsymbol{\xi} = \boldsymbol{\theta}. \quad (2.19)$$

The parameters $\boldsymbol{\theta}$ are discretised FI parameters, which determine discretised Kähler classes of the underlying CY_3 cone Y .

2.3 Quiver representations, θ -stability and Kähler chambers

From a mathematician's point of view, a quiver is nothing but an oriented graph consisting of nodes $i = 1, \dots, G$ and arrows a connecting the nodes. Let us denote by $a = a_{ij}$ an arrow that goes from i to node j . The arrows generate a non-commutative algebra $\mathbb{C}\mathcal{Q}$ consisting of all the paths in the quiver, where the multiplication operation is the obvious concatenation of paths. If we associate to each node the trivial path e_i , the algebra $\mathbb{C}\mathcal{Q}$ has an identity element $\sum_i e_i$.

The quivers we study are also equipped with a superpotential which is a formal sum of quiver loops $l = \{i_1, i_2, \dots, i_{n_l}\}$:

$$W = \sum_{l \in L_0} \pm a_{i_1 i_2} \cdots a_{i_{n_l-1} i_{n_l}}, \quad (2.20)$$

where L_0 denotes some subset of all the closed loops in \mathcal{Q} . Formal derivation with respect to the arrows a_{ij} leads to relations between the paths according to $\partial_a W = 0$. The fundamental algebraic object associated to the quiver \mathcal{Q} is the path algebra obtained after quotienting by superpotential relations,

$$\mathcal{A} \equiv \mathbb{C}\mathcal{Q}/(\partial W). \quad (2.21)$$

For a toric quiver every arrow X_a appears twice in (2.20), with opposite signs.

A *quiver representation* R is a choice of vector space V_i for each node i and of linear map X_a for each arrow a , with the linear maps satisfying the superpotential relations:

$$R : \begin{cases} i \mapsto V_i \cong \mathbb{C}^{N_i} \\ a_{ij} \mapsto X_{ij} \end{cases} \quad \text{such that} \quad \partial_X W = 0. \quad (2.22)$$

The vector

$$\mathbf{N} \equiv (N_1, \dots, N_G) \equiv \dim R \quad (2.23)$$

is the *dimension vector* of R . In physical terms, a quiver representation is a choice of gauge group

$$\mathcal{G} = U(N_1) \times \dots \times U(N_G) \quad (2.24)$$

for a supersymmetric quiver gauge theory, together with a choice of VEVs for the chiral superfields X_{ij} . The dimension vector \mathbf{N} gives the ranks of the gauge group.

Given two quiver representations R and R' , a *morphism* $\phi : R \rightarrow R'$ is a set of linear maps $\phi_i : V_i \rightarrow V'_i$ such that

$$\phi_i X'_a = X_a \phi_j, \quad \forall a = a_{ij}. \quad (2.25)$$

If ϕ is injective, R is called a *subrepresentation* of R' . Two representations R and R' are isomorphic if there exists a bijective morphism between them. As long as we consider holomorphic quantities, the gauge group of the supersymmetric quiver theory is effectively complexified to $\mathcal{G}_{\mathbb{C}} = \prod_i GL(N_i, \mathbb{C})$. Isomorphic quiver representations are simply gauge equivalent supersymmetric vacua in a given quiver gauge theory, which are physically identified. Isomorphism classes of \mathcal{Q} representations can also be understood as \mathcal{A} -modules, i.e. representations of the path algebra (2.21).

The moduli space of quiver representations of dimension $\mathbf{N} = \boldsymbol{\alpha} \equiv (1, 1, \dots, 1)$ is our space Y , seen algebraically:

$$\mathcal{M}(\mathcal{Q}, \boldsymbol{\alpha}) = \{R_{\boldsymbol{\alpha}}\} / \mathcal{G}_{\mathbb{C}} \cong Y. \quad (2.26)$$

We are after a similar description of partial resolutions $\pi : \tilde{Y} \rightarrow Y$, in parallel to the discussion of Kähler and GIT quotients in section 2.1. We need some notion that adds some additional $\mathcal{G}_{\mathbb{C}}$ -orbits to (2.26). The crucial notion to do so is θ -stability [30].

Definition: θ -stability. Consider a quiver \mathcal{Q} with G nodes. Given a vector $\boldsymbol{\theta} \in \mathbb{Z}^G$, a quiver representation R of dimension \mathbf{N} is θ -stable (resp. semi-stable) if and only if $\boldsymbol{\theta} \mathbf{N} = 0$ and for any proper subrepresentation R' of dimension \mathbf{N}' we have $\boldsymbol{\theta} \mathbf{N}' < 0$ (resp. $\boldsymbol{\theta} \mathbf{N}' \leq 0$).

The main result of [30] is that the moduli space of θ -semistable quiver representations of a given dimension \mathbf{N} can be obtained by a GIT quotient. In particular for $\mathbf{N} = \boldsymbol{\alpha}$,

$$\mathcal{M}(\mathcal{Q}, \boldsymbol{\alpha}; \boldsymbol{\theta}) \equiv \{R_{\boldsymbol{\alpha}}\}^{ss} / \mathcal{G}_{\mathbb{C}} \cong \mathcal{M}(\mathcal{Q}; \boldsymbol{\theta})_{GIT}, \quad (2.27)$$

with $\mathcal{M}(\mathcal{Q}; \boldsymbol{\theta})_{GIT}$ defined in (2.18).

One can reformulate the considerations of section 2.1 about Kähler chambers in this quiver language [51, 52]. Consider any $\boldsymbol{\alpha}$ -rep (\mathcal{Q} representation of dimension $\boldsymbol{\alpha}$) $R_\alpha \cong \{\boldsymbol{\alpha}, X_a\}$. Let \mathcal{Q}_{R_α} be the quiver obtained from \mathcal{Q} by deleting any arrow a such that $X_a = 0$ in R_α . Any subrepresentation of R_α is also a representation of \mathcal{Q}_{R_α} , obviously. A representation $R'_\beta \cong \{\boldsymbol{\beta}, X'_a\}$, with $\boldsymbol{\beta} \leq \boldsymbol{\alpha}$, is a subrepresentation of R_α if and only if for any $\beta_i \neq 0$ there exists a non-zero complex number ϕ_i such that (2.25) holds. Denote by I_0 the set of nodes $\{i_0\}$ such that $\beta_{i_0} = 0$; we thus have $\phi_i = 0$ if $i \in I_0$ and $\phi_i \neq 0$ otherwise. From (2.25), we have

$$0 = \phi_j X_a, \quad \forall a = a_{j i_0}, \quad \forall i_0 \in I_0, \quad (2.28)$$

which holds if and only if $j \in I_0$ too. We thus showed that R_β is a subrepresentation of R_α only if the dimension vector $\boldsymbol{\beta}$ is such that for any $i_0 \in I_0$, all nodes j connected to i_0 from the left in the auxiliary quiver \mathcal{Q}_{R_α} (i.e. nodes such that there is a $X_{j i_0} \neq 0$ in R_α) are also in I_0 .

Consequently, any representation R_α such that \mathcal{Q}_{R_α} is strongly connected⁶ has no subrepresentations and is therefore stable for *any* $\boldsymbol{\theta}$. This is what happens for generic R_α representations, corresponding to a D2-brane probing the resolved cone \tilde{Y} away from the exceptional locus B_4 (and away from any singularity that might remain in \tilde{Y}).

On the other hand, the R_α representations corresponding to the exceptional locus $\pi^{-1}(0) \subset \tilde{Y}$ are all representations of a quiver \mathcal{Q}_{B_4} with no closed loop [53] and therefore *not* strongly connected; we call such quiver a “pseudo-Beilinson quiver” for B_4 . Choosing a Kähler chamber in the toric quiver in the sense of (2.7), the exceptional locus B_4 is obtained as a compact toric divisor $\{p_0 = 0\}$, with $p_0 \in \{p_r\}$ corresponding to the strictly internal point w_0 . Therefore the pseudo-Beilinson quiver \mathcal{Q}_{B_4} is obtained from \mathcal{Q} by setting to zero any field X_a appearing in the perfect matching p_0 .

More generally, for any perfect matching or collection of perfect matchings $\{p_k\}$, we define a \mathcal{Q} -representation of dimension $\boldsymbol{\alpha}$ [52]⁷

$$R_{\{p_k\}} : X_a = \begin{cases} 0, & a \in \{p_0\} \\ 1, & a \notin \{p_k\} \end{cases}, \quad (2.29)$$

and a pseudo-Beilinson quiver $\mathcal{Q}_{R_{\{p_k\}}}$. The collection $\{p_k\}$ is called $\boldsymbol{\theta}$ -stable if $R_{\{p_k\}}$ is $\boldsymbol{\theta}$ -stable.

For any choice of Kähler chamber (2.7), we need that every perfect matching $p_r \in KC$ is $\boldsymbol{\theta}$ -stable. This gives inequalities on $\boldsymbol{\theta} \cong \boldsymbol{\xi}$, reproducing the same result as in section 2.1. Given such a Kähler chamber, we further specify a triangulation T_Γ of the toric diagram as a collection of pairs of perfect matchings, $T_\Gamma = \{(p_{r_1}, p_{r_2})\}$, according

⁶A quiver is called *strongly connected* if for any pair of nodes i, j there exists a quiver path $\mathbf{p} : i \rightarrow j$.

⁷It turns out that for perfect matchings this is a good representation [52], which is not completely obvious due to the superpotential relations.

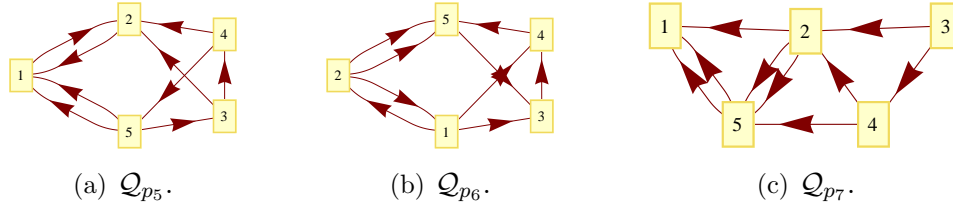


Figure 3: Examples of pseudo-Beilinson quivers obtained from the toric quiver for PdP_2 , for the perfect matchings p_5 , p_6 and p_7 respectively.

to the edges in T_Γ . This triangulation is allowed only for θ such that every pair (p_{r_1}, p_{r_2}) in T_Γ is θ -stable as well.

When implemented on a computer, this gives an algorithm to find all Kähler chambers in FI parameter space which runs in about the same time as the algorithm described in section 2.1. On the other hand, the present method is much more efficient to discuss triangulations of the toric diagram and how they depend on the FI parameters of the quiver, besides being more elegant conceptually.

The PdP_2 example. Consider the PdP_2 quiver introduced before. A Kähler chamber $KC \cong \{p_{(1,0)}, p_{(0,0)}\}$ is such that these two perfect matchings are θ -stable for any θ in the chamber (and θ -semistable on the walls of the chamber). The pseudo-Beilinson quivers associated to some perfect matchings are shown in Figure 3(a). In the case $p_{(1,0)} = p_5$, we easily see from the quiver in Fig. 3(a) that the only subrepresentation of the α -rep R_{p_5} has dimension vector $\beta = (1, 1, 0, 0, 0)$, leading to the θ -stability condition $\theta_1 + \theta_2 < 0$. Similarly, from Fig. 3(b) we find that the only subrepresentation of R_{p_6} has dimension vector $(0, 0, 1, 1, 1)$, so that we should have $\theta_3 + \theta_4 + \theta_5 = -\theta_1 - \theta_2 < 0$. This reproduces (2.13). Similarly for the choice of strictly internal perfect matching: from Fig. 3(c) we see that the subrepresentations of R_{p_7} are $(1, 0, 0, 0, 0)$, $(1, 0, 0, 0, 1)$, $(1, 1, 0, 0, 1)$ and $(1, 1, 0, 1, 1)$, giving the conditions in the first line of (2.14).

Consider the four triangulations $T_\Gamma^{(1)}, \dots, T_\Gamma^{(4)}$ in Figure 2. Any edge between the internal point $(0, 0)$ and a strictly external point is θ -stable whenever $p_{(0,0)}$ is θ -stable. On the other hand any other edge gives a new non-trivial constraint. We find that the choice $p_{(1,0)} = p_6$ (i.e. a choice of FI parameters with $\xi_1 + \xi_2 > 0$) does not allow any of the four complete triangulations. On the other hand, for $p_{(1,0)} = p_5$, the five Kähler chambers $\{p_5, p_{(0,0)}\}$ are compatible with some of the triangulations according to:

Compatible ?	$\{p_5, p_7\}$	$\{p_5, p_8\}$	$\{p_5, p_9\}$	$\{p_5, p_{10}\}$	$\{p_5, p_{11}\}$
$T_\Gamma^{(1)}$	Yes	Yes	Yes	Yes	Yes
$T_\Gamma^{(2)}$	Yes	Yes	No	Yes	Yes
$T_\Gamma^{(3)}$	No	Yes	No	Yes	Yes
$T_\Gamma^{(4)}$	Yes	No	Yes	Yes	Yes

2.4 Tilting collection of line bundles from toric quiver

Branes of type II string theory wrapping holomorphic cycles in Y are described math-

ematically as objects in the B-brane category of Y , also known as derived category of coherent sheaves $D(\text{Coh } \tilde{Y})$. These objects are the branes of the topological B-model, and for that reason they are independent of the Kähler structure, allowing us to probe singular geometries where large α' corrections are expected.

Given a toric variety \tilde{Y} , suppose that we can find a collection of line bundles

$$\mathcal{E} = \{\mathbf{L}_1, \dots, \mathbf{L}_G\} \quad (2.31)$$

such that

$$H^n(\tilde{Y}, \mathbf{L}_j \otimes \mathbf{L}_i^*) = 0, \quad \forall n > 0, \forall i, j, \quad (2.32)$$

and which generates $D(\text{Coh } \tilde{Y})$. Such an object (2.31) is called a *tilting collection* of line bundles and gives a particularly nice generating set of the B-branes on Y . It also has the right properties to be associated to a quiver: each \mathbf{L}_i corresponds to a node of the quiver \mathcal{Q} with path algebra (2.21) given by

$$\mathcal{A}^{\text{op}} \cong \bigoplus_{i,j} \text{Hom}(\mathbf{L}_i, \mathbf{L}_j) = \bigoplus_{i,j} H^0(\tilde{Y}, \mathbf{L}_j \otimes \mathbf{L}_i^*). \quad (2.33)$$

See in particular [54] for more background on this construction.⁸ \mathcal{A} and \mathcal{A}^{op} are related by reversing the orientation of every path, and \mathcal{A} defines the quiver \mathcal{Q} (with superpotential relations) implicitly.

Given a toric quiver \mathcal{Q} corresponding to a toric CY_3 Y , we can construct a tilting collection on any of the partial resolutions \tilde{Y} following [53, 52]. A *weak path* \mathbf{p} is a path in \mathcal{Q} using both the arrows a and their inverse a^{-1} :

$$\mathbf{p} : a_1^{\epsilon_1} a_2^{\epsilon_2} \cdots a_l^{\epsilon_l}, \quad \epsilon = \pm 1. \quad (2.34)$$

To any arrow a , the Ψ -map associates the formal sum of perfect matchings in which X_a appears, $\Psi(a) = \sum_k \mathbf{P}_{ak} p_k$. This extends to any weak path linearly. Consider the resolved space \tilde{Y}_θ associated to some θ parameter, and more generally to some chamber (2.7). We denote by Ψ_θ the Ψ -map with range restricted to θ -stable perfect matchings. Since the latter are associated to rays in the toric fan of \tilde{Y}_θ , thus to toric divisors, Ψ_θ is really mapping paths to divisors of \tilde{Y}_θ . For a weak path (2.34), we have

$$\Psi_\theta(\mathbf{p}) = \sum_{n=1}^l \epsilon_n \sum_{k|p_k \text{ } \theta\text{-stab}} \mathbf{P}_{a_n k} D_k, \quad (2.35)$$

where $D_k \cong \{p_k = 0\}$. Choose some conventional “first node” $i = 1$ in \mathcal{Q} , and associate to every node i a weak path $\mathbf{p}_i : 1 \rightarrow i$ (with \mathbf{p}_1 the trivial path). We can associate a line bundle over \tilde{Y}_θ to every quiver node according to

$$\mathbf{L}_i = \mathcal{O}(\Psi_\theta(\mathbf{p}_i)). \quad (2.36)$$

It was proven in Theorem 4.2 of [52] that the collection $\{\mathbf{L}_i\}_{i=1}^G$ obtained in this way is a tilting collection.

⁸See also [33]. As reviewed there, the line bundles \mathbf{L}_i (or sheaves \mathbf{P}_i in the notation of [33]) correspond to the projective (right) \mathcal{A} -modules $\mathcal{A}e_i$ in the quiver language.

Example. In our PdP_2 example (see Fig. 1(a)), we can take for instance the weak paths $\mathbf{p}_1 = e_1$, $\mathbf{p}_2 = a_{12}$, $\mathbf{p}_3 = a_{13}$, $\mathbf{p}_4 = a_{14}$ and $\mathbf{p}_5 = (a_{51}^1)^{-1}$. The Ψ -map gives us

$$\begin{aligned}\Psi(\mathbf{p}_1) &= 0, & \Psi(\mathbf{p}_2) &= p_1 + p_7 + p_9, \\ \Psi(\mathbf{p}_3) &= p_3 + p_5 + p_7, & \Psi(\mathbf{p}_4) &= p_2 + p_5 + p_7 + p_8, \\ \Psi(\mathbf{p}_5) &= -p_3 - p_4 - p_6 - p_{11}.\end{aligned}\tag{2.37}$$

In any Kähler chamber $KC \cong \{p_{(1,0)}, p_{(0,0)}\}$, the Ψ_θ map restricts (2.37) to the θ -stable perfect matchings, and to the corresponding tilting collections of line bundles (2.36). For instance

$$\begin{aligned}KC \cong \{p_5, p_7\} &: \begin{cases} \mathcal{O}, \mathcal{O}(D_1 + D_{(0,0)}), \mathcal{O}(D_3 + D_{(1,0)} + D_{(0,0)}), \\ \mathcal{O}(D_2 + D_{(1,0)} + D_{(0,0)}), \mathcal{O}(-D_3 - D_4), \end{cases} \\ KC \cong \{p_5, p_8\} &: \begin{cases} \mathcal{O}, \mathcal{O}(D_1), \mathcal{O}(D_3 + D_{(1,0)}), \\ \mathcal{O}(D_2 + D_{(1,0)} + D_{(0,0)}), \mathcal{O}(-D_3 - D_4), \end{cases}\end{aligned}\tag{2.38}$$

and so on for the 10 open string Kähler chambers of this PdP_2 quiver.

2.5 2d toric Fano varieties and brane charge dictionaries

To any Kähler chamber (2.7) we associate a tilting collection of line bundles (2.31). However, the objects L_i are *not* the physical fractional branes. The fractional branes are — loosely speaking — branes wrapping compact cycles. For the algorithm of section 4 below, we will need to know their brane charges, a piece of information which is not so easy to extract in general. In this paper we restrict ourselves to the case in which Y is a complex cone over a *toric Fano variety*. There are 16 of them, with toric diagrams that are reflexive polygons, having a single strictly internal point [55].

Adding the interior point to the toric fan corresponds to a partial resolution

$$\pi : \tilde{Y} \rightarrow Y, \quad \tilde{Y} \cong \mathcal{O}_{B_4}(K),\tag{2.39}$$

with $\mathcal{O}_{B_4}(K)$ the canonical bundle over the Fano variety B_4 . The toric fan of B_4 is obtained from the toric diagram Γ by taking the strictly interior point as the origin and drawing a toric vector to every strictly external point. When there are internal-external points, B_4 has orbifold singularities, which can be resolved by adding the corresponding toric vectors to the fan. The resulting smooth manifold is denoted \tilde{B}_4 .

For all practical purposes we can restrict our attentions to the B-branes on B_4 , which naturally lift to B-branes of \tilde{Y} . Let us denote by $\{p_r^{EI}, p_0\}$ a Kähler chamber, where the perfect matchings p_r^{EI} correspond to external-internal points and p_0 correspond to the strictly internal point. To any such chamber we associate a smooth space \tilde{Y} and a pseudo-Beilinson quiver \mathcal{Q}_{B_4} obtained from \mathcal{Q} by removing all arrows appearing in p_0 . We then associate a collection of line bundles over B_4 to this Kähler chamber by the Ψ_θ -map, for any θ inside the chamber. We write the divisors (2.35)

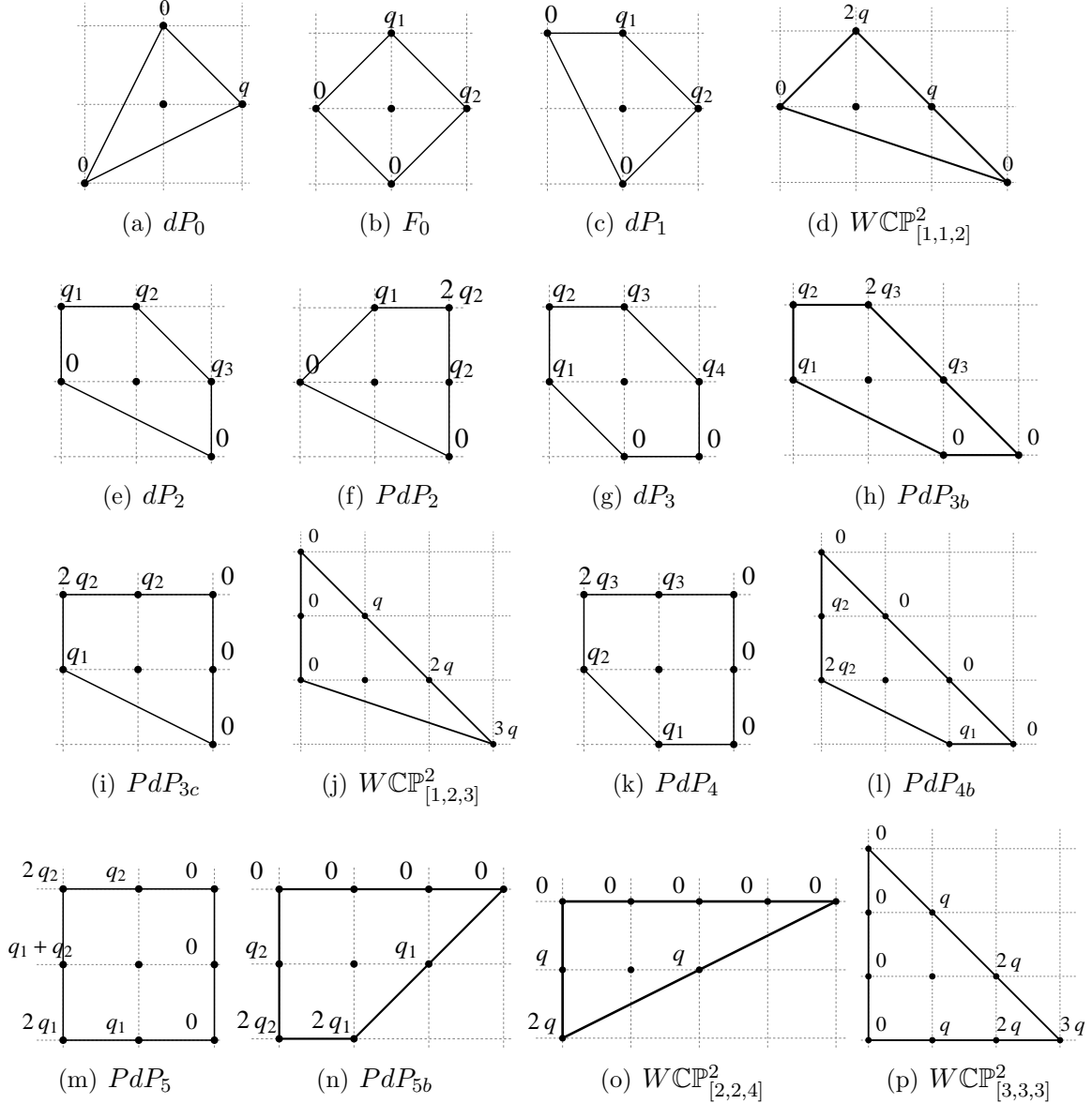


Figure 4: Toric diagrams for the 16 two-dimensional toric Fano varieties. The labels over the external points give the height of the point in the corresponding 3d toric diagrams which we shall introduce later on.

in term of the toric divisors D_k for the external points only (using $D_0 = -\sum_k D_k$ in homology, with $D_0 \cong B_4$ the divisor from the internal point), and these naturally restrict to divisors D_k on B_4 . The resulting collection

$$\mathcal{E} = \{E_1, \dots, E_G\} \tag{2.40}$$

is also a tilting collection for $D(\text{Coh } B_4)$, the B-brane category on B_4 [56].⁹

⁹See Proposition C.1. of that paper; we thank the authors of [56] for bringing our attention to their result. (Remark that it can also be checked explicitly (using the *SAGE* [57] package) that in all

The fractional branes we are looking for are related to the line bundles (2.40), but they are somewhat more complicated objects in $D(\text{Coh } B_4)$. A generic object in the B-brane category is a chain complex of sheaves,

$$\mathbf{E} = \cdots \rightarrow E_{(-2)} \rightarrow E_{(-1)} \rightarrow E_{(0)} \rightarrow E_{(1)} \rightarrow \cdots . \quad (2.41)$$

In this work we will only be concerned with the *charges* of the branes, so that we can ignore the subtleties of the derived category formalism. The charge of a B-brane (2.41) is a K-theory class [58], but for our purpose it suffices to define the charge as the Chern character

$$ch(\mathbf{E}) = \sum_n (-1)^n ch(E_{(n)}) , \quad (2.42)$$

where $ch(E_{(n)})$ are the Chern characters of the individual sheaves. To discuss the most general brane charges we consider the full resolution $\pi : \tilde{B}_4 \rightarrow B_4$, which is what the B-model probes. Let us denote

$$\mathcal{C}_\alpha \in H^2(\tilde{B}_4, \mathbb{Z}), \quad \alpha = 1, \dots, m, \quad \mathcal{C}_\alpha \cdot \mathcal{C}_\beta = \mathcal{I}_{\alpha\beta} . \quad (2.43)$$

a primitive basis of 2-cycles, with \mathcal{I} the intersection matrix. We will generally choose the 2-cycles \mathcal{C}_α to coincide with m of the $m+2$ toric divisors: $\mathcal{C}_\alpha \cong D_\alpha$ with $\{D_\alpha\} \subset \{D_k\}$.

There are $G \equiv m+2$ charges for the compactly supported branes (branes wrapping B_4 , \mathcal{C}_α or a point), and we denote the Chern character (2.42) of a generic B-brane \mathbf{E} by the covector

$$\mathbf{Q}_{\text{branes}}(\mathbf{E}) = ch(\mathbf{E}) = (rk(\mathbf{E}), c_1(\mathbf{E}), ch_2(\mathbf{E})) . \quad (2.44)$$

A natural pairing on the space of charges is given by the Euler character¹⁰

$$\chi(\mathbf{E}_i, \mathbf{E}_j) \equiv \sum_q (-1)^q \dim \text{Ext}^q(\mathbf{E}_i, \mathbf{E}_j) , \quad (2.45)$$

which can be computed by the Riemann-Roch theorem:

$$\chi(\mathbf{E}_i, \mathbf{E}_j) = \int_{\tilde{B}_4} ch(\mathbf{E}_i^*) ch(\mathbf{E}_j) Td(\tilde{B}_4) . \quad (2.46)$$

We can conveniently rewrite this in matrix notation,

$$\chi(\mathbf{E}_i, \mathbf{E}_j) = ch(\mathbf{E}_i) \mathbf{X}_{\tilde{B}_4} ch(\mathbf{E}_j)^T , \quad \text{with} \quad \mathbf{X}_{\tilde{B}_4} = \begin{pmatrix} 1 & \frac{1}{2}c_1 & 1 \\ -\frac{1}{2}c_1 & -\mathcal{I} & 0 \\ 1 & 0 & 0 \end{pmatrix} , \quad (2.47)$$

where \mathcal{I} is defined in (2.43) and $c_1 = c_1(\tilde{B}_4)$; thus the matrix $\mathbf{X}_{\tilde{B}_4}$ is intrinsic to the geometry we consider. Given the tilting collection (2.40) on B_4 , we define

$$S_{ij} \equiv \chi(\mathbf{E}_i, \mathbf{E}_j) = \dim \text{Hom}(\mathbf{E}_i, \mathbf{E}_j) . \quad (2.48)$$

the examples we studied $H^n(\tilde{B}_4, \mathbf{E}_j \otimes \mathbf{E}_i^*) = 0$ for $n > 0$. We thank Noppadol Mekareeya for helping us with that computation.)

¹⁰We refer to [59] for a physical introduction to Ext groups. For the purpose of this paper one could as well take (2.46) as the primary definition.

The matrix element S_{ij} is the number of independent open paths from j to i in the pseudo-Beilinson quiver \mathcal{Q}_{B_4} . It is equal to the number of global sections of the line bundle $\mathbf{E}_j \otimes \mathbf{E}_i^*$,

$$S_{ij} = \dim H^0(\tilde{B}_4, \mathbf{E}_j \otimes \mathbf{E}_i^*), \quad (2.49)$$

which is easily computed by toric methods. The fractional branes form a collection

$$\mathcal{E}^\vee = \{\mathbf{E}_1^\vee, \dots, \mathbf{E}_G^\vee\} \quad (2.50)$$

which is dual to (2.40) with respect to the Euler character:

$$\chi(\mathbf{E}_i, \mathbf{E}_j^\vee) = \delta_{ij}. \quad (2.51)$$

This also implies $\chi(\mathbf{E}_j^\vee, \mathbf{E}_i^\vee) = S_{ij}^{-1}$. We introduce the two $G \times G$ matrices

$$Q = \begin{pmatrix} ch(\mathbf{E}_1) \\ \vdots \\ ch(\mathbf{E}_G) \end{pmatrix}, \quad Q^\vee = \begin{pmatrix} ch(\mathbf{E}_1^\vee) \\ \vdots \\ ch(\mathbf{E}_G^\vee) \end{pmatrix}. \quad (2.52)$$

whose rows are the charges of the B-branes in \mathcal{E} and \mathcal{E}^\vee , respectively. In term of these charge matrices we can rewrite (2.51) and (2.48) in a compact way:

$$Q^{\vee T} = (\mathbf{X}_{\tilde{B}_4})^{-1} Q^{-1}, \quad S = Q \mathbf{X}_{\tilde{B}_4} Q^T. \quad (2.53)$$

The antisymmetric adjacency matrix A of the complete quiver \mathcal{Q} can be found from S , according to

$$A \equiv S^{-1T} - S^{-1}. \quad (2.54)$$

Remark that we did not need to give a concrete definition of the fractional branes \mathbf{E}^\vee in order to extract their brane charges Q^\vee . Instead we will just conjecture that there exist objects in $D(\text{Coh } B_4)$ with the right properties.¹¹ We call the matrix Q^\vee a *dictionary*. It allows to translate between the brane charge basis (2.44) and the fractional brane basis, namely the quiver ranks:

$$\mathbf{Q}_{\text{branes}} = \mathbf{N} Q^\vee. \quad (2.55)$$

Example. Consider the total resolution $P\tilde{d}P_2$ of PdP_2 , whose toric fan looks like the triangulation $T_\Gamma^{(1)}$ from Figure 2. We take our homology basis (2.43) to be

$$\{\mathcal{C}_\alpha\} \cong \{D_3, D_4, D_{(1,0)}\}, \quad \mathcal{I} = \begin{pmatrix} -1 & 1 & 1 \\ 1 & -1 & 0 \\ 1 & 0 & -2 \end{pmatrix}. \quad (2.56)$$

where the divisors of $P\tilde{d}P_2$ are inherited from the divisors of \tilde{Y} . We have the homology relations $D_1 = 2D_3 + D_4 + D_{(1,0)}$ and $D_2 = D_3 + D_4$; we also have the relation

¹¹If \mathcal{E}^\vee is a complete strongly exceptional collection (corresponding to S an upper-triangular matrix), the fractional branes can be obtained from the line bundles \mathbf{E}_i by explicit mutations [60].

$D_{(0,0)} = -4D_3 - 3D_4 - 2D_{(0,0)}$ in \tilde{Y} . The tilting collection (2.40) for $P\tilde{d}P_2$ is directly obtained from (2.38) by using these homology relations. Let us focus on the first Kähler chamber for definiteness. We have:

$$\mathcal{E}_{\{p_5, p_7\}} = \{\mathcal{O}(0, 0, 0), \mathcal{O}(-2, -2, -1), \mathcal{O}(-3, -3, -1), \mathcal{O}(-3, -2, -1), \mathcal{O}(-1, -1, 0)\}$$

in the basis (2.56). The charge matrix for these line bundles is

$$Q = \begin{pmatrix} 1 & 0 & 0 & 0 & 0 \\ 1 & -2 & -2 & -1 & 1 \\ 1 & -3 & -3 & -1 & 2 \\ 1 & -3 & -2 & -1 & \frac{3}{2} \\ 1 & -1 & -1 & 0 & 0 \end{pmatrix}, \quad (2.57)$$

and we have

$$\mathbf{X}_{\tilde{B}_4} = \begin{pmatrix} 1 & \frac{1}{2} & \frac{1}{2} & 0 & 1 \\ -\frac{1}{2} & 1 & -1 & -1 & 0 \\ \frac{1}{2} & -1 & 1 & 0 & 0 \\ 0 & -1 & 0 & 2 & 0 \\ 1 & 0 & 0 & 0 & 0 \end{pmatrix}, \quad S = \begin{pmatrix} 1 & 0 & 0 & 0 & 0 \\ 4 & 1 & 0 & 0 & 2 \\ 6 & 2 & 1 & 1 & 4 \\ 5 & 1 & 0 & 1 & 3 \\ 2 & 0 & 0 & 0 & 1 \end{pmatrix}, \quad (2.58)$$

from which we can compute the dictionary $Q^\vee = Q^{-1T} \mathbf{X}_{\tilde{B}_4}^{-1T}$. The actual dictionary we will use will contain some additional half-integer shift of the charges due to the Freed-Witten anomaly [61].

2.6 Kähler moduli space and quiver locus

Most B-branes on \tilde{Y} are not physical D-branes, because they do not lift to half-BPS objects in physical string theory. The D-brane spectrum at any given value of the Kähler moduli is given by the spectrum of Π -stable B-branes [62]. In the regime of interest to us, Π -stability reduces to θ -stability of quiver representations [62, 63].

To any compactly supported D-brane \mathbf{E}^\vee on Y one associates a complex central charge $Z(\mathbf{E}^\vee)$, which determines which half of the supersymmetry of the closed string background it preserves. Two BPS D-branes \mathbf{E}_1^\vee and \mathbf{E}_2^\vee are mutually BPS if and only if their central charges are aligned,

$$\arg(Z(\mathbf{E}_1^\vee)) = \arg(Z(\mathbf{E}_2^\vee)). \quad (2.59)$$

The central charge depends on the closed string Kähler moduli. Our space \tilde{Y} has m complexified Kähler moduli, corresponding to

$$t_\alpha \equiv \int_{\mathcal{C}_\alpha} (B + iJ) \equiv b_\alpha + i\chi_\alpha, \quad (2.60)$$

where the 2-cycles \mathcal{C}_α , $\alpha = 1, \dots, m$, were defined in (2.43). The *quiver locus* \mathcal{M}_Q is the locus in Kähler moduli space \mathcal{M}_K where the $G = m + 2$ fractional branes (2.50)

are mutually BPS [64]. It has codimension $m + 1$ in \mathcal{M}_K . Since the fractional branes are mutually BPS at the tip of the cone, we expect the quiver locus to be located at

$$\chi_\alpha = 0. \quad (2.61)$$

There is one more constraint on the m B-field periods b_α , which we denote by $\chi_0 = 0$. Let us define a vector

$$\boldsymbol{\chi} \equiv (\chi_0, \chi_\alpha, 0), \quad (2.62)$$

corresponding to the directions transverse to \mathcal{M}_Q in \mathcal{M}_K . As long as the central charges $Z(\mathbf{E}_i^\vee)$ are almost aligned, the quiver \mathcal{Q} is a good description of D-brane physics. The closed string modes (2.62) couple to the fractional branes as FI parameters $\boldsymbol{\xi} = (\xi_i)$ [36], and stability of D-branes corresponds to θ -stability of quiver representations. One can show that the FI parameters are related to the Kähler moduli (2.62) by the dictionary Q^\vee :

$$\boldsymbol{\xi} = Q^\vee \boldsymbol{\chi}. \quad (2.63)$$

The $m - 1$ directions along the quiver locus correspond to marginal gauge couplings for the so-called “non-anomalous” fractional branes, which are D4-branes wrapped on 2-cycles in \tilde{B}_4 dual to non-compact divisors in \tilde{Y} . In the quiver regime, the central charges of the fractional branes are given by

$$Z(\mathbf{E}_i^\vee) \approx \frac{1}{g_i^2} + i\xi_i. \quad (2.64)$$

Whenever the inverse squared gauge coupling of a non-anomalous fractional brane becomes negative, one should change basis of fractional branes, leading to a Seiberg dual quiver (which might be a self-similar quiver, or a new quiver in a different “toric phase”).

2.7 Dictionaries, monodromies and Freed-Witten anomaly

A quiver with its FI parameters $\boldsymbol{\xi}$ describes the fractional branes near a particular point in the quiver locus, probing \mathcal{M}_K in directions transverse to \mathcal{M}_Q . We have seen how the quiver can probe numerous Kähler chambers $\{p_r^{EI}, p_0\}$, related to the multiplicities of points in the toric diagram. Going from one Kähler chamber to the next one in FI parameter space corresponds to crossing a wall of marginal stability in \mathcal{M}_K (a codimension 1 wall where two fractional branes become mutually BPS).

To each of these Kähler chamber we associated a dictionary Q^\vee . However, there are some ambiguities to this procedure, which corresponds physically to the fact that the very concept of brane charge is not well defined on Kähler moduli space, but only on its universal cover (its Teichmüller space).

The central charge of a generic D-brane \mathbf{E} with brane charge (2.44) can be written

$$Z(\mathbf{E}) = \mathbf{Q}_{\text{brane}} \cdot \boldsymbol{\Pi} = r(\mathbf{E}) \Pi_6 + c_1^\alpha(\mathbf{E}^\vee) \Pi_{4,\alpha} + ch_2(\mathbf{E}^\vee) \Pi_2, \quad (2.65)$$

where Π_4 , $\Pi_{2,\alpha}$ and Π_0 are so-called *periods* associated to the states with Chern characters $(1, 0, 0)$, $(0, \delta_\beta^\alpha, 0)$ and $(0, 0, 1)$, respectively. These periods are not single valued functions on \mathcal{M}_K , but instead suffer from *monodromies* around various singular loci. On the other hand the central charge of any physical state is invariant under such monodromies. Denoting by M the monodromy matrix acting on the periods, there is a corresponding action on the brane charges:

$$\mathbf{\Pi} \rightarrow M\mathbf{\Pi}, \quad \mathbf{Q}_{\text{brane}} \rightarrow \mathbf{Q}_{\text{brane}} M^{-1}. \quad (2.66)$$

The best understood monodromies are the monodromies around the large volume limit in \mathcal{M}_K . At large volume, up to instanton corrections to Π_6 , the periods are given by

$$\begin{aligned} \Pi_6 &\simeq \frac{1}{2} \int_{\tilde{B}_4} (B + iJ)^2 + \frac{1}{24} \chi(\tilde{B}_4) \\ \Pi_{4,\alpha} &= t_\alpha \\ \Pi_2 &= 1. \end{aligned} \quad (2.67)$$

The large volume monodromies (LVM) corresponds to the shift of the B-field by some cohomology class in $H^2(\tilde{B}_4)$,

$$B \rightarrow B + \sum_{\alpha} m_{\alpha} [D_{\alpha}], \quad (2.68)$$

for $m_{\alpha} \in \mathbb{Z}$. Its action on the periods $\mathbf{\Pi} = (\Pi_6, \Pi_{4,\alpha}, \Pi_2)$ is given by

$$M_{\infty}(\mathbf{m}) = \begin{pmatrix} 1 & \mathbf{m} & \frac{1}{2} \mathbf{m} \mathcal{I} \mathbf{m} \\ 0 & \mathbf{1} & \mathcal{I} \mathbf{m} \\ 0 & 0 & 1 \end{pmatrix} \quad (2.69)$$

with $\mathbf{m} = (m_{\alpha})$ and \mathcal{I} the intersection matrix. In the algorithm described above to find Q^{\vee} , a different choice of “first node” to construct the line bundles (2.40) corresponds to such a large volume monodromy. Fixing the order of the nodes once and for all, we are still free to perform any LVM, generating new dictionaries which are valid for different values of the background B-field. A generic dictionary takes the form

$$Q^{\vee}[KC, \mathbf{m}] = Q^{\vee}[KC, \mathbf{0}] M_{\infty}(\mathbf{m})^{-1}, \quad (2.70)$$

with $KC \cong \{p_r^{EI}, p_0\}$ a Kähler chamber. We have to fix some convention on what we call $Q^{\vee}[KC, \mathbf{0}]$. In every example studied in this paper we choose convenient conventions which are kept implicit. Instead we state the actual dictionary Q^{\vee} whenever needed.

When the manifold B_4 is not spin, we cannot wrap a D6 over it without turning as well $F = 1/2$ units of worldvolume flux¹² [61], and this results in half-integral shift

¹²More precisely we have to introduce some (ill-defined) line bundle \sqrt{L} such that $\sqrt{TB_4} \otimes \sqrt{L}$ is a well defined spin^c bundle. Heuristically $F = \frac{1}{2}$ is the first Chern class of \sqrt{L} .

of the Page charges — see Appendix A.4. To take this Freed-Witten anomaly into account in our dictionaries, we need to shift them according to

$$Q^\vee[KC, \mathbf{0}] \rightarrow Q^\vee[KC, \mathbf{0}] M_\infty\left(\frac{\mathbf{s}}{2}\right), \quad (2.71)$$

where the Freed-Witten anomaly parameters $\mathbf{s} = (s_\alpha)$ are defined in (A.36).

There are further monodromies apart from the LVM's, generically called quantum monodromies because they arise in the region of \mathcal{M}_K which suffers large α' corrections. We will have little to say about them, but we should keep in mind that there can exist more dictionaries than those of (2.70). In section 7 we will encounter an instance of such extra monodromies which are related to Seiberg duality of quivers [60, 33].

3. Reduction of M-theory on $\mathbb{R}^{1,2} \times CY_4$ to type IIA

In this section we describe the first step of the stringy derivation of the theories on M2 branes probing the toric CY_4 cone over $Y^{p,q}(B_4)$, with B_4 a 2-complex-dimensional toric Fano surface, namely the reduction of the M-theory background $\mathbb{R}^{1,2} \times C(Y^{p,q}(B_4))$ to a type IIA background. In the next section this type IIA background will be used to deduce the field theory on D2-brane probes: its low energy limit is the M2-brane theory we are interested in. We will streamline the presentation, referring the reader to [14] for more background on this kind of computations. We start by discussing aspects of the reduction for general toric CY_4 cones, before applying it to the $C(Y^{p,q}(B_4))$ geometries that are the focus of this paper.

3.1 Generalities

Generalising the idea of [11], the approach of [14] was to Kaluza-Klein reduce the M-theory background along a wisely chosen $U(1)_M$ circle action in the CY_4 , so that the resulting type IIA background is a fibration¹³ of a resolved CY_3 \tilde{Y} over a real line \mathbb{R} parametrised by r_0 , with RR 2-form fluxes and (anti-)D6-branes [14]. The CY_3 fibre over r_0 is the Kähler quotient $\tilde{Y}(r_0) \equiv CY_4 //_{r_0} U(1)_M$. The Kähler volumes $\chi_\alpha(r_0) = \int_{\mathcal{C}_\alpha} J$ of its 2-cycles \mathcal{C}_α are piecewise linear functions of r_0 . The curvature of the $U(1)_M$ fibration yields RR F_2 field strength, whose fluxes $\int_{\mathcal{C}_\alpha} F_2 = \chi'_\alpha(r_0)$ are piecewise constant in r_0 . Discontinuities in these fluxes are due to (anti-)D6-branes, which descend from fixed point loci of the circle action (KK monopoles).

One can use toric methods to derive these data, working with the abelian GLSMs whose vacuum moduli spaces are the toric CY_4 and CY_3 cones. It will be crucial to demand that the GLSM for $CY_4 //_{r_0} U(1)_M$ is in a geometric phase for any r_0 . This gives meaning to the geometric description of the previous paragraph and is a necessary condition for the corresponding 2-brane theory to be a toric quiver gauge theory. We expect that it will also be sufficient if the quiver gauge theory is extended to include

¹³More correctly this is a foliation rather than a fibration because, as we will explain, the topology of the “fibre” can degenerate and vary as we move along the base.

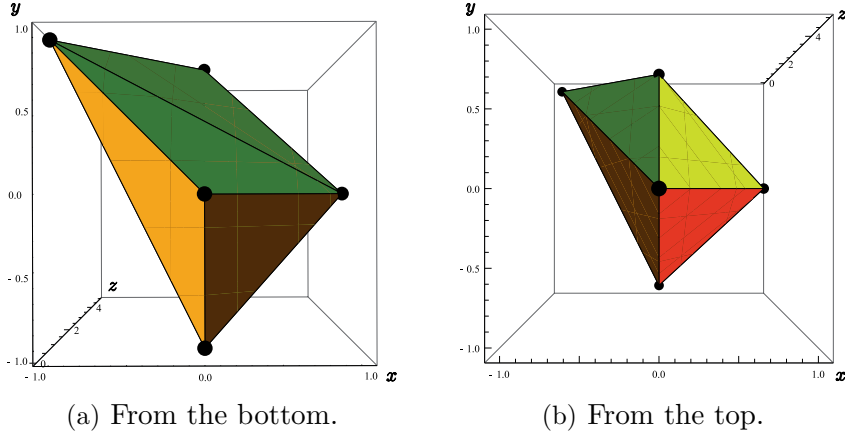


Figure 5: The 3d toric diagram for the cone over $Y^{p, q_1, q_2}(dP_1)$, with $(q_1, q_2, p) = (2, 1, 5)$. Looking at the toric diagram from the top or the bottom, we see the two different triangulations of the 2d toric diagram of $C_C(dP_1)$.

(anti)fundamental matter coming from massless open string modes stretching between D2-branes and D6-branes along *noncompact* divisors, along the lines of [13, 12].

The previous restriction is most easily stated in terms of toric diagrams. We start with the toric diagram of the CY_4 , a 3d convex lattice polytope Γ_3 , and associate by convention the $U(1)_M$ symmetry with the vertical direction in \mathbb{Z}^3 . The 2d toric diagram Γ of $Y = CY_4//U(1)_M$ is obtained by vertical projection of Γ_3 . Each pair of adjacent vertically aligned points belonging to Γ_3 leads to a (anti-)D6-brane embedded along the toric divisor of the CY_3 associated to the point in Γ that the pair of points projects to. Finally, the RR 2-form is determined by the vertical coordinates of the points of the 3d toric diagram, as we will see explicitly in section 3.4.

We can initially focus on CY_4 metric cones: then the D6-branes wrap toric divisors in the conical $\tilde{Y}(0) = Y$ and the GLSM for $\tilde{Y}(r_0) = CY_4//_{r_0}U(1)_M$ is specified by two rays in its FI parameter space, for $r_0 < 0$ and $r_0 > 0$ respectively. Up to an overall dilatation controlled by $|r_0|$, we thus have two toric crepant (partial or complete) resolutions \tilde{Y}_- and \tilde{Y}_+ of the singular CY_3 $Y = \tilde{Y}(0)$ which lies over $r_0 = 0$. It turns out that the triangulated 2d toric diagram Γ_{\mp} for \tilde{Y}_{\mp} can be found by looking at the 3d toric diagram of the CY_4 , viewed as a solid lattice polytope, from below ($-$) and above ($+$) respectively — see Figure 5 for an example. Consider $r_0 < 0$: the CY_3 GLSM is in a geometric phase for all $r_0 < 0$ iff Γ_- contains all its lattice points, possibly joined by segments determining a partial or complete (simplicial) triangulation. Similarly for $r_0 > 0$. Phrased in terms of the original CY_4 , the necessary and sufficient condition is that the intersection of its toric diagram Γ_3 with the set of lattice vertical lines $\mathbb{Z}^2 \times \mathbb{R}$ is a union of vertical segments joining points in \mathbb{Z}^3 . Each such vertical segment has then integer length $h \geq 0$ and leads to h D6 on the associated toric divisor in $\tilde{Y}(0)$. Remark that since Γ_3 is a convex polytope, if the CY_3 Y obtained upon reduction has compact toric divisors then a sufficient number of D6-branes must wrap each of those

compact divisors to ensure that the CY_3 GLSM is in a geometric phase for any r_0 .

In the following we will restrict our attention to families of toric CY_4 such that the toric CY_3 \tilde{Y} obtained upon KK reduction to IIA, in addition to being in a geometric phase for all values of r_0 , has a single compact toric divisor and no D6-branes along noncompact toric divisors. The former requirement restricts us to CY_3 Y which are total spaces of canonical bundles over one of the 16 toric Fano surfaces introduced in section 2.5; the latter guarantees that the resulting 2-brane theory is a quiver gauge theory with only bifundamental matter. The extension of the stringy derivation to M2-brane theories for the entire class of toric CY_4 geometries that reduce to geometric CY_3 fibrations with both compact and noncompact D6-branes and RR F_2 fluxes is an interesting challenge that we leave for future investigation.

3.2 Cones over toric $Y^{p,q}(B_4)$ Sasaki-Einstein 7-folds

Let us then consider a toric CY_4 cone whose 3d toric diagram contains a single vertical line of $p \geq 1$ points $s_a = (0, 0, a)$, $a = 1, \dots, p$, lying above the point $s_0 = (0, 0, 0)$ in the toric diagram. In addition there are $m + 2$ points $t_i = (x_i, y_i, z_i)$, $i = 1, 2, \dots, m + 2$, having different horizontal coordinates (x_i, y_i) , one for each generator of the toric fan of one of the 16 2-complex-dimensional toric Fano surfaces B_4 of Fig. 4, with $H_2(B_4, \mathbb{Z}) = \mathbb{Z}^m$. $\{s_0, \dots, s_p, t_1, \dots, t_{m+2}\}$ are all the lattice points belonging to the polytope Γ_3 . The vertical projection of Γ_3 is the toric diagram Γ of the CY_3 Y , the total space of $\mathcal{O}_{B_4}(K)$, which is also the toric fan of B_4 .

To ensure that the CY_3 GLSM is always in a geometric phase and that there are no D6 along noncompact divisors, we need *a)* Γ_3 to have no vertical faces nor edges and *b)* s_0 and s_p to be external points. *a)* requires that each external point $v_i = (x_i, y_i) \in \Gamma$ lifts to a single point $t_i = (x_i, y_i, z_i) \in \Gamma_3$. For singular B_4 it also requires that the lattice points belonging to an external edge of Γ lift to aligned lattice points in Γ_3 , otherwise there would be a vertical face. This imposes some equalities between the heights z_i of lattice points belonging to the same external edge of Γ . On the other hand *b)* imposes a number of inequalities among linear combinations of the z_i and 0 or p , as we will see explicitly in examples.

Using the subgroup of the $SL(3, \mathbb{Z})$ acting on Γ_3 that leaves Γ and s_0 invariant, we are free to set the z_i of two lattice points $v_1 = (x_1, y_1)$ and $v_2 = (x_2, y_2)$ of Γ to 0, as long as v_1 , v_2 and $(0, 0)$ form a triangle of minimal area. We then call $z_{i+2} = q_i$ the vertical coordinates of the remaining m external lattice points in Γ . We made one such choice for each of the 16 toric Fano surfaces: in Fig. 4 we show next to each point v_i the assignment of q_i , $i = 1, \dots, m$ which fulfils requirement *a)*. We will stick to these conventions in section 5. For each toric Fano B_4 , we thus have a $(v - 1)$ -parameter family of toric CY_4 cones labelled by p and the set of independent $\mathbf{q} = (q_i)$, where v is the number of vertices of Γ . Generalising the nomenclature of [26], we call $Y^{p,\mathbf{q}}(B_4)$ the SE_7 base of the CY_4 cone.

We still need to impose that s_0 and s_p are external in Γ_3 . We will assume that this has been done in the remainder of this section, postponing to section 5 the list

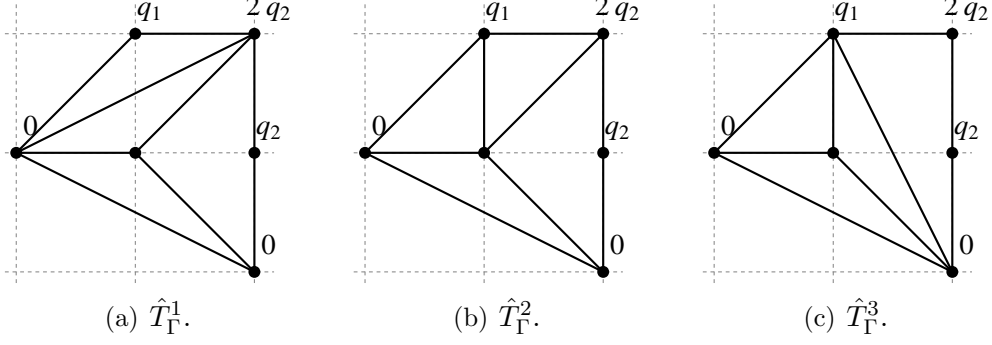


Figure 6: The three partial triangulations \hat{T}_Γ^i , $i = 1, 2, 3$, of the toric diagram of PdP_2 relevant for the reduction of $C(Y^{p, q_1, q_2}(PdP_2))$.

of inequalities that this imposes on the geometric parameters (p, \mathbf{q}) for each B_4 . Here we consider the illustrative example of $C(Y^{p, q_1, q_2}(PdP_2))$, which has a non-isolated singularity. The relevant partial triangulations of the toric diagram are shown in Fig. 6. We wrote the z_i coordinates of external points, fulfilling condition *a*) above. We still need to impose that s_0 and s_p are external points in Γ_3 : that restricts q_1 and q_2 by the inequalities

$$0 \leq \frac{q_1}{3}, \frac{q_2}{2} \leq p. \quad (3.1)$$

When one of the inequalities is saturated, s_0 or s_p lies inside an external face, otherwise they are strictly external. We can further refine the class of geometries into subclasses, depending on which partial triangulation T_{Γ_\pm} of Γ_\pm results from the reduction:

$$T_{\Gamma_-} = \begin{cases} \hat{T}_\Gamma^1 & \text{if } q_1 > 2q_2 \\ \hat{T}_\Gamma^2 & \text{if } q_2 < q_1 < 2q_2 \\ \hat{T}_\Gamma^3 & \text{if } q_1 < q_2 \end{cases}, \quad T_{\Gamma_+} = \begin{cases} \hat{T}_\Gamma^1 & \text{if } q_1 < 2q_2 - p \\ \hat{T}_\Gamma^2 & \text{if } 2q_2 - p < q_1 < q_2 + p \\ \hat{T}_\Gamma^3 & \text{if } q_1 > q_2 + p \end{cases}. \quad (3.2)$$

When one of the above inequalities becomes an equality the triangulation of Γ has fewer edges. The choices for T_{Γ_-} and T_{Γ_+} are interchanged by the \mathbb{Z}_2 symmetry $(q_1, q_2) \mapsto (3p - q_1, 2p - q_2)$ which identifies $C(Y^{p, q_1, q_2}(PdP_2)) \cong C(Y^{p, 3p - q_1, 2p - q_2}(PdP_2))$ and sends $r_0 \mapsto -r_0$. In total there are 7 possibilities

$$(T_{\Gamma_-}, T_{\Gamma_+}) = \begin{cases} (\hat{T}_\Gamma^1, \hat{T}_\Gamma^2) & \text{if } 2q_2 < q_1 < q_2 + p \\ (\hat{T}_\Gamma^1, \hat{T}_\Gamma^3) & \text{if } q_1 > q_2 + p, 2q_2 \\ (\hat{T}_\Gamma^2, \hat{T}_\Gamma^3) & \text{if } q_2 + p < q_1 < 2q_2 \\ (\hat{T}_\Gamma^2, \hat{T}_\Gamma^2) & \text{if } q_2, 2q_2 - p < q_1 < q_2 + p, 2q_2 \\ (\hat{T}_\Gamma^3, \hat{T}_\Gamma^2) & \text{if } 2q_2 - p < q_1 < q_2 \\ (\hat{T}_\Gamma^3, \hat{T}_\Gamma^1) & \text{if } q_1 < 2q_2 - p, q_2 \\ (\hat{T}_\Gamma^2, \hat{T}_\Gamma^1) & \text{if } q_2 < q_1 < 2q_2 - p \end{cases} \quad (3.3)$$

the last 3 of which are equivalent to the first 3 under the \mathbb{Z}_2 identification above.

3.3 GLSM for the CY_3 fibres in type IIA

The toric CY_4 , including all its toric crepant resolutions, can be realised as the moduli space of a supersymmetric abelian gauged linear sigma model for specific choices of the associated FI parameters. In our examples the GLSM for the CY_4 can be written as follows (excluding the last row, which appears for future reference):

$$\begin{array}{c|cccccccccc|c}
 CY_4 & t_1 & \cdots & t_{m+2} & s_0 & s_1 & s_2 & \cdots & s_{p-2} & s_{p-1} & s_p & \text{FI} \\
 \hline
 & Q_1^\alpha & \cdots & Q_{m+2}^\alpha & Q_{(s_0)}^\alpha & Q_{(s_1)}^\alpha & 0 & \cdots & 0 & 0 & 0 & \xi_\alpha^c \\
 & 0 & \cdots & 0 & 1 & -2 & 1 & \cdots & 0 & 0 & 0 & \xi_2 \\
 & 0 & \cdots & 0 & 0 & 1 & -2 & \cdots & 0 & 0 & 0 & \xi_3 \\
 & \vdots & \ddots & \vdots & \vdots & \vdots & \vdots & \ddots & \vdots & \vdots & \vdots & \vdots \\
 & 0 & \cdots & 0 & 0 & 0 & 0 & \cdots & -2 & 1 & 0 & \xi_{p-1} \\
 & 0 & \cdots & 0 & 0 & 0 & 0 & \cdots & 1 & -2 & 1 & \xi_p \\
 \hline
 U(1)_M & 0 & \cdots & 0 & 1 & -1 & 0 & \cdots & 0 & 0 & 0 & r_0
 \end{array} \tag{3.4}$$

The first row denotes the fields of the GLSM, one for each point in the 3d toric diagram. The second row with $\alpha = 1, \dots, m$ denotes their charges under a $U(1)^m$ subgroup. The subset $\{t_1, \dots, t_{m+2}\}$ with $U(1)^m$ charges Q_i^α describes the compact Fano surface B_4 . The following $p - 1$ lines describe the GLSM for a $\mathbb{C}^2/\mathbb{Z}_2$ singularity, fibred over B_4 . The charges $Q_{(s_0)}^\alpha$ and $Q_{(s_1)}^\alpha$ determine how the $\mathbb{C}^2/\mathbb{Z}_p$ fibre is twisted over the base B_4 . The last column lists FI parameters of the GLSM which control resolutions of the geometry. $\xi_{2, \dots, p}$ have to be non-negative to keep the GLSM of the CY_4 in a geometric phase. Similar inequalities involve linear combinations of ξ_α^c .

The last row in (3.4) specifies our choice of $U(1)_M$ symmetry acting on the M-theory circle, visualised as the vertical direction in the 3d toric diagram of CY_4 [13]. Including the last row in (3.4) yields a GLSM for the Kähler quotient $\tilde{Y}(r_0) = CY_4 //_{r_0} U(1)_M$. The type IIA geometry obtained by KK reduction along the $U(1)_M$ circle involves a fibration of this $\tilde{Y}(r_0)$ over the real line parametrised by the moment map r_0 [11]. To obtain the precise form of the fibration, we define

$$\zeta_0 = -\infty, \quad \zeta_1 = 0, \quad \zeta_a = \sum_{b=2}^a \xi_b \quad (a = 2, \dots, p), \quad \zeta_{p+1} = +\infty \tag{3.5}$$

and rewrite the GLSM for $CY_4 //_{r_0} U(1)_M$ in (3.4), including the last line, as

$$\begin{array}{c|cccccccccc|c}
 CY_3 & t_1 & \cdots & t_{m+2} & s_0 & s_1 & s_2 & \cdots & s_{p-2} & s_{p-1} & s_p & \text{FI} \\
 \hline
 & Q_1^\alpha & \cdots & Q_{m+2}^\alpha & Q_{(s_0)}^\alpha & Q_{(s_1)}^\alpha & 0 & \cdots & 0 & 0 & 0 & \xi_\alpha^c \\
 & 0 & \cdots & 0 & 1 & -1 & 0 & \cdots & 0 & 0 & 0 & r_0 - \zeta_1 \\
 & 0 & \cdots & 0 & 0 & 1 & -1 & \cdots & 0 & 0 & 0 & r_0 - \zeta_2 \\
 & 0 & \cdots & 0 & 0 & 0 & 1 & \cdots & 0 & 0 & 0 & r_0 - \zeta_3 \\
 & \vdots & \ddots & \vdots & \vdots & \vdots & \vdots & \ddots & \vdots & \vdots & \vdots & \vdots \\
 & 0 & \cdots & 0 & 0 & 0 & 0 & \cdots & 1 & -1 & 0 & r_0 - \zeta_{p-1} \\
 & 0 & \cdots & 0 & 0 & 0 & 0 & \cdots & 0 & 1 & -1 & r_0 - \zeta_p
 \end{array} \tag{3.6}$$

This is a redundant description of $\tilde{Y}(r_0)$:¹⁴ all but one of the $s_{a=0,\dots,p}$ can be eliminated in favour of a remaining unconstrained variable, which depends on the value of r_0 as

$$t_0 = s_a \quad \text{if} \quad \zeta_a \leq r_0 \leq \zeta_{a+1}. \quad (3.7)$$

We can rewrite the $\tilde{Y}(r_0)$ GLSM in its minimal form

$$\frac{CY_3 \mid t_1 \cdots t_{m+2} \ t_0 \mid \text{FI}}{\mathcal{C}_\alpha \mid Q_1^\alpha \cdots Q_{m+2}^\alpha \ Q_0^\alpha \mid \chi_\alpha(r_0)} \quad (3.8)$$

where

$$Q_0^\alpha \equiv Q_{(s_0)}^\alpha + Q_{(s_1)}^\alpha = - \sum_{i=1}^{m+2} Q_i^\alpha = - \int_{\mathcal{C}_\alpha} c_1(B_4). \quad (3.9)$$

The FI parameters are

$$\chi_\alpha(r_0) = \xi_\alpha^c - \left(\sum_{i=1}^{m+2} z_i Q_i^\alpha \right) (r_0 - \zeta_1) - Q_0^\alpha \sum_{b=1}^p (r_0 - \zeta_b) \Theta(r_0 - \zeta_b), \quad (3.10)$$

with $\Theta(x)$ the Heaviside step function. We used the relation

$$-Q_{(s_1)}^\alpha = \sum_{i=1}^{m+2} z_i Q_i^\alpha \quad (3.11)$$

which follows from the toric diagram. Abusing notation we have identified the m $U(1)$ gauge groups of the GLSM with holomorphic 2-cycles \mathcal{C}_α .

The FI parameters $\chi_\alpha(r_0)$ of the minimal GLSM, which are the Kähler parameters in the fibred $\tilde{Y}(r_0)$ if the GLSM is in a geometric phase (as we impose) and the \mathcal{C}_α are effective curves in the Mori cone, are continuous piecewise linear functions of r_0 with first derivatives jumping by $-Q_0^\alpha$ at $r_0 = \zeta_{a=1,\dots,p}$, where the unconstrained coordinate jumps from s_{a-1} to s_a . This is due to the presence of an anti-D6-brane wrapping the exceptional toric divisor D_0 in $\tilde{Y}(\zeta_a)$.¹⁵ If the CY_4 is conical, that is $\zeta_a = \xi_\alpha^c = 0$ for all a and α , the resolution parameters of $\tilde{Y}(r_0)$ are simply

$$\chi_\alpha(r_0) = \left[- \left(\sum_{i=1}^{m+2} z_i Q_i^\alpha \right) - p Q_0^\alpha \Theta(r_0) \right] r_0. \quad (3.12)$$

¹⁴This redundancy parallels the one encountered in the GLSM for perfect matching variables of section 2.1. Here it is due to the Kähler quotient from the CY_4 to the CY_3 geometry, rather than from the master space \mathcal{Z} to the CY_3 mesonic moduli space of the abelian toric quiver gauge theory.

¹⁵See [14] for the explanation of why the object which is mutually BPS with the D2-brane along the quiver locus is a $\overline{\text{D6}}$ rather than a D6.

3.4 RR 2-form flux and D6-branes

Generically the M-theory circle fibration is nontrivial, so its curvature gives a nonvanishing RR 2-form field strength in type IIA. By the same arguments as in [14], its cohomology class is

$$[F_2] = - \sum_{i=1}^{m+2} z_i [D_i] - \sum_{a=1}^p a [D_{(s_a)}], \quad (3.13)$$

where $[D_i]$ is the cohomology class Poincaré dual of the toric divisor $D_i = \{t_i = 0\}$. This expression is still in terms of the redundant GLSM for the CY_3 . Using the reduced GLSM in (3.8) which minimally describes the resolved CY_3 geometry we find

$$[F_2](r_0) = - \sum_{i=1}^{m+2} z_i [D_i] - [D_0] \sum_{a=1}^p \Theta(r_0 - \zeta_a). \quad (3.14)$$

The flux $[F_2]$ jumps by $-[D_0]$ at $r_0 = \zeta_{a=1, \dots, p}$: the discontinuity is due to a magnetic source for F_2 , a $\overline{D6}$ -brane wrapping the toric divisor D_0 in $\tilde{Y}(\zeta_a)$. The $\mathbb{C}^2/\mathbb{Z}_p$ Kähler parameters ξ_a are the separations in the r_0 direction between p $\overline{D6}$ -branes wrapping D_0 . When the CY_4 is conical, that is $\xi_\alpha^c = \xi_a = 0$, the type IIA background has p coincident $\overline{D6}$ -branes wrapping the collapsed divisor D_0 in $\tilde{Y}(0) = Y$.

The fluxes of F_2 through the holomorphic 2-cycles \mathcal{C}_α of $\tilde{Y}(r_0)$ are

$$\int_{\mathcal{C}_\alpha} F_2(r_0) = - \sum_i z_i Q_i^\alpha - Q_0^\alpha \sum_{a=1}^p \Theta(r_0 - \zeta_a) = \chi'_\alpha(r_0), \quad (3.15)$$

where recall that $\sum_i z_i Q_i^\alpha = -Q_{(s_1)}^\alpha$. The equality between 2-form fluxes and derivatives of Kähler parameters is a consequence of supersymmetry. In the conical case

$$\int_{\mathcal{C}_\alpha} F_2(r_0) = - \sum_i z_i Q_i^\alpha - p Q_0^\alpha \Theta(r_0). \quad (3.16)$$

3.5 Torsion G_4 and generic type IIA background

The Sasaki-Einstein seven-manifold $Y^{p,q}(B_4)$ has a rather interesting fourth cohomology group which is finite:

$$H^4(Y^{p,q}(B_4), \mathbb{Z}) = \Gamma, \quad (3.17)$$

with Γ given in (A.23) in the Appendix. In M-theory, we can turn on discrete torsion G_4 flux for any element of Γ . Equivalently we can wrap an M5-brane on the Poincaré dual 3-cycle, known as “fractional M2-brane” [65]. This gives rise to a large family of $AdS_4 \times Y^{p,q}(B_4)$ backgrounds which are otherwise undistinguishable. Moving in Γ corresponds to changing the ranks and Chern-Simons levels of the dual Chern-Simons quiver theory [65, 14]. In Appendix A we collect some results on the topology of $Y^{p,q}(B_4)$ and of the 6-manifold M_6 (an S^2 bundle over B_4) which appears in the type IIA limit of the AdS_4/CFT_3 correspondence, in the type IIA background $AdS_4 \times_w M_6$.

Torsion G_4 flux corresponds to quantised D4-brane Page charges in type IIA, which results in a dynamical quantization of the background B-field [66, 14]. In the conical

setup discussed here, we also have explicit D4-branes wrapped on vanishing 2-cycles of Y at $r_0 = 0$. This type IIA background is characterised by background fluxes measured at $r_0 < 0$ and $r_0 > 0$, which we denote

$$\mathbf{Q}_{\text{flux},\pm} \equiv (-Q_{4;\pm} \mid Q_{6;\alpha\pm} \mid 0), \quad (3.18)$$

and by the explicit D-brane sources: the p $\overline{\text{D6}}$ -branes discussed in section 3.4, the D4-branes discussed in the Appendix (section A.6), and of course the N D2-branes corresponding to the N M2-branes we seek to describe. We denote the corresponding brane charges by

$$\mathbf{Q}_{\text{source}} \equiv (Q_{D6} \mid (\mathcal{I}^{-1})^{\alpha\beta} Q_{D4;\beta} \mid Q_{D2}). \quad (3.19)$$

The sources account for the jump of the background fluxes between $r_0 < 0$ and $r_0 > 0$, according to

$$Q_{4;+} - Q_{4;-} = \mathcal{I}_{0\alpha} (\mathcal{I}^{-1})^{\alpha\beta} Q_{D4;\beta}, \quad Q_{6;\alpha+} - Q_{6;\alpha-} = \mathcal{I}_{0\alpha} Q_{D6}, \quad (3.20)$$

with $\mathcal{I}_{\alpha\beta}$ defined in (2.43) and $\mathcal{I}_{0\alpha} = Q_0^\alpha$ the intersection number between B_4 and \mathcal{C}_α in Y . In Appendix A we give the explicit form of $\mathbf{Q}_{\text{flux},\pm}$, $\mathbf{Q}_{\text{source}}$ for the $Y^{p,q}(B_4)$ geometry with torsion flux $(n_0, n_\alpha) \in \Gamma$ — see equation (A.46). In the following we will mainly focus on the torsionless case $(n_0, n_\alpha) = (0, 0)$, in which case (A.46) reduces to

$$\begin{aligned} \mathbf{Q}_{\text{flux},-} &= \left(\frac{1}{2} s_\alpha q_\beta \mathcal{I}^{\alpha\beta} \mid -\mathcal{I}_{\alpha\beta} q^\beta \mid 0 \right), \\ \mathbf{Q}_{\text{source}} &= \left(-p \mid -\frac{1}{2} s_\alpha p \mid N - \frac{1}{8} s_\alpha s_\beta \mathcal{I}^{\alpha\beta} p \right). \end{aligned} \quad (3.21)$$

We will discuss the case of torsion flux in a simple example in section 7.

4. From type IIA to CS quiver gauge theories and back

Once the type IIA background is understood, the technology of section 2 can be used to derive the low energy worldvolume theory of M2-branes probing the CY_4 . The type IIA background obtained from a conical CY_4 in M-theory is foliated by CY_3 leaves \tilde{Y} along $\mathbb{R} \cong \{r_0\}$. Algebraically we can characterise it by a choice of *two* partial resolutions of Y , \tilde{Y}_- and \tilde{Y}_+ at $r_0 < 0$ and $r_0 > 0$ respectively. The fluxes on \tilde{Y}_\pm are encoded in the flux vectors (3.18), while the D-branes wrapped on vanishing cycles at $r_0 = 0$ are encoded in the source vector (3.19).

4.1 Translating from IIA background to CS quiver

The IIA background is a resolved toric CY_3 $\tilde{Y}(r_0)$ fibred along $\mathbb{R} \cong \{r_0\}$, as described previously. The fibre $\tilde{Y}(r_0)$ can change to a different partial resolution of Y as we cross $r_0 = 0$, while at $r_0 = 0$ we have the singular cone Y .¹⁶ The Kähler parameters of $\tilde{Y}(r_0)$

¹⁶If the CY_4 has a non-isolated singularity we can have a singular Y on a half-line as well.

are given by

$$\chi_{\pm} = \begin{cases} -\mathbf{Q}_{\text{flux},-}(-r_0) & \text{for } r_0 < 0 \\ \mathbf{Q}_{\text{flux},+}r_0 & \text{for } r_0 > 0 \end{cases} \quad (4.1)$$

where χ was defined in (2.62). This gives us two distinct spaces \tilde{Y}_+ and \tilde{Y}_- . To translate this into the quiver language, we need to consider the toric quiver \mathcal{Q} describing D-branes on the CY_3 . The background value of the B-field determines in principle which toric phase to use, corresponding to a particular point in the quiver locus. In practice we do not know the exact central charges of all the fractional branes along the quiver locus, and thus we do not know the location of all the Seiberg duality walls. In this paper we will discuss various toric phases for each geometry; it turns out that all the resulting Chern-Simons quivers are 3d Seiberg dual in the sense of [32, 33].

D2-branes in the background (4.1) correspond to θ -stable quiver representations, with θ depending on the sign of r_0 . According to (2.63), we have

$$\begin{aligned} \tilde{Y}(r_0 < 0) \simeq \tilde{Y}_- & : & \theta_- &= -Q_-^{\vee} \mathbf{Q}_{\text{flux},-}, \\ \tilde{Y}(r_0 > 0) \simeq \tilde{Y}_+ & : & \theta_+ &= Q_+^{\vee} \mathbf{Q}_{\text{flux},+}, \end{aligned} \quad (4.2)$$

with Q_{\pm}^{\vee} the relevant dictionaries. We find the correct dictionaries by scanning explicitly over all the Kähler chambers (and over large volume monodromies in each chamber), retaining only those dictionaries Q_{\pm}^{\vee} for which θ_{\pm} as defined in (4.2) lies in the corresponding open string Kähler chambers. We call such dictionaries Q_{\pm}^{\vee} the *consistent dictionaries* for \tilde{Y}_{\pm} .

In general there might be several pairs of consistent dictionaries for a given $\mathbf{Q}_{\text{flux},\pm}$, corresponding either to the fact that the type IIA fluxes sets \tilde{Y}_- and/or \tilde{Y}_+ on a Kähler wall (in which case the different choice of dictionaries lead to the same CS quiver theory), or else to Seiberg-like dualities among different CS gauge theories. For torsionless backgrounds the former situation always occurs, since the $\overline{\text{D6}}$ -brane wrapping B_4 is mutually BPS with the D2.

Choosing some consistent dictionaries Q_{\pm}^{\vee} , the derivation of the field theory is straightforward. Away from the tip $r_0 = 0$, the mobile D2-brane is a stable bound state of G fractional D2-branes \mathbf{E}_i^{\vee} . The $U(1)$ gauge field on \mathbf{E}_i^{\vee} acquires a Chern-Simons interaction from its Wess-Zumino action¹⁷

$$\int_{\mathbb{R}^{1,2}} A_{3d} \wedge F_{3d} \int_{B_4} ch(\mathbf{E}_i^{\vee}) \wedge F^{(P)}, \quad (4.3)$$

due to the background fluxes $F^{(P)}$ encoded in $\mathbf{Q}_{\text{flux},\pm}$. Here $F_{3d} = dA_{3d}$ is the world-volume flux along the $\mathbb{R}^{1,2}$ directions and $F^{(P)} = e^B F$ the Page current, where F is the improved gauge invariant RR field strength polyform. From (4.3) we read the Chern-Simons levels

$$\mathbf{k}_{\pm} = Q_{\pm}^{\vee} \mathbf{Q}_{\text{flux},\pm}, \quad (4.4)$$

¹⁷We neglect the gravitational coupling in the Wess-Zumino action, because it does not affect our derivation. See [33] for some comments on that point.

for a D2-brane at $r_0 > 0$ or $r_0 < 0$. Remark that we have $\theta_{\pm} = \pm \mathbf{k}_{\pm}$. At $r_0 = 0$, the worldvolume gauge theory acquires the CS levels

$$\mathbf{k} = \frac{1}{2}(\mathbf{k}_- + \mathbf{k}_+). \quad (4.5)$$

The ranks \mathbf{N} of the CS quiver theory are related to the explicit sources, which we encoded in $\mathbf{Q}_{\text{source}}$. In order to use the dictionaries and read the quiver ranks from the branes, we need to split these D-brane sources to the left and right of $r_0 = 0$:

$$\mathbf{Q}_{\text{source},-} = \delta \mathbf{Q}_{\text{source}}, \quad \mathbf{Q}_{\text{source},+} = \mathbf{Q}_{\text{source}} - \delta \mathbf{Q}_{\text{source}}, \quad (4.6)$$

in such a way that the bunches $\mathbf{Q}_{\text{source},\pm}$ still lie inside the Kähler chambers where Q_{\pm}^{\vee} are respectively valid; since these branes affect the background flux, this is a non-trivial constraint. In practice we take an arbitrary splitting $\delta \mathbf{Q}_{\text{source}}$, and compute

$$\mathbf{N}_{\text{trial}} = \mathbf{Q}_{\text{source},-}(Q_-^{\vee})^{-1} + \mathbf{Q}_{\text{source},+}(Q_+^{\vee})^{-1}, \quad (4.7)$$

which depends on some of the unknowns in the arbitrary splitting $\delta \mathbf{Q}_{\text{source}}$. It only depends on the the so-called *anomalous D-branes*, which wrap cycles dual to compact cycles and therefore source the fluxes $\mathbf{Q}_{\text{flux},+}$. The anomalous D-branes are the D6-brane wrapped on \tilde{B}_4 and the D4-brane on the dual 2-cycle. In term of quiver representations, the distinction between non-anomalous or anomalous D-brane is whether the corresponding dimension vector β is or not in the kernel of the antisymmetric adjacency matrix A : $A\beta = 0$ for non-anomalous branes.¹⁸ The correct \mathbf{N} is found by requiring that

$$A\mathbf{N}_{\text{trial}} = \mathbf{k}_+ - \mathbf{k}_-. \quad (4.8)$$

This algorithm gives us a Chern-Simons quiver gauge theory $(\mathcal{Q}, \mathbf{N}, \mathbf{k})$ for any choice of consistent dictionaries Q_-^{\vee}, Q_+^{\vee} . We will show next that the semi-classical moduli space of $(\mathcal{Q}, \mathbf{N}, \mathbf{k})$ reproduces by construction the type IIA geometry we started with.

4.2 Semi-classical moduli space of CS quiver theories and type IIA geometry

Three dimensional $\mathcal{N} = 2$ supersymmetric quiver gauge theories have complex scalar fields X_{ij} in bifundamental representations and real scalar fields σ_i in adjoint representations, leading to a potentially rich semi-classical moduli space. The classical vacuum equations are¹⁹

$$\begin{aligned} \partial_X W &= 0, \\ \sigma_i X_{ij} - X_{ij} \sigma_j &= 0, \\ \sum_{X_{ij}} X_{ij}^{\dagger} X_{ij} - \sum_{X_{ji}} X_{ji} X_{ji}^{\dagger} &= \sigma_i k_i, \end{aligned} \quad (4.9)$$

¹⁸Let us stress that there is nothing anomalous about these “anomalous” fractional D2-branes: the terminology is inherited from the related setup with fractional D3-branes in type IIB, where a quiver theory with $AN \neq 0$ would have a gauge anomaly and the IIB background a RR tadpole.

¹⁹To keep formulae simpler, we rescaled $\sigma \rightarrow 2\pi\sigma$ with respect to common conventions.

whose general solution could be rather intricate. A general analysis of these classical equations was performed in [4, 5, 6], whereas the generalization to the one-loop corrected moduli space was given in [14]. Let us write the ranks as $N_i = \tilde{N} + N_i$, with $\tilde{N} = \min(N_i)$. We focus on the *geometric branch*, which we define by setting

$$\sigma_i = \text{diag}(\sigma_1, \dots, \sigma_{\tilde{N}}, 0, \dots, 0), \quad \forall i. \quad (4.10)$$

In the case $\tilde{N} = 1$, the low energy theory at any fixed $\sigma \neq 0$ is Abelian, with vacuum equations

$$\partial_X W = 0, \quad \sum_{X_{ij}} |X_{ij}|^2 - \sum_{X_{ji}} |X_{ji}|^2 = \sigma k_i^{eff}(\sigma), \quad (4.11)$$

where the effective CS levels \mathbf{k}^{eff} are given by [14]

$$\mathbf{k}^{eff}(\sigma) = \begin{cases} \mathbf{k}_- & \text{if } \sigma < 0 \\ \mathbf{k}_+ & \text{if } \sigma > 0 \end{cases}, \quad \text{with } \mathbf{k}_{\pm} = \mathbf{k} \pm \frac{1}{2} A \mathbf{N}, \quad (4.12)$$

due to one-loop corrections upon integrating out massive chiral multiplets. Remark that \mathbf{k}_{\pm} are integers. The equations (4.11) lead to the Kähler quotient description of a resolved CY_3 cone \tilde{Y} , with FI parameters $\sigma \mathbf{k}^{eff}(\sigma)$. The full geometric branch for $\tilde{N} = 1$ is a resolved cone \tilde{Y} fibred on a line $\mathbb{R} \cong \{\sigma\}$ according to (4.11)-(4.12). We have two distinct partial resolutions \tilde{Y}_{\pm} depending on the sign of σ . Equivalently, we can describe the spaces \tilde{Y} by the GIT quotient (2.18), or in term of semi-stable quiver representations. The θ -stability parameters are given by the effective Chern-Simons levels according to

$$\boldsymbol{\theta}_{\pm} = \pm \mathbf{k}_{\pm}. \quad (4.13)$$

This identity is what makes θ -stability such a natural tool to study Chern-Simons quivers. For $\tilde{N} > 1$, the geometric branch is the \tilde{N} -symmetric product of the above result (due to the residual gauge symmetry permuting the non-zero eigenvalues σ_i). Therefore we reproduce the type IIA geometry probed by \tilde{N} mobile D2-branes, with the identification $r_0 = \sigma$. The parameters $\boldsymbol{\theta}_{\pm} = \pm \mathbf{k}_{\pm}$ of the CS quiver determine which open Kahler chambers we sit in at σ positive or negative, and which consistent dictionaries we should use. The Kähler parameters $\boldsymbol{\chi}$ of \tilde{Y}_{\pm} are found from $\boldsymbol{\theta}_{\pm}$ by inverting the relations (4.2).

4.3 Monopole operators and GIT quotient

The real scalar σ is naturally complexified using the dual photon φ . Good homomorphic coordinates on the Coulomb branch are provided by the monopole operators $t \sim \exp(\frac{2\pi}{g^2} \sigma + i\varphi)$. In the conventions of [14], we have

$$t = T, \quad \text{for } \sigma < 0, \quad t = \tilde{T}, \quad \text{for } \sigma > 0. \quad (4.14)$$

Denoting $t_- = T$ and $t_+ = \tilde{T}$, the bare monopole operators have electric charges $\mathbf{g}(t_{\pm}) = -\boldsymbol{\theta}_{\pm} = \mp \mathbf{k}_{\pm}$, respectively, under the torus $\mathcal{G} = U(1)^G$. On the other hand, in

the GIT construction (2.18) we have the function t on the trivial line bundle which has charges $-\boldsymbol{\theta}$ under \mathcal{G} [50], and the $\mathcal{G}_{\mathbb{C}}(\boldsymbol{\theta})$ -invariant functions are of the form $f_{n\boldsymbol{\theta}}t^n$ for n any non-negative integer, with $f_{n\boldsymbol{\theta}}$ an homogenous polynomial in the coordinates z_a of degree $n\boldsymbol{\theta}$ under (2.17). Thus we have

$$\tilde{Y}_{\pm} \cong \mathcal{M}(\mathcal{Q}, \boldsymbol{\alpha}; \boldsymbol{\theta}_{\pm})_{GIT} \cong \text{Proj} \bigoplus_{n \geq 0} \mathbb{C}[f_{n\boldsymbol{\theta}_{\pm}} t_{\pm}^n]. \quad (4.15)$$

Note that the rings $\mathbb{C}[f_{n\boldsymbol{\theta}_{\pm}} t_{\pm}^n]$ are in general not freely generated, despite the short-hand notation: there can be *syzygies*, i.e. relations between the generators which follow from their definition in term of the variables z_a, t_{\pm} ; the rings above are thus obtained by further dividing the free ring of gauge invariants by a syzygy ideal which is left implicit. The invariant functions $f_{n\boldsymbol{\theta}_{\pm}} t_{\pm}^n$ with $n > 0$ are the gauge invariant diagonal monopole operators discussed at length in [14], and the ring $\mathbb{C}[f_{n\boldsymbol{\theta}_{\pm}} t_{\pm}^n]$ is graded by the magnetic charge n . While the singular cone Y corresponds to the spectrum of the $n = 0$ subring,

$$Y = \text{Spec } \mathbb{C}[f_0], \quad (4.16)$$

the Proj construction in (4.15) corresponds to a partial resolution $\pi : \tilde{Y} \rightarrow Y$. The local coordinates on the exceptional locus are basically the monopole operators $f_{\boldsymbol{\theta}}t$.

The construction (4.15) “projectivises” the affine variety one would obtain from the spectrum of the free ring $\mathbb{C}[f_{\boldsymbol{\theta}}t]$. To obtain the full CY_4 geometric branch of the Chern-Simons quiver one would naively replace Proj with Spec in (4.15), but the complete story is more subtle. It was shown in various examples [67, 13, 12] and conjectured in general in [14] that the full geometric branch can be obtained as

$$\mathcal{M}_{M2\text{-branes}} = \text{Spec} \frac{\bigoplus_{n \geq 0} \mathbb{C}[f_{n\boldsymbol{\theta}_-} t_-^n, f_{n\boldsymbol{\theta}_+} t_+^n]}{\mathcal{I}_{QR}}, \quad (4.17)$$

and that for $\tilde{N} = 1$ this is a conical CY fourfold. The ideal \mathcal{I}_{QR} corresponds to so-called *quantum relations* involving the monopoles operators. It could not be determined from first principle so far. In the examples which have been worked out, it was enough to conjecture that \mathcal{I}_{QR} is generated by any binomial²⁰ of the monopoles $f_{n\boldsymbol{\theta}_{\pm}} t_{\pm}^n$ homogeneous under all the global symmetries.²¹

Example: The ABJM theory. As a simple example, consider the ABJM theory, which is the CY_3 quiver for D-branes on the conifold. Take the Abelian theory $U(1)_k \times U(1)_{-k}$; there are four bifundamental fields A_{α}, B_{β} ($\alpha, \beta = 1, 2$) from node 1 to 2 and from node 2 to 1, respectively. We have

$$\mathcal{Z} \cong \mathbb{C}^4 \cong \{w_1, \dots, w_4\}, \quad \text{with} \quad w_1 = A_1 B_2, w_2 = A_2 B_1, w_3 = A_1 B_1, w_4 = A_2 B_2.$$

²⁰That the relations are of the form “binomial= 0” is necessary for $\mathcal{M}_{M2\text{-branes}}$ to be a toric space. In non-toric cases such as in [67] the relations are not binomial.

²¹It was pointed out to us by Daniel Gulotta that this conjecture fails in some special cases, where one can write down relations amongst monopoles which are allowed by the symmetries but would ruin the identification (4.17). In those special cases we should modify the conjecture accordingly.

and (there are no one-loop correction in this non-chiral case)

$$\boldsymbol{\theta}_- = (-k, k), \quad \boldsymbol{\theta}_+ = (k, -k). \quad (4.18)$$

Consider the $k = 1$ case for simplicity. The gauge invariant monopole operators are $B_\beta t_-$ and $A_\alpha t_+$ at $\sigma < 0$ and $\sigma > 0$, respectively. Explicitly, the Proj in (4.15) is obtained by separating the functions $\{w_1, \dots, w_4\}$ with $n = 0$ from the functions \tilde{w}_i with $n > 0$, considering $\mathbb{C}^4 \cong \{w\}$ and $\mathbb{C}^d \cong \{\tilde{w}\}$, taking the zero set of all the relations between the (w, \tilde{w}) (syzygies) on $\mathbb{C}^4 \times \mathbb{C}^d \setminus 0$, and further quotienting by the \mathbb{C}^* action given by the n -grading. Let us define

$$a_\alpha = A_\alpha t_+, \quad b_\beta = B_\beta t_-. \quad (4.19)$$

We have

$$\begin{aligned} \tilde{Y}_+ &= \text{Proj } \mathbb{C}[w_1, \dots, w_2] \oplus \mathbb{C}[a_1, a_2] \oplus \dots \\ &\sim \text{Spec } \mathbb{C}[w_1, \dots, w_2] / (w_1 w_2 - w_3 w_4) \times \frac{\mathbb{C}[a_1, a_2]}{\mathbb{C}^*}, \end{aligned} \quad (4.20)$$

describing the resolved conifold $\mathcal{O}(-1) \oplus \mathcal{O}(-1) \rightarrow \mathbb{C}\mathbb{P}^1$. The small resolution locus is spanned by the monopoles $[a_1, a_2]$, which are the homogenous coordinates of the $\mathbb{C}\mathbb{P}^1$ at the tip. Similarly \tilde{Y}_- is the resolved conifold with the flopped $\mathbb{C}\mathbb{P}^1$ described by $[b_1, b_2]$. On the other hand the geometric branch (4.17) is given by

$$\mathcal{M}_{\text{M2-branes}} = \text{Spec } \frac{\mathbb{C}[w_{\alpha\beta}, a_\alpha, b_\beta]}{(a_\alpha b_\beta - w_{\alpha\beta})} = \text{Spec } \mathbb{C}[a_\alpha, b_\beta] \cong \mathbb{C}^4 \quad (4.21)$$

with $w_{\alpha\beta} = A_\alpha B_\beta$, corresponding to the moduli space of a single M2-brane.

5. M2-brane theories for backgrounds without torsion G_4 flux

In this section we use the type IIA stringy derivation method explained in sections 3 and 4 to find the low energy worldvolume theory on M2-branes probing toric CY_4 cones over the toric $Y^{p,q}(B_4)$ Sasaki-Einstein 7-folds introduced in section 3.2. We will consider all the 16 2d toric Fano varieties B_4 of section 2.5, starting with smooth del Pezzo surfaces and then moving to singular pseudo del Pezzo surfaces including some weighted $\mathbb{C}\mathbb{P}^2$'s.

5.1 $dP_0 \equiv \mathbb{C}\mathbb{P}^2$

This example was discussed in great depth in [14], to which we refer for more details. We review here some of the results as a warm-up before delving into new examples. We slightly changed conventions with respect to [14] for later convenience.

The toric diagram of the 2-parameter family of toric CY_4 cones over $Y^{p,q}(\mathbb{C}\mathbb{P}^2)$, shown in Fig. 7(a) (or Fig. 4(a)), is the convex hull of

$$(0, 0, 0), (0, 0, p), (-1, -1, 0), (0, 1, 0), (1, 0, q). \quad (5.1)$$

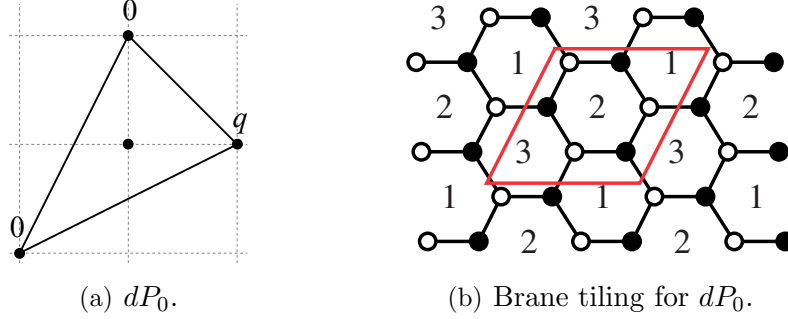


Figure 7: Toric diagram and brane tiling for the complex cone over dP_0 . The toric diagram is a projection on the plane of the 3d toric diagram of $C(Y^{p,q}(\mathbb{CP}^2))$, with the vertical height of the external points indicated on the figure.

We are interested in geometric parameters in the range $0 \leq q \leq 3p$, so that all the points (5.1) are external. The geometries are identified under the \mathbb{Z}_2 action $q \mapsto 3p - q$. The metrics for the Sasaki-Einstein bases are explicitly known [26]. The minimal GLSM for the $\tilde{Y}(r_0)$ fibre in IIA is

$$\frac{CY_3 \mid p_1 \ p_2 \ p_3 \ p_0 \mid \chi(r_0)}{\mathcal{C} \mid 1 \ 1 \ 1 \ -3 \mid (3p\Theta(r_0) - q) r_0} \quad (5.2)$$

where the Kähler volume of the exceptional $\mathcal{C} = \mathbb{CP}^1 \subset \mathbb{CP}^2$ in the $\tilde{Y}(r_0)$ fibre is

$$\chi(r_0) = (3p\Theta(r_0) - q) r_0. \quad (5.3)$$

The toric quiver gauge theory for the complex cone over $dP_0 = \mathbb{CP}^2$ is specified by the brane tiling of Fig. 7(b), with superpotential

$$W = \epsilon_{ijh} X_{13}^i X_{32}^j X_{21}^h. \quad (5.4)$$

The dimer model has 3 internal perfect matchings $\{p[4], p[5], p[6]\}$, associated to the open string Kähler chambers

$$p[4]: \quad -\xi_1 \geq 0, \quad \xi_3 \geq 0 \quad (5.5)$$

$$p[5]: \quad -\xi_3 \geq 0, \quad \xi_2 \geq 0 \quad (5.6)$$

$$p[6]: \quad -\xi_2 \geq 0, \quad \xi_1 \geq 0 \quad (5.7)$$

each one with its own dictionary matrix up to large volume monodromies.

A quiver CS theory for the whole class of $C(Y^{p,q}(\mathbb{CP}^2))$ geometries can be proposed as follows. Both at $\sigma < 0$ and $\sigma > 0$ we are on the Kähler wall between the maximal dimensional chamber associated to dictionary

$$Q^\vee[dP_0, \{p[5]\}, \{0\}] = \begin{pmatrix} -2 & 0 & \frac{3}{4} \\ 1 & \frac{1}{2} & \frac{1}{8} \\ 1 & -\frac{1}{2} & \frac{1}{8} \end{pmatrix} \quad (5.8)$$

and the one associated to dictionary

$$Q^\vee[dP_0, \{p[6]\}, \{-1\}] = \begin{pmatrix} 1 & \frac{3}{2} & \frac{9}{8} \\ 1 & \frac{1}{2} & \frac{1}{8} \\ -2 & -2 & -\frac{1}{4} \end{pmatrix} \quad (5.9)$$

The wall between these two chambers is given by the cone

$$\xi_2 = 0, \quad \xi_1 = -\xi_3 \geq 0 \quad (5.10)$$

in FI parameter space. Using either one of these dictionaries, both at $\sigma < 0$ and $\sigma > 0$, we find that the 3d quiver theory has ranks and bare CS levels

$$\mathbf{N} = (N, N - p, N) \quad (5.11)$$

$$\mathbf{k} = \left(\frac{3}{2}p - q, 0, -\frac{3}{2}p + q\right) \quad (5.12)$$

so that the effective CS levels are

$$-\mathbf{k}^- = (q, 0, -q) \quad (5.13)$$

$$+\mathbf{k}^+ = (3p - q, 0, -3p + q). \quad (5.14)$$

The inequality $0 \leq q \leq 3$ ensures that the effective FI parameters of this CS toric quiver gauge theory lie precisely on the Kähler wall (5.10) associated to the dictionaries that we used to derive the 3d theory. Using formula (2.63), we find that on this wall the volume of the $\mathbb{CP}^1 \subset \mathbb{CP}^2$ in the fibred CY_3 , computed from the field theory, is

$$\chi(\sigma) = \xi_1^{eff}(\sigma) = (3p\Theta(\sigma) - q)\sigma \quad (5.15)$$

in agreement with the geometric result (5.3) of the reduction if $\sigma = r_0$.

5.2 $\mathbb{F}_0 \equiv \mathbb{CP}^1 \times \mathbb{CP}^1$

The toric diagram of the 3-parameter family of toric CY_4 cones over $Y^{p, q_1, q_2}(\mathbb{CP}^1 \times \mathbb{CP}^1)$, shown in Fig. 4(b), is the convex hull of

$$(0, 0, 0), (0, 0, p), (0, -1, 0), (-1, 0, 0), (0, 1, q_1), (1, 0, q_2). \quad (5.16)$$

We are interested in geometric parameters in the range

$$0 \leq \frac{q_1}{2}, \frac{q_2}{2} \leq p \quad (5.17)$$

so that all the points (5.16) are external. The metrics for the Sasaki-Einstein bases are known [26, 68, 69].²² The geometries are identified under the $\mathbb{Z}_2 \times \mathbb{Z}_2$ action

$$g : (q_1, q_2) \mapsto (2p - q_1, 2p - q_2), \quad g' : (q_1, q_2) \mapsto (q_2, q_1). \quad (5.18)$$

²²See also the recent [31], which dubbed these Sasaki-Einstein 7-folds $A^{q_1 q_2 p}$ and studied Romans mass deformations of the type IIA $AdS_4 \times_w M_6$ backgrounds resulting from KK reduction of the $AdS_4 \times A^{q_1 q_2 p}$ backgrounds of 11d supergravity. We changed notation for the sake of uniformity.

The CY_4 singularity is not isolated when at least one of the inequalities (5.17) is saturated. In that case the CY_3 lying over $r_0 < 0$ or over $r_0 > 0$ is not completely resolved. Indeed, the minimal GLSM for the $\tilde{Y}(r_0)$ fibre in IIA is

$$\begin{array}{c|ccccc|c} CY_3 & p_1 & p_2 & p_3 & p_4 & p_0 & \chi(r_0) \\ \hline \mathcal{C}_3 & 0 & 1 & 0 & 1 & -2 & (2p\Theta(r_0) - q_2)r_0 \\ \mathcal{C}_4 & 1 & 0 & 1 & 0 & -2 & (2p\Theta(r_0) - q_1)r_0 \end{array} \quad (5.19)$$

with the volumes of the two \mathbb{P}^1 's, \mathcal{C}_3 and \mathcal{C}_4 ,

$$\chi_3(r_0) = (2p\Theta(r_0) - q_2)r_0, \quad \chi_4(r_0) = (2p\Theta(r_0) - q_1)r_0. \quad (5.20)$$

5.2.1 Phase a of \mathbb{F}_0

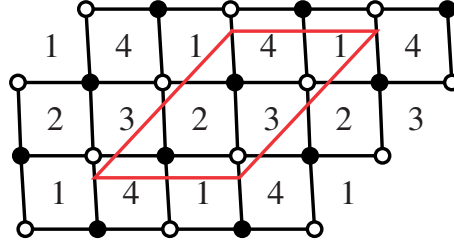


Figure 8: Brane tiling for toric phase a of \mathbb{F}_0 .

The toric quiver gauge theory for toric phase a of the complex cone over F_0 is specified by the brane tiling of Fig. 8, with superpotential

$$W = \epsilon_{ij}\epsilon_{khl} X_{12}^i X_{23}^h X_{34}^j X_{41}^k. \quad (5.21)$$

The dimer model has 4 internal perfect matchings $\{p[5], \dots, p[8]\}$, associated to the open string Kähler chambers

$$p[5]: \quad -\xi_1 \geq 0, \quad \xi_2 \geq 0, \quad \xi_2 + \xi_3 \geq 0 \quad (5.22)$$

$$p[6]: \quad -\xi_1 - \xi_2 \geq 0, \quad -\xi_2 \geq 0, \quad \xi_3 \geq 0 \quad (5.23)$$

$$p[7]: \quad -\xi_1 - \xi_2 - \xi_3 \geq 0, \quad -\xi_2 - \xi_3 \geq 0, \quad -\xi_3 \geq 0 \quad (5.24)$$

$$p[8]: \quad \xi_1 \geq 0, \quad \xi_1 + \xi_2 \geq 0, \quad \xi_1 + \xi_2 + \xi_3 \geq 0 \quad (5.25)$$

each one with its own dictionary matrix up to large volume monodromies.

A quiver CS theory for the whole class of $C(Y^{p, q_1, q_2}(F_0))$ geometries based on this toric phase can be proposed as follows. Both at $\sigma < 0$ and $\sigma > 0$ we are on the Kähler wall between the maximal dimensional chamber associated to dictionary

$$Q^\vee[(\mathbb{F}_0)_a, \{p[5]\}, \{0, -1\}] = \begin{pmatrix} 1 & 0 & 0 & 0 \\ 1 & 0 & 1 & 0 \\ -1 & 1 & -1 & 1 \\ -1 & -1 & 0 & 0 \end{pmatrix} \quad (5.26)$$

and the one associated to dictionary

$$Q^\vee[(\mathbb{F}_0)_a, \{p[8]\}, \{0, 0\}] = \begin{pmatrix} 1 & 0 & 0 & 0 \\ -1 & 0 & 1 & 0 \\ -1 & 1 & -1 & 1 \\ 1 & -1 & 0 & 0 \end{pmatrix} \quad (5.27)$$

The wall between these two chambers is given by the cone

$$\xi_1 = 0, \quad \xi_2 \geq 0, \quad \xi_2 + \xi_3 \geq 0 \quad (5.28)$$

in FI parameter space. Using either one of these dictionaries, both at $\sigma < 0$ and $\sigma > 0$, we find that the 3d quiver theory has ranks and bare CS levels

$$\mathbf{N} = (N - p, N, N, N) \quad (5.29)$$

$$\mathbf{k} = (0, p - q_1, q_1 - q_2, -p + q_2) \quad (5.30)$$

so that the effective CS levels are

$$-\mathbf{k}^- = (0, q_1, -q_1 + q_2, -q_2) \quad (5.31)$$

$$+\mathbf{k}^+ = (0, 2p - q_1, q_1 - q_2, -2p + q_2). \quad (5.32)$$

It is straightforward to see that the geometric inequalities (5.17) imply that the effective FI parameters of this CS toric quiver gauge theory lie precisely on the Kähler wall (5.28) associated to the dictionaries used to derive the 3d theory.

This guarantees the consistency of the stringy derivation and that the semiclassical computation of the geometric branch of the moduli space reproduces the type IIA geometry, as shown in section 4.2. Let us see it explicitly. In the Kähler chamber $p[5]$, using formula (2.63) with dictionary (5.26), the volumes $\chi_{3,4}$ of the two \mathbb{P}^1 's are

$$\chi_3 = \xi_2 + \xi_3, \quad \chi_4 = -\xi_1 + \xi_2. \quad (5.33)$$

In the Kähler chamber $p[8]$, using formula (2.63) with dictionary (5.27), the volumes of the two \mathbb{P}^1 's are

$$\chi_3 = 2\xi_1 + \xi_2 + \xi_3, \quad \chi_4 = \xi_1 + \xi_2. \quad (5.34)$$

Therefore on the wall $\xi_1 = 0$ between these two chambers the volumes are

$$\chi_3 = \xi_2 + \xi_3 = -\xi_4, \quad \chi_4 = \xi_2. \quad (5.35)$$

Plugging in the effective CS levels (5.31)-(5.32), we find the volumes

$$\chi_3(\sigma) = (2p\Theta(\sigma) - q_2)\sigma, \quad \chi_4(\sigma) = (2p\Theta(\sigma) - q_1)\sigma, \quad (5.36)$$

which reproduce the volumes of the two \mathbb{P}^1 's in the type IIA background (5.20), with the identification $\sigma = r_0$.

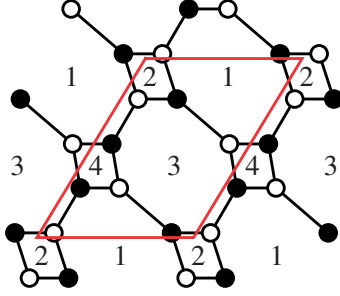


Figure 9: Brane tiling for toric phase b of \mathbb{F}_0 .

5.2.2 Phase b of \mathbb{F}_0

The toric quiver gauge theory for toric phase b of the complex cone over F_0 is specified by the brane tiling of Fig. 9, with superpotential

$$W = \epsilon_{ij}\epsilon_{kh} X_{12}^i X_{23}^h X_{31}^{jk} - \epsilon_{ij}\epsilon_{kh} X_{14}^h X_{43}^i X_{31}^{jk} . \quad (5.37)$$

The dimer model has 5 internal perfect matchings $\{p[5], \dots, p[9]\}$, each one associated to an open string Kähler chamber and a dictionary matrix up to large volume monodromies.

A quiver CS theory for the whole class of $C(Y^{p, q_1, q_2}(F_0))$ geometries based on this toric phase can be obtained by Seiberg duality on gauge group 4 of the theory of phase a. Since the effective FI parameters $\xi_4^\pm \leq 0$, the brane charge dictionaries are obtained by double left mutation $M_{(4;L)}$ of the dictionaries (5.26) and (5.27) [33], giving

$$M_{(4;L)} Q^\vee[(F_0)_a, \{p[5]\}, \{0, -1\}] = \begin{pmatrix} 1 & 0 & 0 & 0 \\ 1 & 0 & 1 & 0 \\ -3 & -1 & -1 & 1 \\ 1 & 1 & 0 & 0 \end{pmatrix} \quad (5.38)$$

and

$$M_{(4;L)} Q^\vee[(F_0)_a, \{p[8]\}, \{0, 0\}] = \begin{pmatrix} 1 & 0 & 0 & 0 \\ -1 & 0 & 1 & 0 \\ 1 & -1 & -1 & 1 \\ -1 & 1 & 0 & 0 \end{pmatrix} . \quad (5.39)$$

Note that these are related to dictionaries

$$Q^\vee[(\mathbb{F}_0)_b, \{p[5]\}, \{0, 0\}] = \begin{pmatrix} 1 & 0 & 0 & 0 \\ 1 & 1 & 0 & 0 \\ -3 & -1 & -1 & 1 \\ 1 & 0 & 1 & 0 \end{pmatrix} \quad (5.40)$$

and

$$Q^\vee[(\mathbb{F}_0)_b, \{p[9]\}, \{0, 0\}] = \begin{pmatrix} 1 & 0 & 0 & 0 \\ -1 & 1 & 0 & 0 \\ 1 & -1 & -1 & 1 \\ -1 & 0 & 1 & 0 \end{pmatrix} \quad (5.41)$$

by a quantum \mathbb{Z}_2 monodromy interchanging the role of the two \mathbb{P}^1 's. The wall between the two chambers is given by the cone

$$\xi_1 = 0, \quad \xi_2 \geq 0, \quad \xi_4 \geq 0 \quad (5.42)$$

in FI parameter space. On this wall the volumes of the two \mathbb{P}^1 's are

$$\chi_3 = \xi_4, \quad \chi_4 = \xi_2. \quad (5.43)$$

Using either one of the mutated dictionaries (5.38) and (5.39), both at $\sigma < 0$ and $\sigma > 0$, we find the 3d quiver theory with ranks and bare CS levels

$$\mathbf{N} = (N - p, N, N, N) \quad (5.44)$$

$$\mathbf{k} = (0, p - q_1, -2p + q_1 + q_2, p - q_2) \quad (5.45)$$

so that the effective CS levels are

$$-\mathbf{k}^- = (0, q_1, -q_1 - q_2, q_2) \quad (5.46)$$

$$+\mathbf{k}^+ = (0, 2p - q_1, -4p + q_1 + q_2, 2p - q_2). \quad (5.47)$$

The geometric inequalities (5.17) ensure that the effective FI parameters of this CS toric quiver gauge theory lie precisely on the Kähler wall (5.42) associated to the dictionaries used to derive the 3d theory. The volumes of the 2-cycles in the CY_3 are again

$$\chi_3(\sigma) = (2p \Theta(\sigma) - q_2) \sigma, \quad \chi_4(\sigma) = (2p \Theta(\sigma) - q_1) \sigma. \quad (5.48)$$

An important remark is in order here: the stringy derivation is subtler if $q_i = 0, 2p$, which introduces a non-isolated singularity in the CY_4 due to the fibration of an isolated singularity of the CY_3 . Let us consider $q_2 = 2p$ for simplicity. There is an extra 1-complex-dimensional Coulomb branch, due to $k_4^+ = 0$. If this extra branch of the moduli space is parametrised by a monopole operator turning on one unit of flux in gauge group in one of the phases, it is parametrised in the dual phase by an extra singlet coupled in the superpotential to an analogous monopole operator [70, 32]. As in simpler brane realizations of 3d Seiberg duality like the type IIB setup of [71], it is not known how to account for these extra singlets in terms of branes: the stringy derivation, as developed so far, is not sensitive to these details. It is thus unclear in which of the two toric phases the singlet should be. Similar considerations hold for Seiberg duality on gauge group 2 and q_1 . In conclusion, the stringy derivation is unambiguous only when the CY_3 fibres are completely resolved, so that those extra branches of the moduli space and extra singlets are not there.

5.3 dP_1

The toric diagram of the 3-parameter family of toric CY_4 cones over $Y^{p, q_1, q_2}(dP_1)$, shown in Fig. 4(c), is the convex hull of

$$(0, 0, 0), (0, 0, p), (0, -1, 0), (-1, 1, 0), (0, 1, q_1), (1, 0, q_2). \quad (5.49)$$

We are interested in geometric parameters in the range

$$0 \leq \frac{q_1}{2}, \frac{q_2}{3} \leq p \quad (5.50)$$

so that all the points (5.49) are external. The geometries are identified under the \mathbb{Z}_2 action $(q_1, q_2) \mapsto (2p - q_1, 3p - q_2)$. The minimal GLSM for the $\tilde{Y}(r_0)$ fibre in IIA is

$$\begin{array}{c|ccccc|c} CY_3 & p_1 & p_2 & p_3 & p_4 & p_0 & \chi(r_0) \\ \hline \mathcal{C}_3 & 0 & 1 & -1 & 1 & -1 & (p \Theta(r_0) + q_1 - q_2) r_0 \\ \mathcal{C}_4 & 1 & 0 & 1 & 0 & -2 & (2p \Theta(r_0) - q_1) r_0 \end{array} \quad (5.51)$$

If $0 < q_2 - q_1 < p$, the triangulations Γ_{\pm} are the same: both \tilde{Y}_{\pm} contain a blown up dP_1 . When $q_2 - q_1$ crosses 0 (resp. p), the curve $\mathcal{C}_3 \cong \mathbb{P}^1$ undergoes a flop transition in \tilde{Y}_- (resp. \tilde{Y}_+), resulting in a \mathbb{P}^1 intersecting a \mathbb{P}^2 .

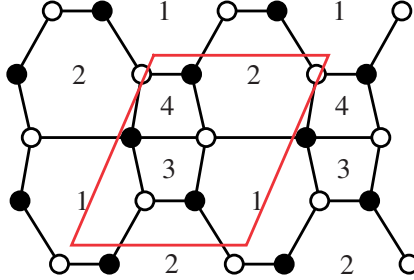


Figure 10: Brane tiling for dP_1 .

The toric quiver gauge theory for the complex cone over dP_1 is specified by the brane tiling of Fig. 10, with superpotential

$$\begin{aligned} W = & X_{21}^1 X_{14} X_{42}^1 + X_{21}^2 X_{13}^1 X_{32} + X_{42}^2 X_{21}^3 X_{13}^2 X_{34} + \\ & - X_{13}^2 X_{32} X_{21}^1 - X_{14} X_{42}^2 X_{21}^2 - X_{21}^3 X_{13}^1 X_{34} X_{42}^1. \end{aligned} \quad (5.52)$$

The dimer model has 4 internal perfect matchings $\{p[5], \dots, p[8]\}$ and corresponding open string Kähler chambers (before triangulating the toric diagram of the CY_3)

$$p[5]: \quad \xi_1 + \xi_2 \geq 0, \quad \xi_2 \geq 0, \quad \xi_1 + \xi_2 + \xi_3 \geq 0 \quad (5.53)$$

$$p[6]: \quad \xi_1 \geq 0, \quad -\xi_2 \geq 0, \quad \xi_1 + \xi_3 \geq 0 \quad (5.54)$$

$$p[7]: \quad -\xi_1 \geq 0, \quad -\xi_1 - \xi_2 \geq 0, \quad \xi_3 \geq 0 \quad (5.55)$$

$$p[8]: \quad -\xi_1 - \xi_2 - \xi_3 \geq 0, \quad -\xi_1 - \xi_3 \geq 0, \quad -\xi_3 \geq 0 \quad (5.56)$$

each one with its own dictionary matrix up to large volume monodromies.

A quiver CS theory for the whole class of $C(Y^{p, q_1, q_2}(dP_1))$ geometries (*i.e.* also for any triangulations of \tilde{Y}_\pm) can be proposed as follows. Both at $\sigma < 0$ and $\sigma > 0$ we are on the Kähler wall between the maximal dimensional chamber associated to dictionary

$$Q^\vee[dP_1, \{p[5]\}, \{0, 0\}] = \begin{pmatrix} -2 & 1 & 0 & 1 \\ 1 & 0 & \frac{1}{2} & 0 \\ 0 & -1 & 0 & 0 \\ 1 & 0 & -\frac{1}{2} & 0 \end{pmatrix} \quad (5.57)$$

and the one associated to dictionary

$$Q^\vee[dP_1, \{p[6]\}, \{-1, -1\}] = \begin{pmatrix} 1 & 1 & \frac{3}{2} & 1 \\ 1 & 0 & \frac{1}{2} & 0 \\ -1 & -1 & -\frac{1}{2} & 0 \\ -1 & 0 & -\frac{3}{2} & 0 \end{pmatrix} \quad (5.58)$$

The wall between these two chambers is given by the cone

$$\xi_1 \geq 0, \quad \xi_2 = 0, \quad \xi_1 + \xi_3 \geq 0 \quad (5.59)$$

in FI parameter space.²³ Using either one of these dictionaries, both at $\sigma < 0$ and $\sigma > 0$, we find that the 3d quiver theory has ranks and bare CS levels

$$\mathbf{N} = (N, N - p, N, N) \quad (5.60)$$

$$\mathbf{k} = \left(\frac{3p}{2} - q_2, 0, -\frac{p}{2} - q_1 + q_2, -p + q_1 \right) \quad (5.61)$$

so that the effective CS levels are

$$-\mathbf{k}^- = (q_2, 0, q_1 - q_2, -q_1) \quad (5.62)$$

$$+\mathbf{k}^+ = (3p - q_2, 0, -p - q_1 + q_2, -2p + q_1) . \quad (5.63)$$

The geometric inequalities (5.50) imply that the effective FI parameters of this CS toric quiver gauge theory lie precisely on the Kähler wall (5.59) associated to the dictionaries used to derive the 3d theory. This guarantees the consistency of the derivation and that the semiclassical computation of the geometric branch of the moduli space reproduces the type IIA geometry: plugging the effective FI parameters and any of the dictionaries (5.57)-(5.58) into formula (2.63), the volumes of 2-cycles of $\tilde{Y}(\sigma)$ computed in field theory match the IIA data (5.51) with $r_0 = \sigma$.

²³This cone can be further refined into two cones with $\xi_3 \leq 0$ and $\xi_3 \geq 0$ respectively, which the dictionaries translate to $\chi_3 \geq 0$ and $\chi_3 \leq 0$. This subdivision is sensitive to the triangulation of the toric diagram: \tilde{Y} undergoes a flop transition at the common boundary of the two subcones.

5.4 dP_2

The toric diagram of the 4-parameter family of toric CY_4 cones over $Y^{p, q_1, q_2, q_3}(dP_2)$, shown in Fig. 4(e), is the convex hull of

$$(0, 0, 0), (0, 0, p), (1, -1, 0), (-1, 0, 0), (-1, 1, q_1), (0, 1, q_2), (1, 0, q_3). \quad (5.64)$$

We are interested in geometric parameters in the range

$$0 \leq \frac{q_1}{2}, \frac{q_2}{3}, \frac{q_3}{2} \leq p \quad (5.65)$$

so that all the points (5.64) are external. The geometries are identified under the \mathbb{Z}_2 action $(q_1, q_2, q_3) \mapsto (2p - q_1, 3p - q_2, 2p - q_3)$. The minimal GLSM for the $\tilde{Y}(r_0)$ fibre in IIA is

CY_3	p_1	p_2	p_3	p_4	p_5	p_0	$\chi(r_0)$
\mathcal{C}_3	0	1	-1	1	0	-1	$(p \Theta(r_0) + q_1 - q_2) r_0$
\mathcal{C}_4	0	0	1	-1	1	-1	$(p \Theta(r_0) - q_1 + q_2 - q_3) r_0$
\mathcal{C}_5	1	0	0	1	-1	-1	$(p \Theta(r_0) - q_2 + q_3) r_0$

(5.66)

5.4.1 Phase a of dP_2

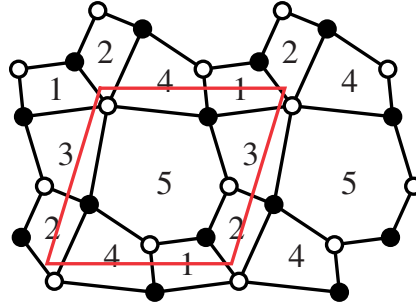


Figure 11: Brane tiling for toric phase a of dP_2 .

The brane tiling for toric phase a of dP_2 is in Fig. 11. The superpotential is

$$W = X_{25} X_{53}^2 X_{32} + X_{51} X_{14} X_{45}^2 + X_{31} X_{12} X_{24} X_{45}^1 X_{53}^1 + \quad (5.67)$$

$$- X_{25} X_{51} X_{12} - X_{53}^1 X_{32} X_{24} X_{45}^2 - X_{53}^2 X_{31} X_{14} X_{45}^1.$$

The dimer model has 5 internal perfect matchings $\{p[6], \dots, p[10]\}$.

The quiver CS theory for M2-branes at $C(Y^{p, q_1, q_2, q_3}(dP_2))$ in the absence of torsion G_4 flux is on the wall between the chamber of dictionary

$$Q^\vee[(dP_2)_a, \{p[7]\}, \{0, 0, 1\}] = \begin{pmatrix} -1 & 0 & -\frac{1}{2} & 1 & \frac{9}{8} \\ 0 & -1 & 0 & 0 & 0 \\ -1 & 1 & \frac{1}{2} & 0 & \frac{1}{8} \\ 1 & 0 & -\frac{1}{2} & -1 & -\frac{1}{8} \\ 1 & 0 & \frac{1}{2} & 0 & -\frac{1}{8} \end{pmatrix} \quad (5.68)$$

and the one of dictionary

$$Q^\vee[(dP_2)_a, \{p[8]\}, \{-1, -1, 0\}] = \begin{pmatrix} 0 & 0 & 0 & 1 & 1 \\ -1 & -1 & -\frac{1}{2} & 0 & \frac{1}{8} \\ 1 & 1 & \frac{3}{2} & 0 & -\frac{1}{8} \\ -1 & 0 & -\frac{3}{2} & -1 & \frac{1}{8} \\ 1 & 0 & \frac{1}{2} & 0 & -\frac{1}{8} \end{pmatrix}. \quad (5.69)$$

In FI parameter space the wall is the cone

$$\xi_1 + \xi_3 \geq 0, \quad \xi_3 \geq 0, \quad -\xi_4 \geq 0, \quad \xi_5 = 0. \quad (5.70)$$

The gauge ranks and bare CS levels of the M2-brane theory are

$$\mathbf{N} = (N, N, N, N, N - p) \quad (5.71)$$

$$\mathbf{k} = \left(\frac{1}{2}p - q_2 + q_3, -\frac{1}{2}p - q_1 + q_2, p - q_3, -p + q_1, 0\right) \quad (5.72)$$

The effective CS levels

$$-\mathbf{k}^- = (q_2 - q_3, q_1 - q_2, q_3, -q_1, 0) \quad (5.73)$$

$$+\mathbf{k}^+ = (p - q_2 + q_3, -p - q_1 + q_2, 2p - q_3, -2p + q_1, 0) \quad (5.74)$$

are such that the effective FI parameters lie in the cone (5.70) for geometric parameters in the window (5.65). Then the dictionary matrices translate the effective FI parameters $\xi(\sigma)$ of the gauge theory into the GLSM FI parameters $\chi(r_0)$ of $\tilde{Y}(r_0)$, with $r_0 = \sigma$.

5.4.2 Phase b of dP_2

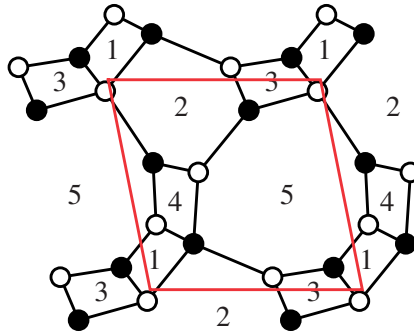


Figure 12: Brane tiling for toric phase b of dP_2 .

The brane tiling for toric phase b of dP_2 is in Fig. 12. The superpotential is

$$W = X_{25}^2 X_{53}^2 X_{32} + X_{15} X_{54}^2 X_{41} + X_{25}^3 X_{54}^1 X_{42} + X_{12} X_{25}^1 X_{53}^1 X_{31} + \\ - X_{25}^1 X_{54}^2 X_{42} - X_{15} X_{53}^2 X_{31} - X_{25}^3 X_{53}^1 X_{32} - X_{12} X_{25}^2 X_{54}^1 X_{41}. \quad (5.75)$$

The dimer model has 6 internal perfect matchings $\{p[6], \dots, p[11]\}$.

We can propose a quiver CS theory for M2-branes probing $C(Y^{p, q_1, q_2, q_3}(dP_2))$, for the entire class of geometries specified by $q_1 \in [0, 2p]$, $q_2 \in [0, 3p]$ and $q_3 \in [0, 2p]$: it is on the wall between the chamber associated to dictionary

$$Q^\vee[(dP_2)_b, \{p[9]\}, \{0, 0, 1\}] = \begin{pmatrix} 0 & 0 & -1 & 0 & 1 \\ 1 & -1 & -\frac{1}{2} & -1 & -\frac{1}{8} \\ -1 & 1 & \frac{1}{2} & 0 & \frac{1}{8} \\ -1 & 0 & \frac{1}{2} & 1 & \frac{1}{8} \\ 1 & 0 & \frac{1}{2} & 0 & -\frac{1}{8} \end{pmatrix} \quad (5.76)$$

and the one associated to

$$Q^\vee[(dP_2)_b, \{p[10]\}, \{0, -1, 0\}] = \begin{pmatrix} -1 & 0 & -\frac{3}{2} & 0 & \frac{9}{8} \\ -2 & -1 & -2 & -1 & \frac{1}{4} \\ 1 & 1 & \frac{3}{2} & 0 & -\frac{1}{8} \\ 1 & 0 & \frac{3}{2} & 1 & -\frac{1}{8} \\ 1 & 0 & \frac{1}{2} & 0 & -\frac{1}{8} \end{pmatrix}, \quad (5.77)$$

which in FI parameter space is given by the cone

$$-\xi_2 \geq 0, \quad \xi_3 \geq 0, \quad \xi_4 \geq 0, \quad \xi_5 = 0. \quad (5.78)$$

The gauge ranks and bare CS levels are

$$\mathbf{N} = (N, N, N, N, N - p) \quad (5.79)$$

$$\mathbf{k} = \left(-\frac{1}{2}p + q_1 - q_2 + q_3, -\frac{3}{2}p + q_2, p - q_3, p - q_1, 0\right), \quad (5.80)$$

and the effective CS levels are

$$-\mathbf{k}^- = (-q_1 + q_2 - q_3, -q_2, q_3, q_1, 0) \quad (5.81)$$

$$+\mathbf{k}^+ = (-p + q_1 - q_2 + q_3, -3p + q_2, 2p - q_3, 2p - q_1, 0), \quad (5.82)$$

so that the effective FI parameters belong to the cone (5.78) thanks to the geometric inequalities (5.65). This quiver CS theory is nothing but the dual of the theory in phase a of section 5.4.1 under a maximally chiral Seiberg duality of gauge group 4 [32]. The dictionaries (5.76) and (5.77) are obtained by left mutation $M_{(4;L)}$ of the dictionaries (5.68) and (5.69) of phase a respectively, with no need of quantum monodromies.

5.5 dP_3

The toric diagram of the 5-parameter family of toric CY_4 cones over $Y^{p, q_1, q_2, q_3, q_4}(dP_3)$, shown in Fig. 4(g), is the convex hull of

$$(0, 0, 0), (0, 0, p), (1, -1, 0), (0, -1, 0), (-1, 0, q_1), (-1, 1, q_2), (0, 1, q_3), (1, 0, q_4). \quad (5.83)$$

We require that the points (5.83) are all external, which means

$$0 \leq \frac{q_1 + q_4}{2}, \frac{q_2}{2}, \frac{q_3}{2}, \frac{q_1 + q_3}{3}, \frac{q_2 + q_4}{3} \leq p. \quad (5.84)$$

The geometries are identified under the \mathbb{Z}_2 action $(q_1, q_2, q_3, q_4) \mapsto (p - q_1, 2p - q_2, 2p - q_3, p - q_4)$. The minimal GLSM for the $\tilde{Y}(r_0)$ fibre in IIA is

CY_3	p_1	p_2	p_3	p_4	p_5	p_6	p_0	$\chi(r_0)$
\mathcal{C}_3	0	1	-1	1	0	0	-1	$(p\Theta(r_0) + q_1 - q_2)r_0$
\mathcal{C}_4	0	0	1	-1	1	0	-1	$(p\Theta(r_0) - q_1 + q_2 - q_3)r_0$
\mathcal{C}_5	0	0	0	1	-1	1	-1	$(p\Theta(r_0) - q_2 + q_3 - q_4)r_0$
\mathcal{C}_6	1	0	0	0	1	-1	-1	$(p\Theta(r_0) - q_3 + q_4)r_0$

(5.85)

5.5.1 Phase d of dP_3

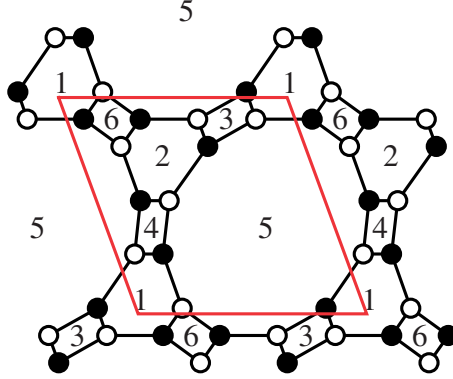


Figure 13: Brane tiling for toric phase d of dP_3 .

Toric phase d of dP_3 is specified by the brane tiling of Fig. 13. The superpotential is

$$\begin{aligned}
W = & X_{32}X_{25}^2X_{53}^2 + X_{31}X_{15}^1X_{53}^1 + X_{41}X_{15}^3X_{54}^2 + X_{42}X_{25}^3X_{54}^1 + \\
& + X_{56}^1X_{62}X_{25}^1 + X_{56}^2X_{61}X_{15}^2 - X_{31}X_{15}^3X_{53}^2 - X_{32}X_{25}^3X_{53}^1 + \\
& - X_{42}X_{25}^1X_{54}^2 - X_{41}X_{15}^2X_{54}^1 - X_{56}^1X_{61}X_{15}^1 - X_{56}^2X_{62}X_{25}^2.
\end{aligned} \quad (5.86)$$

The dimer model has 11 internal perfect matchings $\{p[7], \dots, p[17]\}$ and corresponding open string Kähler chambers (before triangulating the toric diagram of the CY_3), each one with its own dictionary matrix up to large volume monodromies.

A quiver CS theory for the whole class of $C(Y^{p, q_1, q_2, q_3, q_4}(dP_3))$ geometries can be proposed as follows. Both at $\sigma < 0$ and $\sigma > 0$ we are on the Kähler wall between the

maximal dimensional chamber associated to dictionary

$$Q^\vee[(dP_3)_d, \{p[13]\}, \{1, 0, 0, 0\}] = \begin{pmatrix} 1 & \frac{1}{2} & -1 & -1 & -\frac{1}{2} & -\frac{1}{4} \\ 1 & -\frac{1}{2} & -1 & -1 & \frac{1}{2} & -\frac{1}{4} \\ -1 & \frac{1}{2} & 1 & 0 & -\frac{1}{2} & \frac{1}{4} \\ -1 & -\frac{1}{2} & 1 & 1 & -\frac{1}{2} & \frac{5}{4} \\ 1 & \frac{1}{2} & 0 & 0 & \frac{1}{2} & -\frac{1}{4} \\ -1 & -\frac{1}{2} & 0 & 1 & \frac{1}{2} & \frac{1}{4} \end{pmatrix} \quad (5.87)$$

and the one associated to dictionary

$$Q^\vee[(dP_3)_d, \{p[14]\}, \{1, 0, 0, -1\}] = \begin{pmatrix} -2 & -1 & -1 & -1 & -2 & \frac{1}{2} \\ -2 & -2 & -1 & -1 & -1 & \frac{1}{2} \\ 1 & \frac{3}{2} & 1 & 0 & \frac{1}{2} & -\frac{1}{4} \\ 1 & \frac{1}{2} & 1 & 1 & \frac{1}{2} & \frac{3}{4} \\ 1 & \frac{1}{2} & 0 & 0 & \frac{1}{2} & -\frac{1}{4} \\ 1 & \frac{1}{2} & 0 & 1 & \frac{3}{2} & -\frac{1}{4} \end{pmatrix}. \quad (5.88)$$

The wall between these two Kähler chambers is given by the cone

$$-\xi_1 \geq 0, \quad -\xi_2 \geq 0, \quad \xi_3 \geq 0, \quad \xi_4 \geq 0, \quad \xi_5 = 0, \quad \xi_6 \geq 0 \quad (5.89)$$

in FI parameter space. Using either one of these dictionaries, both at $\sigma < 0$ and $\sigma > 0$, we find that the 3d quiver theory has ranks and bare CS levels

$$\mathbf{N} = (N, N, N, N, N - p, N) \quad (5.90)$$

$$\mathbf{k} = \left(-\frac{3}{2}p + q_1 + q_3, -\frac{3}{2}p + q_2 + q_4, p - q_3, p - q_1 - q_4, 0, p - q_2\right) \quad (5.91)$$

so that the effective CS levels are

$$-\mathbf{k}^- = (-q_1 - q_3, -q_2 - q_4, q_3, q_1 + q_4, 0, q_2) \quad (5.92)$$

$$+\mathbf{k}^+ = (-3p + q_1 + q_3, -3p + q_2 + q_4, 2p - q_3, 2p - q_1 - q_4, 0, 2p - q_2). \quad (5.93)$$

It is straightforward to see that the geometric inequalities (5.84) ensure that the effective FI parameters of this CS toric quiver gauge theory lie on the Kähler wall (5.89) associated to the dictionaries used to derive the 3d theory. This guarantees the consistency of the stringy derivation and that the semiclassical computation of the geometric branch of the moduli space reproduces the type IIA geometry (5.85).

5.5.2 Phase c of dP_3

We next move to phase c of the dP_3 quiver, which is obtained upon a “maximally chiral” Seiberg duality on gauge group 4 [32]. In D-brane terms [33] it is a double right

mutation $M_{(4;R)}$ on the dictionary matrices (5.87)-(5.88), giving the dictionaries

$$M_{(4;R)} Q^\vee[(dP_3)_d, \{p[13]\}, \{1, 0, 0, 0\}] = \begin{pmatrix} 0 & 0 & 0 & 0 & -1 & 1 \\ 0 & -1 & 0 & 0 & 0 & 1 \\ -1 & \frac{1}{2} & 1 & 0 & -\frac{1}{2} & \frac{1}{4} \\ 1 & \frac{1}{2} & -1 & -1 & \frac{1}{2} & -\frac{5}{4} \\ 1 & \frac{1}{2} & 0 & 0 & \frac{1}{2} & -\frac{1}{4} \\ -1 & -\frac{1}{2} & 0 & 1 & \frac{1}{2} & \frac{1}{4} \end{pmatrix} \quad (5.94)$$

and

$$M_{(4;R)} Q^\vee[(dP_3)_d, \{p[14]\}, \{1, 0, 0, -1\}] = \begin{pmatrix} -1 & -\frac{1}{2} & 0 & 0 & -\frac{3}{2} & \frac{5}{4} \\ -1 & -\frac{3}{2} & 0 & 0 & -\frac{1}{2} & \frac{5}{4} \\ 1 & \frac{3}{2} & 1 & 0 & \frac{1}{2} & -\frac{1}{4} \\ -1 & -\frac{1}{2} & -1 & -1 & -\frac{1}{2} & -\frac{3}{4} \\ 1 & \frac{1}{2} & 0 & 0 & \frac{1}{2} & -\frac{1}{4} \\ 1 & \frac{1}{2} & 0 & 1 & \frac{3}{2} & -\frac{1}{4} \end{pmatrix}. \quad (5.95)$$

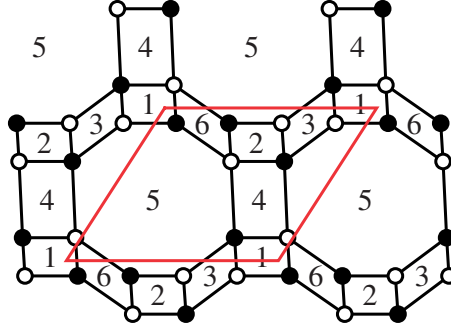


Figure 14: Brane tiling for toric phase c of dP_3 .

The brane tiling for toric phase c is in Fig. 14, with superpotential

$$W = X_{25}X_{53}^2X_{32} + X_{31}X_{15}X_{53}^1 + X_{56}^1X_{62}X_{24}X_{45}^1 + X_{56}^2X_{61}X_{14}X_{45}^2 + \\ - X_{25}X_{56}^2X_{62} - X_{61}X_{15}X_{56}^1 - X_{53}^1X_{32}X_{24}X_{45}^2 - X_{53}^2X_{31}X_{14}X_{45}^1. \quad (5.96)$$

The dimer model has 8 internal perfect matchings $\{p[7], \dots, p[14]\}$ and corresponding open string Kähler chambers. From the D6-charges we can infer that (5.94) is valid in the Kähler chamber of perfect matching $p[9]$ and that (5.95) is valid in the Kähler chamber of perfect matching $p[10]$. The wall in FI parameter space between the corresponding maximal dimensional chambers is

$$-\xi_1 - \xi_4 \geq 0, \quad -\xi_2 - \xi_4 \geq 0, \quad \xi_3 \geq 0, \quad -\xi_4 \geq 0, \quad \xi_5 = 0, \quad \xi_6 \geq 0. \quad (5.97)$$

Using either one of these mutated dictionaries, both at $\sigma < 0$ and $\sigma > 0$, or applying the Seiberg duality rules of [32] to the theory in phase d, we find a 3d quiver

theory in phase c with gauge ranks and bare CS levels

$$\mathbf{N} = (N, N, N, N, N - p, N) \quad (5.98)$$

$$\mathbf{k} = \left(-\frac{1}{2}p + q_3 - q_4, -\frac{1}{2}p + q_2 - q_1, p - q_3, -p + q_1 + q_4, 0, p - q_2\right) \quad (5.99)$$

so that the effective CS levels are

$$-\mathbf{k}^- = (-q_3 + q_4, -q_2 + q_1, q_3, -q_1 - q_4, 0, q_2) \quad (5.100)$$

$$+\mathbf{k}^+ = (-p + q_3 - q_4, -p + q_2 - q_1, 2p - q_3, -2p + q_1 + q_4, 0, 2p - q_2) . \quad (5.101)$$

Once again (5.84) ensures that the effective FI parameters of the gauge theory are in the cone (5.97) and therefore that the type IIA geometry (5.85) is reproduced.

5.5.3 Phase b of dP_3

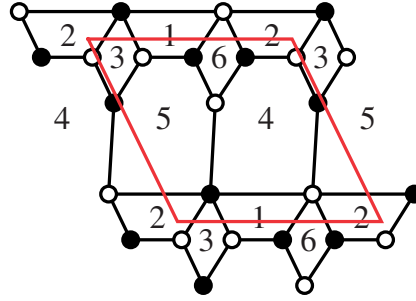


Figure 15: Brane tiling for toric phase b of dP_3 .

We next move to phase b of the dP_3 quiver by means of a Seiberg duality on gauge group 2 of the quiver of phase c. We see from the effective CS levels (5.100) that the Seiberg duality in question is maximally chiral if $0 \leq q_2 - q_1 \leq p$ (a double $M_{(2;L)}$ left mutation), whereas it is minimally chiral if $q_2 - q_1 < 0$ ($M_{(2;R)}/M_{(2;L)}$ mutation at $\sigma < 0/\sigma < 0$ resp.) or $q_2 - q_1 > p$ ($M_{(2;L)}/M_{(2;R)}$ mutation). As a consequence, three windows will be needed to cover the full class of geometries using toric phase b.

The brane tiling of toric phase b is in figure 15, with superpotential

$$\begin{aligned} W = & X_{31}X_{15}X_{53} + X_{42}X_{23}X_{34} + X_{56}X_{64}X_{45}^1 + X_{52}X_{26}X_{61}X_{14}X_{45}^2 + \\ & - X_{42}X_{26}X_{64} - X_{53}X_{34}X_{45}^2 - X_{56}X_{61}X_{15} - X_{14}X_{45}^1X_{52}X_{23}X_{31} . \end{aligned} \quad (5.102)$$

The dimer model has 7 internal perfect matchings $\{p[7], \dots, p[13]\}$ and corresponding open string Kähler chambers.

In the window $0 \leq q_2 - q_1 \leq p$, we are both at $\sigma < 0$ and $\sigma > 0$ on the Kähler wall between dictionaries $\{\{p[7]\}, \{-1, 0, 1, 0\}\}$ and $\{\{p[13]\}, \{-1, 0, 1, 1\}\}$, which gives the cone

$$\xi_2 \geq 0, \quad \xi_2 + \xi_3 \geq 0, \quad \xi_2 + \xi_6 \geq 0, \quad \xi_1 + \xi_4 \leq 0, \quad \xi_4 \leq 0, \quad \xi_5 = 0 \quad (5.103)$$

in FI parameter space. The ranks and bare levels of the CS theory are

$$\mathbf{N} = (N, N, N, N, N - p, N) \quad (5.104)$$

$$\mathbf{k} = \left(-\frac{p}{2} + q_3 - q_4, \frac{p}{2} + q_1 - q_2, \frac{p}{2} - q_1 + q_2 - q_3, -p + q_1 + q_4, 0, \frac{p}{2} - q_1\right) \quad (5.105)$$

so that the effective CS levels are

$$-\mathbf{k}^- = (-q_3 + q_4, -q_1 + q_2, q_1 - q_2 + q_3, -q_1 - q_4, 0, q_1) \quad (5.106)$$

$$+\mathbf{k}^+ = (-p + q_3 - q_4, p + q_1 - q_2, p - q_1 + q_2 - q_3, -2p + q_1 + q_4, 0, p - q_1) . \quad (5.107)$$

In order for the dictionaries we used in the derivation to be consistent, the effective FI parameters must lie in the cone (5.103): this indeed requires that $0 \leq q_2 - q_1 \leq p$.

We can leave the Kähler cone (5.103) either by going to $q_2 - q_1 \leq 0$ or to $q_2 - q_1 \geq p$, changing sign to the effective ξ_2 at $\sigma < 0$ or $\sigma > 0$: we end up on the wall between dictionaries $\{\{p[8]\}, \{0, 0, 0, -1\}\}$ and $\{\{p[13]\}, \{0, 0, 1, 1\}\}$, which gives the cone

$$\xi_2 \leq 0, \quad \xi_3 \geq 0, \quad \xi_6 \geq 0, \quad \xi_1 + \xi_4 \leq 0, \quad \xi_4 \leq 0, \quad \xi_2 + \xi_5 = 0 \quad (5.108)$$

in FI parameter space.

In the window $q_2 - q_1 \leq 0$, the field theory is on the wall (5.108) at $\sigma < 0$ and on the wall (5.103) at $\sigma > 0$. The ranks and bare levels of the CS theory are

$$\mathbf{N} = (N, N + q_1 - q_2, N, N, N - p, N) \quad (5.109)$$

$$\mathbf{k} = \left(-\frac{p}{2} + q_3 - q_4, \frac{p}{2} + q_1 - q_2, \frac{p}{2} - \frac{q_1}{2} + \frac{q_2}{2} - q_3, \right. \quad (5.110)$$

$$\left. -p + \frac{q_1}{2} + \frac{q_2}{2} + q_4, -\frac{q_1}{2} + \frac{q_2}{2}, \frac{p}{2} - \frac{q_1}{2} - \frac{q_2}{2}\right) \quad (5.111)$$

so that the effective CS levels are

$$-\mathbf{k}^- = (-q_3 + q_4, -q_1 + q_2, q_3, -q_2 - q_4, q_1 - q_2, q_2) \quad (5.112)$$

$$+\mathbf{k}^+ = (-p + q_3 - q_4, p + q_1 - q_2, p - q_1 + q_2 - q_3, -2p + q_1 + q_4, 0, p - q_1) . \quad (5.113)$$

The dictionaries we used are consistent when $q_2 - q_1 \leq 0$ in addition to (5.84).

Conversely, in the window $q_2 - q_1 \geq p$, the field theory is on the wall (5.103) at $\sigma < 0$ and on the wall (5.108) at $\sigma > 0$. The ranks and levels of the CS theory are

$$\mathbf{N} = (N, N - p - q_1 + q_2, N, N, N - p, N) \quad (5.114)$$

$$\mathbf{k} = \left(-\frac{p}{2} + q_3 - q_4, \frac{p}{2} + q_1 - q_2, p - \frac{q_1}{2} + \frac{q_2}{2} - q_3, \right. \quad (5.115)$$

$$\left. -\frac{3}{2}p + \frac{q_1}{2} + \frac{q_2}{2} + q_4, -\frac{p}{2} - \frac{q_1}{2} + \frac{q_2}{2}, p - \frac{q_1}{2} - \frac{q_2}{2}\right) \quad (5.116)$$

so that the effective CS levels are

$$-\mathbf{k}^- = (-q_3 + q_4, -q_1 + q_2, q_1 - q_2 + q_3, -q_1 - q_4, 0, q_2) \quad (5.117)$$

$$+\mathbf{k}^+ = (-p + q_3 - q_4, p + q_1 - q_2, 2p - q_3, -3p + q_2 + q_4, -p - q_1 + q_2, 2p - q_2) . \quad (5.118)$$

The dictionaries we used are consistent when $q_2 - q_1 \geq p$ in addition to (5.84).

Joining the three windows that we described in this subsection, we have provided M2-brane theories for the full class of $Y^{p,q}(dP_3)$ geometries with (5.84).

One can similarly Seiberg dualise to toric phase a, where again several windows associated to pairs of consistent dictionaries are needed. We leave that as an exercise to the readers and move instead to singular toric Fano surfaces.

5.6 $W\mathbb{CP}_{[1,1,2]}^2$

The toric diagram of the 2-parameter family of toric CY_4 cones over $Y^{p,q}(W\mathbb{CP}_{[1,1,2]}^2)$, shown in Fig. 4(d), is the convex hull of

$$(0, 0, 0), (0, 0, p), (0, 1, 2q), (1, 0, q), (2, -1, 0). \quad (5.119)$$

We are interested in geometric parameters in the range

$$0 \leq \frac{q}{2} \leq p \quad (5.120)$$

so that the points (5.119) are all external. The geometries are identified under the \mathbb{Z}_2 action $q \mapsto 2p - q$. We further restricted the CY_4 geometries to avoid the presence in the IIA reduction of D6-branes along the exceptional divisor $\mathbb{P}^1 \times \mathbb{C}$ corresponding to the toric point $(1, 0)$ That is achieved by picking its vertical coordinate to be q and the ones of $(1, -1)$ and $(1, 1)$ to be 0 and $2q$ respectively. The CY_3 fibre is only partially resolved because that exceptional \mathbb{P}^1 vanishes.

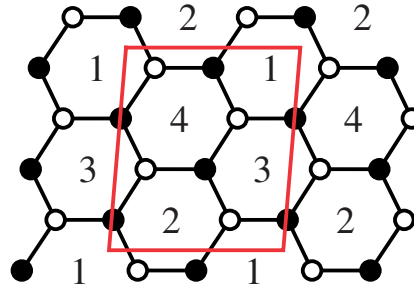


Figure 16: Brane tiling for $W\mathbb{CP}_{[1,1,2]}^2$.

The brane tiling for D-branes at the complex cone over $W\mathbb{CP}_{[1,1,2]}^2$ is in Fig. 16 and has superpotential

$$W = X_{12}^1 X_{24} X_{41}^1 + X_{31} X_{12}^2 X_{23}^1 + X_{34}^2 X_{42} X_{23}^2 + X_{41}^2 X_{13} X_{34}^1 + \quad (5.121)$$

$$- X_{12}^1 X_{23}^2 X_{31} - X_{13} X_{34}^2 X_{41}^1 - X_{34}^1 X_{42} X_{23}^1 - X_{41}^2 X_{12}^2 X_{24} .$$

The dimer model has 3 strictly external perfect matchings, 2 internal-external perfect matchings $\{p[4], p[5]\}$ and 4 strictly internal perfect matchings $\{p[6], \dots, p[9]\}$. There are 8 open string Kähler chambers, but we will not need to choose between $p[4]$ and $p[5]$ since the associated exceptional \mathbb{P}^1 will remain blown down in the CY_3 fibre.

A quiver CS theory for the whole class of $C(Y^{p,q}(W\mathbb{C}P_{[1,1,2]}^2))$ geometries can be proposed as follows. Both at $\sigma < 0$ and $\sigma > 0$ we are on the Kähler wall between the maximal dimensional chambers associated to perfect matchings $\{p[4], p[6]\}$, $\{p[4], p[7]\}$, $\{p[5], p[6]\}$ and $\{p[5], p[7]\}$, with suitable large volume monodromies. The intersection of these 4 Kähler chambers is the cone

$$\xi_2 = \xi_4 = 0, \quad \xi_1 = -\xi_3 \geq 0 \quad (5.122)$$

in FI parameter space. Using any of these dictionaries, both at $\sigma < 0$ and $\sigma > 0$, we find that the 3d quiver theory has ranks and bare CS levels

$$\mathbf{N} = (N, N, N, N - p) \quad (5.123)$$

$$\mathbf{k} = (p - q, 0, -p + q, 0) \quad (5.124)$$

so that the effective CS levels are

$$-\mathbf{k}^- = (q, 0, -q, 0) \quad (5.125)$$

$$+\mathbf{k}^+ = (2p - q, 0, -2p + q, 0). \quad (5.126)$$

The geometric inequalities (5.120) imply that the effective FI parameters belong to the cone (5.122) where all the four dictionaries that can be used to derive the 3d theory are valid. This guarantees that the semiclassical computation of the geometric branch of the moduli space reproduces the type IIA geometry.

5.7 PdP_2

The toric diagram of the 3-parameter family of toric CY_4 cones over $Y^{p,q_1,q_2}(PdP_2)$, shown in Fig. 4(f), is the convex hull of

$$(0, 0, 0), (0, 0, p), (-1, 0, 0), (0, 1, q_1), (1, 1, 2q_2), (1, 0, q_2), (1, -1, 0). \quad (5.127)$$

We are interested in geometric parameters in the range

$$0 \leq \frac{q_1}{3}, \frac{q_2}{2} \leq p \quad (5.128)$$

so that the points (5.127) are all external. The geometries are identified under $(q_1, q_2) \mapsto (3p - q_1, 2p - q_2)$. We restricted the CY_4 geometries to avoid D6-branes along noncompact toric divisors in the IIA background. The CY_3 fibre is only partially resolved.

The quiver diagram and brane tiling for D-branes at the complex cone over PdP_2 were shown in figures 1(a)-1(b). The superpotential is (2.9). As reviewed in section 2.1, the dimer model has 4 strictly external perfect matchings, 2 internal-external perfect

matchings $\{p[5], p[6]\}$ and 5 strictly internal perfect matchings $\{p[7], \dots, p[11]\}$. There are 10 open string Kähler chambers, but we will not need to choose between $p[5]$ and $p[6]$ since the associated exceptional \mathbb{P}^1 will remain blown down.

A quiver CS theory for the whole class of $C(Y^{p, q_1, q_2}(PdP_2))$ geometries can be proposed as follows. Both at $\sigma < 0$ and $\sigma > 0$ we are on the Kähler wall between the maximal dimensional chambers associated to perfect matchings $\{p[5], p[10]\}$, $\{p[6], p[10]\}$, $\{p[5], p[11]\}$ and $\{p[6], p[11]\}$ with suitable LVM's. The intersection of these 4 chambers is the cone

$$\xi_1 = -\xi_2 \geq 0, \quad \xi_1 + \xi_3 \geq 0, \quad \xi_5 = 0 \quad (5.129)$$

in FI parameter space. Using any of these dictionaries, both at $\sigma < 0$ and $\sigma > 0$, we find that the 3d quiver theory has ranks and bare CS levels

$$\mathbf{N} = (N, N, N, N, N - p) \quad (5.130)$$

$$\mathbf{k} = (p - q_2, -p + q_2, \frac{1}{2}p - q_1 + q_2, -\frac{1}{2}p + q_1 - q_2, 0) \quad (5.131)$$

so that the effective CS levels are

$$-\mathbf{k}^- = (q_2, -q_2, q_1 - q_2, -q_1 + q_2, 0) \quad (5.132)$$

$$+\mathbf{k}^+ = (2p - q_2, -2p + q_2, p - q_1 + q_2, -p + q_1 - q_2, 0). \quad (5.133)$$

The geometric inequalities (5.128) imply that the effective FI parameters belong to the cone (5.129) where all the four dictionaries that can be used to derive the 3d theory are valid. This guarantees that the semiclassical computation of the geometric branch of the moduli space reproduces the type IIA geometry.

5.8 PdP_{3b}

The toric diagram of the 4-parameter family of toric CY_4 cones over $Y^{p, q_1, q_2, q_3}(PdP_{3b})$, shown in Fig. 4(h), is the convex hull of

$$(0, 0, 0), (0, 0, p), (2, -1, 0), (1, -1, 0), (-1, 0, q_1), (-1, 1, q_2), (0, 1, 2q_3), (1, 0, q_3). \quad (5.134)$$

We are interested in geometric parameters in the range

$$0 \leq \frac{q_1 + q_3}{2}, \frac{q_2}{2}, \frac{q_1 + q_2}{3}, \frac{q_1 + 2q_3}{3} \leq p \quad (5.135)$$

so that the points (5.134) are all external. We avoided D6-branes along noncompact toric divisors in type IIA. The CY_3 fibre is only partially resolved.

5.8.1 Phase c of PdP_{3b}

Toric phase c of PdP_{3b} is specified by the brane tiling of Fig. 17, with superpotential

$$\begin{aligned} W = & X_{21}X_{16}X_{62}^1 + X_{24}X_{43}X_{32}^1 + X_{25}^1X_{53}X_{32}^2 + X_{51}X_{13}X_{35} + X_{54}X_{46}X_{62}^2X_{25}^2 \\ & - X_{21}X_{13}X_{32}^2 - X_{24}X_{46}X_{62}^1 - X_{25}^2X_{53}X_{32}^1 - X_{54}X_{43}X_{35} - X_{51}X_{16}X_{62}^2X_{25}^1. \end{aligned} \quad (5.136)$$

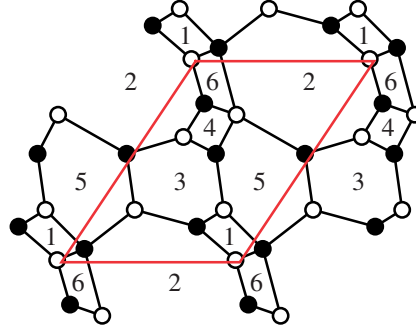


Figure 17: Brane tiling for toric phase c of PdP_{3b} .

The dimer model has 5 strictly external perfect matchings, 2 internal-external perfect matchings $\{p[6], p[7]\}$ and 8 strictly internal perfect matchings $\{p[8], \dots, p[15]\}$. Correspondingly there are 32 open string Kähler chambers, but we will not need to choose between $p[6]$ and $p[7]$ since the associated exceptional \mathbb{P}^1 will remain blown down.

A quiver CS theory for the whole class of $C(Y^{p, q_1, q_2, q_3}(PdP_{3b}))$ geometries can be proposed as follows. Both at $\sigma < 0$ and $\sigma > 0$ we are on the Kähler wall between the maximal dimensional chambers associated to internal perfect matchings $\{p[6], p[14]\}$, $\{p[7], p[14]\}$, $\{p[6], p[15]\}$ and $\{p[7], p[15]\}$, with suitable large volume monodromies in the dictionaries. The intersection of these four Kähler chambers is the cone

$$\xi_2 = \xi_3 + \xi_5 = 0, \quad \xi_5 \geq 0, \quad \xi_1 + \xi_5 \geq 0, \quad \xi_4 + \xi_5 \geq 0, \quad \xi_1 + \xi_4 \geq 0 \quad (5.137)$$

in FI parameter space. Using any of these dictionaries, both at $\sigma < 0$ and $\sigma > 0$, we find that the 3d quiver theory has ranks and bare CS levels

$$\mathbf{N} = (N, N - p, N, N, N, N) \quad (5.138)$$

$$\mathbf{k} = \left(\frac{1}{2}p - q_3, 0, -p + q_1 + q_3, \frac{1}{2}p - q_2 + q_3, p - q_1 - q_3, -p + q_2\right) \quad (5.139)$$

so that the effective CS levels are

$$-\mathbf{k}^- = (q_3, 0, -q_1 - q_3, q_2 - q_3, q_1 + q_3, -q_2) \quad (5.140)$$

$$+\mathbf{k}^+ = (p - q_3, 0, -2p + q_1 + q_3, p - q_2 + q_3, 2p - q_1 - q_3, -2p + q_2). \quad (5.141)$$

The geometric inequalities (5.135) imply that the effective FI parameters belong to the cone (5.137) where all the four dictionaries that can be used to derive the 3d theory are valid. This guarantees that the semiclassical computation of the geometric branch of the moduli space reproduces the type IIA geometry.

A maximally chiral Seiberg duality on node 6 (a double $M_{(6;L)}$ mutation on the dictionaries) leads to a quiver CS theory which is just the CP-conjugate of the original one, up to a relabelling $(4, 3) \leftrightarrow (1, 5)$: without relabelling, ranks and levels are

$$\mathbf{N} = (N, N - p, N, N, N, N) \quad (5.142)$$

$$\mathbf{k} = \left(-\frac{1}{2}p + q_2 - q_3, 0, -p + q_1 + q_3, -\frac{1}{2}p + q_3, p - q_1 - q_3, p - q_2\right) \quad (5.143)$$

and the superpotential is

$$W = x_{26}^2 x_{64} X_{43} X_{32}^1 + X_{25}^1 X_{53} X_{32}^2 + X_{51} X_{13} X_{35} + X_{54} M_{42}^2 X_{25}^2 + x_{61} M_{12}^2 x_{26}^1 + \\ - x_{26}^2 x_{61} X_{13} X_{32}^2 - X_{25}^2 X_{53} X_{32}^1 - X_{54} X_{43} X_{35} - X_{51} M_{12}^2 X_{25}^1 - x_{64} M_{42}^2 x_{26}^1 . \quad (5.144)$$

We can also reach toric phase b by a Seiberg duality on node 1 or 4. Let us consider duality on node 1 for definiteness. The duality is maximally chiral if $0 \leq q_3 \leq p$ (double right mutation $M_{(1;R)}$), whereas it is minimally chiral if $p < q_3 \leq \frac{3}{2}p$ (mutations $M_{(1;R)}$ at $r_0 < 0$ and $M_{(1;L)}$ at $r_0 > 0$), so the resulting theory in phase b needs more than one window to cover the whole class of geometries (5.135). We leave this and further duality to phase a as an exercise to the interested reader.

5.9 PdP_{3c}

The toric diagram of the 3-parameter family of toric CY_4 cones over $Y^{p, q_1, q_2}(PdP_{3c})$, shown in Fig. 4(i), is the convex hull of

$$(0, 0, 0), (0, 0, p), (1, 1, 0), (1, 0, 0), (1, -1, 0), \\ (-1, 0, q_1), (-1, 1, 2q_2), (0, 1, q_2). \quad (5.145)$$

We are interested in geometric parameters in the range

$$0 \leq \frac{q_1}{2}, q_2 \leq p \quad (5.146)$$

so that the points (5.145) are all external. We avoided D6-branes along noncompact toric divisors in the type IIA background.

5.9.1 Phase b of PdP_{3c}

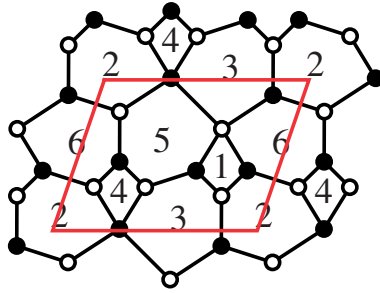


Figure 18: Brane tiling for toric phase b of PdP_{3c} .

Toric phase b of PdP_{3c} is specified by the brane tiling of Fig. 18, with superpotential

$$W = X_{31} X_{12} X_{23} + X_{34} X_{45} X_{53}^2 + X_{56} X_{62} X_{25} + X_{64} X_{42} X_{26} + X_{61} X_{15} X_{53}^1 X_{36} + \\ - X_{31} X_{15} X_{53}^2 - X_{36} X_{62} X_{23} - X_{56} X_{64} X_{45} - X_{61} X_{12} X_{26} - X_{25} X_{53}^1 X_{34} X_{42} . \quad (5.147)$$

The dimer model has 4 strictly external perfect matchings, 2 pairs of internal-external perfect matchings $\{p[5], p[6]\}$ and $\{p[7], p[8]\}$, and 7 strictly internal perfect matchings $\{p[9], \dots, p[15]\}$. Correspondingly there are 28 open string Kähler chambers, but we will not need to choose between internal-external perfect matching variables since the associated exceptional \mathbb{P}^1 's will remain blown down.

A quiver CS theory for the whole class of $C(Y^{p, q_1, q_2}(PdP_{3c}))$ geometries can be proposed as follows. Both at $\sigma < 0$ and $\sigma > 0$ we are on the Kähler wall between the maximal dimensional chambers associated to strictly internal perfect matchings $p[11]$ and $p[15]$, as well as on the wall between $p[5]$ and $p[6]$ and between $p[7]$ and $p[8]$, with suitable large volume monodromies in the dictionaries. The intersection of these eight Kähler chambers is the cone

$$\begin{aligned} \xi_3 &= \xi_1 + \xi_4 + \xi_5 = \xi_2 + \xi_4 = 0, \\ \xi_1 + \xi_5 &\leq 0, \quad \xi_5 \leq 0, \quad \xi_1 + \xi_2 + \xi_5 \leq 0, \quad \xi_2 + \xi_5 \leq 0. \end{aligned} \tag{5.148}$$

in FI parameter space. The 3d quiver theory has ranks and bare CS levels

$$\mathbf{N} = (N, N, N - p, N, N, N) \tag{5.149}$$

$$\mathbf{k} = \left(\frac{p}{2} - q_1 + q_2, -\frac{p}{2} + q_2, 0, \frac{p}{2} - q_2, -p + q_1, \frac{p}{2} - q_2\right) \tag{5.150}$$

so that the effective CS levels are

$$-\mathbf{k}^- = (q_1 - q_2, -q_2, 0, q_2, -q_1, q_2) \tag{5.151}$$

$$+\mathbf{k}^+ = (p - q_1 + q_2, -p + q_2, 0, p - q_2, -2p + q_1, p - q_2). \tag{5.152}$$

The geometric inequalities (5.146) ensure that the effective FI parameters belong to the cone (5.148) where all the eight dictionaries that can be used to derive the 3d theory are valid. Consequently the semiclassical computation of the geometric branch of the moduli space reproduces the type IIA geometry.

A single proposal for all the geometries can be made in toric phase a too: it is obtained by a maximally chiral Seiberg duality on node 4.

5.10 $WC\mathbb{P}_{[1,2,3]}^2$

The toric diagram of the 2-parameter family of toric CY_4 cones over $Y^{p, q}(WC\mathbb{P}_{[1,2,3]}^2)$, shown in Fig. 4(j), is the convex hull of

$$(0, 0, 0), (0, 0, p), (-1, 0, 0), (-1, 1, 0), (-1, 2, 0), (0, 1, q), (1, 0, 2q), (2, -1, 3q). \tag{5.153}$$

We impose that all the points (5.153) are external:

$$0 \leq q \leq p. \tag{5.154}$$

The geometries are identified under the \mathbb{Z}_2 action $q \mapsto p - q$. We restricted the CY_4 geometries to avoid the presence in the reduction to type IIA of D6-branes along non-compact toric divisors.

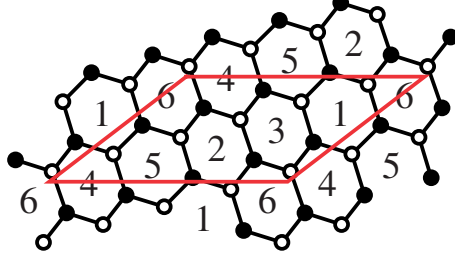


Figure 19: Brane tiling for $W\mathbb{C}\mathbb{P}^2_{[1,2,3]}$.

The brane tiling for D-branes at the complex cone over $W\mathbb{C}\mathbb{P}^2_{[1,2,3]}$ is in Fig. 19 and has superpotential

$$\begin{aligned}
W = & X_{12}X_{26}X_{61} + X_{24}X_{43}X_{32} + X_{35}X_{51}X_{13} + X_{41}X_{15}X_{54} + X_{56}X_{62}X_{25} + \\
& + X_{63}X_{34}X_{46} - X_{12}X_{25}X_{51} - X_{24}X_{46}X_{62} - X_{35}X_{54}X_{43} - X_{41}X_{13}X_{34} + \\
& - X_{56}X_{61}X_{15} - X_{63}X_{32}X_{26} .
\end{aligned} \tag{5.155}$$

The dimer model has 3 strictly external perfect matchings, internal-external perfect matchings $\{p[4], p[5]\}$, $\{p[6], p[7], p[8]\}$ and $\{p[9], p[10], p[11]\}$, and 6 strictly internal perfect matchings $\{p[12], \dots, p[17]\}$. There are 108 open string Kähler chambers, but we will not need to choose between internal-external perfect matching variables associated to the same lattice point, since the associated exceptional \mathbb{P}^1 will remain blown down in the CY_3 fibre.

A quiver CS theory for the whole class of $C(Y^{p,q}(W\mathbb{C}\mathbb{P}^2_{[1,2,3]}))$ geometries has ranks and bare CS levels

$$\mathbf{N} = (N, N, N, N, N, N - p) \tag{5.156}$$

$$\mathbf{k} = \left(\frac{p}{2} - q, 0, \frac{p}{2} - q, -\frac{p}{2} + q, -\frac{p}{2} + q, 0\right) \tag{5.157}$$

so that the effective CS levels are

$$-\mathbf{k}^- = (q, 0, q, -q, -q, 0) \tag{5.158}$$

$$+\mathbf{k}^+ = (p - q, 0, p - q, -p + q, -p + q, 0) . \tag{5.159}$$

The geometric inequalities (5.154) guarantee that the semiclassical computation of the geometric branch of the moduli space reproduces the type IIA geometry.

5.11 PdP_4

The toric diagram of the 4-parameter family of toric CY_4 cones over $Y^{p,q_1,q_2,q_3}(PdP_4)$, shown in Fig. 4(k), is the convex hull of

$$\begin{aligned}
& (0, 0, 0), (0, 0, p), (1, 1, 0), (1, 0, 0), (1, -1, 0), \\
& (0, -1, q_1), (-1, 0, q_2), (-1, 1, 2q_3), (0, 1, q_3).
\end{aligned} \tag{5.160}$$

We are interested in geometric parameters in the range

$$0 \leq \frac{q_1 + q_3}{2}, \frac{q_2}{2}, q_3, \frac{q_1 + q_2}{3} \leq p \quad (5.161)$$

so that the points (5.160) are all external. We avoided D6-branes along noncompact toric divisors in the type IIA background.

5.11.1 Phase c of PdP_4

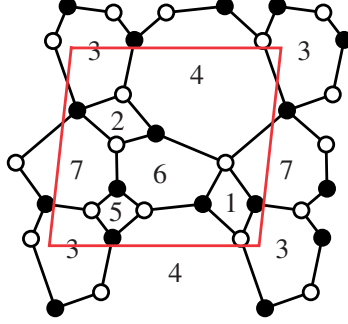


Figure 20: Brane tiling for toric phase c of PdP_4 .

Toric phase c of PdP_4 is specified by the brane tiling of Fig. 20, with superpotential

$$\begin{aligned} W = & X_{41}X_{13}X_{34}^1 + X_{42}X_{23}X_{34}^2 + X_{45}X_{56}X_{64}^1 + X_{67}X_{72}X_{26} + X_{75}X_{53}X_{37} + \\ & - X_{41}X_{16}X_{64}^1 - X_{42}X_{26}X_{64}^2 - X_{45}X_{53}X_{34}^2 - X_{67}X_{75}X_{56} - X_{71}X_{13}X_{37} + \\ & + X_{47}X_{71}X_{16}X_{64}^2 - X_{47}X_{72}X_{23}X_{34}^1 . \end{aligned} \quad (5.162)$$

The dimer model has 5 strictly external perfect matchings, 2 pairs of internal-external perfect matchings $\{p[6], p[7]\}$ and $\{p[8], p[9]\}$, and 12 strictly internal perfect matchings $\{p[10], \dots, p[21]\}$. Correspondingly there are 48 open string Kähler chambers, but we will not need to choose between internal-external perfect matching variables since the associated exceptional \mathbb{P}^1 's will remain blown down.

A quiver CS theory for the whole class of $C(Y^{p, q_1, q_2, q_3}(PdP_4))$ geometries can be proposed as follows. Both at $\sigma < 0$ and $\sigma > 0$ we are on the Kähler wall between the maximal dimensional chambers associated to strictly internal perfect matchings $p[10]$ and $p[21]$, as well as on the wall between $p[6]$ and $p[7]$ and between $p[8]$ and $p[9]$, with suitable large volume monodromies in the dictionaries. The intersection of these eight Kähler chambers is the cone

$$\begin{aligned} \xi_4 = \xi_1 + \xi_5 + \xi_6 = \xi_2 + \xi_3 + \xi_5 = 0, \quad \xi_3 \leq 0, \quad \xi_6 \leq 0, \\ \xi_1 + \xi_2 + \xi_3 + \xi_6 \leq 0, \quad \xi_1 + \xi_3 + \xi_6 \leq 0, \quad \xi_3 + \xi_5 + \xi_6 \leq 0, \quad \xi_2 + \xi_3 \leq 0. \end{aligned} \quad (5.163)$$

in FI parameter space. The 3d quiver theory has ranks and bare CS levels

$$\mathbf{N} = (N, N, N, N - p, N, N, N) \quad (5.164)$$

$$\mathbf{k} = \left(\frac{1}{2}p - q_2 + q_3, \frac{1}{2}p - q_1, -p + q_1 + q_3, 0, \frac{1}{2}p - q_3, -p + q_2, \frac{1}{2}p - q_3 \right) \quad (5.165)$$

so that the effective CS levels are

$$-\mathbf{k}^- = (q_2 - q_3, q_1, -q_1 - q_3, 0, q_3, -q_2, q_3) \quad (5.166)$$

$$+\mathbf{k}^+ = (p - q_2 + q_3, p - q_1, -2p + q_1 + q_3, 0, p - q_3, -2p + q_2, p - q_3) . \quad (5.167)$$

The geometric inequalities (5.161) ensure that the effective FI parameters belong to the cone (5.163) where all the eight dictionaries that can be used to derive the 3d theory are valid. Consequently the semiclassical computation of the geometric branch of the moduli space reproduces the type IIA geometry.

A single proposal for all the geometries can be made in toric phase a too: it is obtained by a maximally chiral Seiberg duality on node 5. More windows are needed in phase b.

5.12 PdP_{4b}

The toric diagram of the 3-parameter family of toric CY_4 cones over $Y^{p, q_1, q_2}(PdP_{4b})$, shown in Fig. 4(l), is the convex hull of

$$\begin{aligned} &(0, 0, 0), (0, 0, p), (-1, 2, 0), (0, 1, 0), (1, 0, 0), (2, -1, 0), \\ &(-1, 1, q_1), (-1, 0, 2q_2), (-1, 1, q_2) . \end{aligned} \quad (5.168)$$

We impose that all the points (5.168) are external:

$$0 \leq \frac{q_1 + q_2}{2}, q_2 \leq p . \quad (5.169)$$

The geometries are identified under the \mathbb{Z}_2 action $(q_1, q_2) \mapsto (p - q_1, p - q_2)$. We avoided D6-branes along noncompact toric divisors in IIA.

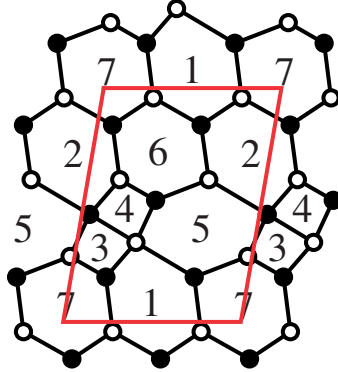


Figure 21: Brane tiling for PdP_{4b} .

The brane tiling for D-branes at the complex cone over PdP_{4b} is in Fig. 21 and has superpotential

$$\begin{aligned} W = & X_{21}X_{17}X_{72} + X_{42}X_{26}X_{64} + X_{56}X_{62}X_{25} + X_{67}X_{71}X_{16} + \\ & + X_{75}X_{53}X_{37} + X_{13}X_{34}X_{45}X_{51} - X_{13}X_{37}X_{71} - X_{16}X_{62}X_{21} + \\ & - X_{56}X_{64}X_{45} - X_{67}X_{72}X_{26} - X_{75}X_{51}X_{17} - X_{25}X_{53}X_{34}X_{42} . \end{aligned} \quad (5.170)$$

The dimer model has 4 strictly external perfect matchings, 2 + 3 + 3 internal-external perfect matchings and 9 strictly internal perfect matchings.

The quiver CS theory for the whole class of $C(Y^{p, q_1, q_2}(PdP_{4b}))$ geometries has ranks and bare CS levels

$$\mathbf{N} = (N, N, N, N, N - p, N, N) \quad (5.171)$$

$$\mathbf{k} = \left(\frac{p}{2} - q_2, -\frac{p}{2} + q_2, \frac{p}{2} - q_1, -\frac{p}{2} + q_1, 0, \frac{p}{2} - q_2, -\frac{p}{2} + q_2\right) \quad (5.172)$$

so that the effective CS levels are

$$-\mathbf{k}^- = (q_2, -q_2, q_1, -q_1, 0, q_2, -q_2) \quad (5.173)$$

$$+\mathbf{k}^+ = (p - q_2, -p + q_2, p - q_1, -p + q_1, 0, p - q_2, -p + q_2). \quad (5.174)$$

The geometric inequalities (5.169) guarantee that the semiclassical computation of the geometric branch of the moduli space reproduces the type IIA geometry.

5.13 PdP_5

The toric diagram of the 3-parameter family of toric CY_4 cones over $Y^{p, q_1, q_2}(PdP_5)$, shown in Fig. 4(m), is the convex hull of

$$\begin{aligned} &(0, 0, 0), (0, 0, p), (1, 1, 0), (1, 0, 0), (1, -1, 0), (0, -1, q_1), \\ &(-1, -1, 2q_1), (-1, 0, q_1 + q_2), (-1, 1, 2q_2), (0, 1, q_1). \end{aligned} \quad (5.175)$$

We impose that all the points (5.175) are external:

$$0 \leq q_1, q_2 \leq p. \quad (5.176)$$

The CY_4 geometries are identified under the \mathbb{Z}_2 action $(q_1, q_2) \mapsto (p - q_1, p - q_2)$. We restricted them to avoid D6-branes along noncompact toric divisors in IIA.

There are 4 toric phases for the D-brane quiver gauge theory. Using each of them it is possible to find a single proposal for a CS quiver gauge theory that is valid for the whole class of CY_4 geometries. In the following we will present only toric phase a.

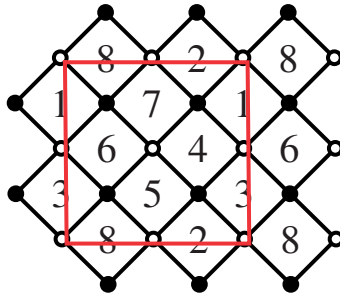


Figure 22: Brane tiling for toric phase a of PdP_5 .

The brane tiling in phase a for D-branes at the complex cone over PdP_5 , which is a $\mathbb{Z}_2 \times \mathbb{Z}_2$ orbifold of the conifold, is in Fig. 22 and has superpotential

$$W = X_{23}X_{38}X_{81}X_{12} + X_{41}X_{16}X_{63}X_{34} + X_{67}X_{74}X_{45}X_{56} + X_{85}X_{52}X_{27}X_{78} + \\ - X_{27}X_{74}X_{41}X_{12} - X_{45}X_{52}X_{23}X_{34} - X_{63}X_{38}X_{85}X_{56} - X_{81}X_{16}X_{67}X_{78} . \quad (5.177)$$

The dimer model has 4 strictly external perfect matchings, 2+2+2+2 internal-external perfect matchings and 12 strictly internal perfect matchings. The quiver CS theory for the whole class of $C(Y^{p, q_1, q_2}(PdP_5))$ geometries has ranks and bare CS levels

$$\mathbf{N} = (N, N, N, N, N, N, N, N - p) \quad (5.178)$$

$$\mathbf{k} = \left(\frac{p}{2} - q_1, q_1 - q_2, -\frac{p}{2} + q_2, 0, \frac{p}{2} - q_1, q_1 - q_2, -\frac{p}{2} + q_2, 0\right) \quad (5.179)$$

so that the effective CS levels are

$$-\mathbf{k}^- = (q_1, -q_1 + q_2, -q_2, 0, q_1, -q_1 + q_2, -q_2, 0) \quad (5.180)$$

$$+\mathbf{k}^+ = (p - q_1, q_1 - q_2, -p + q_2, 0, p - q_1, q_1 - q_2, -p + q_2, 0) . \quad (5.181)$$

The geometric inequalities (5.176) guarantee that the semiclassical computation of the geometric branch of the moduli space reproduces the type IIA geometry.

5.14 PdP_{5b}

The toric diagram of the 3-parameter family of toric CY_4 cones over $Y^{p, q_1, q_2}(PdP_{5b})$, shown in Fig. 4(n), is the convex hull of

$$(0, 0, 0), (0, 0, p), (-1, 1, 0), (0, 1, 0), (1, 1, 0), (2, 1, 0), \\ (1, 0, q_1), (0, -1, 2q_1), (-1, -1, 2q_2), (-1, 0, q_2). \quad (5.182)$$

We impose that all the points (5.182) are external:

$$0 \leq q_1, q_2 \leq p . \quad (5.183)$$

The CY_4 geometries are identified under the \mathbb{Z}_2 action $(q_1, q_2) \mapsto (p - q_1, p - q_2)$. We restricted them to avoid D6-branes along noncompact toric divisors in IIA.

The D-brane quiver gauge theory has 2 toric phases. Here we only introduce phase b, which allows us to propose a theory that is valid for the whole class of geometries.

The brane tiling in phase a for D-branes at the complex cone over PdP_{5b} , which is a \mathbb{Z}_2 orbifold of the real cone over the $SE_5 L^{1,3,1}$, is in Fig. 23 and has superpotential

$$W = X_{31}X_{18}X_{83} + X_{42}X_{23}X_{34} + X_{53}X_{37}X_{75} + X_{67}X_{72}X_{26} + X_{78}X_{81}X_{17} + \\ + X_{86}X_{64}X_{48} + X_{14}X_{45}X_{56}X_{61} - X_{14}X_{48}X_{81} - X_{42}X_{26}X_{64} - X_{53}X_{34}X_{45} \\ - X_{67}X_{75}X_{56} - X_{78}X_{83}X_{37} - X_{86}X_{61}X_{18} - X_{17}X_{72}X_{23}X_{31} . \quad (5.184)$$

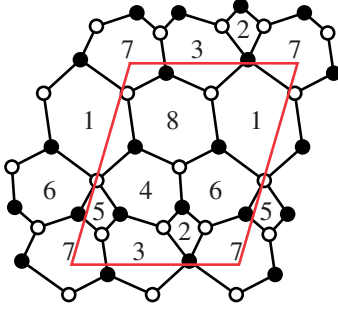


Figure 23: Brane tiling for toric phase b of PdP_{5b} .

The dimer model has 4 strictly external perfect matchings, 3+3+2+2 internal-external perfect matchings and 14 strictly internal perfect matchings. The quiver CS theory for the whole class of $C(Y^{p, q_1, q_2}(PdP_{5b}))$ geometries has ranks and bare CS levels

$$\mathbf{N} = (N - p, N, N, N, N, N, N, N) \quad (5.185)$$

$$\mathbf{k} = (0, -q_1 + q_2, -\frac{p}{2} + q_1, \frac{p}{2} - q_1, q_1 - q_2, -\frac{p}{2} + q_2, \frac{p}{2} - q_2, 0) \quad (5.186)$$

so that the effective CS levels are

$$-\mathbf{k}^- = (0, q_1 - q_2, -q_1, q_1, -q_1 + q_2, -q_2, q_2, 0) \quad (5.187)$$

$$+\mathbf{k}^+ = (0, -q_1 = q_2, -p + q_1, p - q_1, q_1 - q_2, -p + q_2, p - q_2, 0). \quad (5.188)$$

The geometric inequalities (5.183) guarantee that the semiclassical computation of the geometric branch of the moduli space reproduces the type IIA geometry.

5.15 $W\mathbb{C}\mathbb{P}_{[2,2,4]}^2$

The toric diagram of the 2-parameter family of toric CY_4 cones over $Y^{p, q}(W\mathbb{C}\mathbb{P}_{[2,2,4]}^2)$, shown in Fig. 4(o), is the convex hull of

$$\begin{aligned} & (0, 0, 0), (0, 0, p), (-1, 1, 0), (0, 1, 0), (1, 1, 0), (2, 1, 0), (3, 1, 0), \\ & (1, 0, q), (-1, -1, 2q), (-1, 0, q). \end{aligned} \quad (5.189)$$

We impose that all the points (5.189) are external:

$$0 \leq q \leq p. \quad (5.190)$$

The geometries are identified under the \mathbb{Z}_2 action $q \mapsto p - q$. We restricted the CY_4 geometries to avoid D6-branes along noncompact toric divisors in type IIA.

The brane tiling for D-branes at the complex cone over $W\mathbb{C}\mathbb{P}_{[2,2,4]}^2$ is in Fig. 24 and has superpotential

$$\begin{aligned} W = & X_{17}X_{72}X_{21} + X_{28}X_{81}X_{12} + X_{31}X_{14}X_{43} + X_{42}X_{23}X_{34} + \\ & + X_{53}X_{36}X_{65} + X_{64}X_{45}X_{56} + X_{75}X_{58}X_{87} + X_{86}X_{67}X_{78} + \\ & - X_{17}X_{78}X_{81} - X_{28}X_{87}X_{72} - X_{31}X_{12}X_{23} - X_{42}X_{21}X_{14} + \\ & - X_{53}X_{34}X_{45} - X_{64}X_{43}X_{36} - X_{75}X_{56}X_{67} - X_{86}X_{65}X_{58}. \end{aligned} \quad (5.191)$$

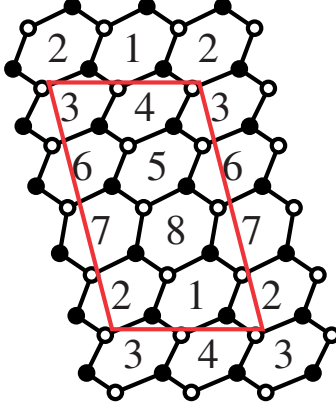


Figure 24: Brane tiling for $W\mathbb{C}\mathbb{P}^2_{[2,2,4]}$.

A quiver CS theory for the $C(Y^{p,q}(W\mathbb{C}\mathbb{P}^2_{[2,2,4]}))$ geometries has ranks and bare CS levels

$$\mathbf{N} = (N, N, N - p, N, N, N, N, N) \quad (5.192)$$

$$\mathbf{k} = \left(\frac{p}{2} - q, -\frac{p}{2} + q, 0, 0, -\frac{p}{2} + q, \frac{p}{2} - q, 0, 0\right) \quad (5.193)$$

so that the effective CS levels are

$$-\mathbf{k}^- = (q, -q, 0, 0, -q, q, 0, 0) \quad (5.194)$$

$$+\mathbf{k}^+ = (p - q, -p + q, 0, 0, -p + q, p - q, 0, 0) . \quad (5.195)$$

The geometric inequalities (5.190) guarantee that the semiclassical computation of the geometric branch of the moduli space reproduces the type IIA geometry.

5.16 $W\mathbb{C}\mathbb{P}^2_{[3,3,3]}$

The toric diagram of the 2-parameter family of toric CY_4 cones over $Y^{p,q}(W\mathbb{C}\mathbb{P}^2_{[3,3,3]})$, shown in Fig. 4(p), is the convex hull of

$$\begin{aligned} &(0, 0, 0), (0, 0, p), (-1, -1, 0), (-1, 0, 0), (-1, 1, 0), (-1, 2, 0), \\ &(0, 1, q), (1, 0, 2q), (2, -1, 3q), (1, -1, 2q), (0, -1, q) . \end{aligned} \quad (5.196)$$

We impose that all the points (5.196) are external:

$$0 \leq q \leq p . \quad (5.197)$$

The geometries are identified under the \mathbb{Z}_2 action $q \mapsto p - q$. We restricted the CY_4 geometries to avoid D6-branes along noncompact toric divisors in type IIA.

The brane tiling for D-branes at the complex cone over $W\mathbb{C}\mathbb{P}^2_{[3,3,3]}$ is in Fig. 25 and has superpotential

$$\begin{aligned} W = &X_{15}X_{56}X_{61} + X_{29}X_{91}X_{12} + X_{31}X_{18}X_{83} + X_{42}X_{23}X_{34} + X_{53}X_{37}X_{75} + \\ &+ X_{67}X_{72}X_{26} + X_{78}X_{89}X_{97} + X_{86}X_{64}X_{48} + X_{94}X_{45}X_{59} - X_{15}X_{59}X_{91} + \\ &- X_{29}X_{97}X_{72} - X_{31}X_{12}X_{23} - X_{42}X_{26}X_{64} - X_{53}X_{34}X_{45} - X_{67}X_{75}X_{56} + \\ &- X_{78}X_{83}X_{37} - X_{86}X_{61}X_{18} - X_{94}X_{48}X_{89} . \end{aligned} \quad (5.198)$$

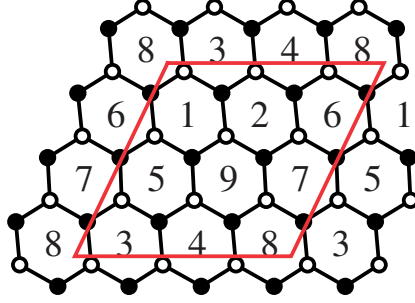


Figure 25: Brane tiling for $W\mathbb{C}\mathbb{P}^2_{[3,3,3]}$.

A quiver CS theory for the whole class of $C(Y^{p,q}(W\mathbb{C}\mathbb{P}^2_{[3,3,3]}))$ geometries has ranks and bare CS levels

$$\mathbf{N} = (N, N, N, N, N, N, N, N - p, N) \quad (5.199)$$

$$\mathbf{k} = \left(-\frac{p}{2} + q, 0, \frac{p}{2} - q, -\frac{p}{2} + q, 0, \frac{p}{2} - q, -\frac{p}{2} + q, 0, \frac{p}{2} - q\right) \quad (5.200)$$

so that the effective CS levels are

$$-\mathbf{k}^- = (-q, 0, q, -q, 0, q, -q, 0, q) \quad (5.201)$$

$$+\mathbf{k}^+ = (-p + q, 0, p - q, -p + q, 0, p - q, -p + q, 0, p - q). \quad (5.202)$$

The geometric inequalities (5.197) guarantee that the semiclassical computation of the geometric branch of the moduli space reproduces the type IIA geometry.

6. Partial resolutions and Higgsing

In this section we study partial or complete resolutions of the CY_4 cones over $Y^{p,q}(B_4)$ from the perspective of the moduli space of the M2-brane field theories that we proposed. Since for any toric Fano B_4 we found at least a toric phase in which the conformal field theory could be derived using the same dictionaries at r_0 negative and positive, we restrict our attention to such models. Then the ranks of the gauge groups all equal N , except for the group associated to the D6 wrapped on B_4 , whose rank is $N - p$, and which we relabel to be node 1 in the quiver. Following [14], we can generalise the analysis of the geometric branch of the moduli space in section 4, allowing bare FI parameters ξ_i and common extra p eigenvalues for the $G - 1$ $U(N)$ gauge groups:

$$\begin{aligned} \sigma_1 &= \text{diag}(\sigma_1, \dots, \sigma_{N-p}) \\ \sigma_i &= \text{diag}(\sigma_1, \dots, \sigma_{N-p}, \tilde{\sigma}_1, \dots, \tilde{\sigma}_p), \quad \forall i = 2, \dots, p. \end{aligned} \quad (6.1)$$

The extra eigenvalues $\tilde{\sigma}_a$ of σ_i parametrise the location of the p wrapped $\overline{D6}$ -branes along the $\sigma = r_0$ real line and modify the real masses of bifundamental matter fields, low energy modes of open strings stretched between D-branes separated in the \mathbb{R} direction.

Integrating out these massive chiral multiplets shifts the CS levels at one loop and affects the effective FI parameters. The 1-loop effective FI parameters for the Cartan $U(1)$'s are

$$\begin{aligned}\xi_1^{eff}(\sigma_a) &= \xi_1 \\ \xi_i^{eff}(\sigma_a) &= \xi_i + k_i \sigma_a + \frac{1}{2} A_{i1} \sum_{\tilde{b}=1}^p |\sigma_a - \tilde{\sigma}_{\tilde{b}}| \quad (i = 2, \dots, p) \\ \xi_i^{eff}(\tilde{\sigma}_{\tilde{a}}) &= \xi_i^{eff}(\sigma_a)|_{\sigma_a \rightarrow \tilde{\sigma}_{\tilde{a}}} \quad (i = 2, \dots, p).\end{aligned}\tag{6.2}$$

These effective FI parameters appear in D-term equations involving chiral superfields with vanishing real mass. The D-term equations split into two sets: those for the first $N - p$ eigenvalues, each one giving a $U(1)^G$ quiver of massless fields which describes a regular D2-brane probing the type IIA geometry; those for the extra p eigenvalues, each one giving a $U(1)^{G-1}$ quiver of massless fields, lacking node 1 and the fields charged under it, which describes a D2- $\overline{D6}$ bound state with a mobile D2 on the $\overline{D6}$ [14].

Let us consider the $U(1)^{G-1}$ quiver first. Since no matter is charged under its diagonal $U(1)$, a necessary conditions for having D-flat solutions is

$$0 = \sum_{i=2}^G \xi_i^{eff}(\tilde{\sigma}_{\tilde{a}}) = \sum_{i=2}^G \xi_i = \sum_{i=2}^G \xi_i^{eff}(\sigma_a) \implies \xi_1 = 0.\tag{6.3}$$

Demanding that the D-terms of the $U(1)^{G-1}$ subquiver can be solved restricts the effective FI parameters $\xi_i^{eff}(\tilde{\sigma}_{\tilde{a}})$, $i = 2, \dots, G$, to belong to its Kähler cone, a subcone of the Kähler cone of the full $U(1)^G$ quiver theory.

We leave a general analysis of the Kähler cone of the $U(1)^{G-1}$ subquivers and of the full nonabelian theory to future work, and we content ourselves here with a simple example of such an analysis. Let us then consider the field theory for M2-branes probing $C(Y^{p, q_1, q_2}(\mathbb{F}_0))$ of section 5.2.1 as a concrete example. The D-term equations for the $U(1)^3$ subquiver for a D2- $\overline{D6}$ bound state read

$$\xi_2^{eff}(\tilde{\sigma}_{\tilde{a}}) = \sum_{i=1}^2 |\tilde{x}_{23}^j|^2\tag{6.4}$$

$$\xi_3^{eff}(\tilde{\sigma}_{\tilde{a}}) = - \sum_{i=1}^2 |\tilde{x}_{23}^j|^2 + \sum_{i=1}^2 |\tilde{x}_{34}^j|^2\tag{6.5}$$

$$\xi_4^{eff}(\tilde{\sigma}_{\tilde{a}}) = - \sum_{i=1}^2 |\tilde{x}_{34}^j|^2\tag{6.6}$$

therefore we need the effective CS levels $\xi_i^{eff}(\tilde{\sigma}_{\tilde{a}})$ to belong to the cone

$$\xi_2^{eff}(\tilde{\sigma}_{\tilde{a}}) \geq 0, \quad \xi_4^{eff}(\tilde{\sigma}_{\tilde{a}}) \leq 0 \quad \forall \tilde{\sigma}_{\tilde{a}}, \quad \tilde{a} = 1, \dots, p.\tag{6.7}$$

The effective FI parameters $\xi_i^{eff}(\sigma)$ of the $U(1)^4$ D2-brane quiver are

$$\xi_1^{eff}(\sigma) = \xi_1 = 0 \tag{6.8}$$

$$\xi_2^{eff}(\sigma) = \xi_2 + (p - q_1)\sigma + \sum_{\tilde{a}=1}^p |\sigma - \tilde{\sigma}_{\tilde{a}}| \tag{6.9}$$

$$\xi_3^{eff}(\sigma) = \xi_3 + (q_1 - q_2)\sigma \tag{6.10}$$

$$\xi_4^{eff}(\sigma) = \xi_4 + (q_2 - p)\sigma - \sum_{\tilde{a}=1}^p |\sigma - \tilde{\sigma}_{\tilde{a}}|. \tag{6.11}$$

$\xi_2^{eff}(\sigma)$ and $\xi_4^{eff}(\sigma)$ take their minimum and maximum respectively at $\sigma = \tilde{\sigma}_{\tilde{a}}$ for some special \tilde{a} , therefore (6.7) implies the same inequalities for $\xi_i^{eff}(\sigma)$: we have learned that the effective FI parameters are forced to remain on the Kähler wall (5.28) associated to the dictionaries used to derive the superconformal theory. Consequently, the semi-classical moduli space of the gauge theory matches the type IIA geometry, as long as the GLSM of the fibred $CY_3 \tilde{Y}(r_0)$ is in a geometric phase.

This last comment deserves a more detailed explanation. Recall that in the derivation of the field theory we had to require the type IIA background to be in a geometric phase of the GLSM. That constrained the conical CY_4 geometry in M-theory to satisfy inequalities like (5.17), and also its partial resolutions. For instance, consider sending to infinity the volume of an exceptional \mathbb{P}^1 's in the $\mathbb{C}^2/\mathbb{Z}_p$ fibre to reduce $p \rightarrow p - 1$ and remove the point s_p from the toric diagram. Iterating this process, at some point the inequality (5.17) will be violated. In type IIA, after sending too many $\overline{D6}$ -branes to infinity, the GLSM of the fibred $CY_3 \tilde{Y}(r_0)$ is no longer in a geometric phase for all r_0 . This has a neat counterpart in field theory: if we try to increase the $\tilde{\sigma}$ eigenvalues accordingly, the effective FI parameters $\xi_i^{eff}(\tilde{\sigma}_{\tilde{a}})$ at some point leave the Kähler cone of the $U(1)^{G-1} = U(1)^3$ subquiver (6.7) and the gauge theory is no longer in a supersymmetric vacuum. Hence the quiver gauge theory only probes partial resolutions of the CY_4 that keep the $\tilde{Y}(r_0)$ GLSM in a geometric phase, due to the extra p components of the D-term equations for the $U(1)^{G-1}$ subquiver.²⁴

6.1 Higgsings

In the remainder of this section we will keep the $p \overline{D6}$ -branes on top of each other, $\tilde{\sigma}_{\tilde{a}} = 0$, and consider instead partial resolutions of the exceptional B_4 surface. In field theory this is achieved by turning on a VEV for a bifundamental which is uncharged under the $\overline{D6}$ gauge group, together with bare FI parameters so that the D-term equations are solved. We will only consider some representative Higgsings among models studied in section 5. More general Higgsings leading to noncompact D6-branes in type IIA will be analysed elsewhere [72].

²⁴This corrects the claim made in [14] that the quiver gauge theory can describe in its supersymmetric moduli space all the toric crepant resolutions of the CY_4 cone. We thank Francesco Benini for discussions on this point.

Higgsing phase d of dP_3 to phase b of dP_2

Consider the theory for phase d of dP_3 with bare FI parameters $\xi_6 = -\xi_1 \equiv \xi > 0$, and the VEV $\langle X_{61} \rangle = \xi I_{N \times N}$ so that D-term equations are solved. Integrating out massive matter leads to a low energy CS quiver theory for phase b of dP_2 , with the brane tiling in figure 12, gauge ranks and bare CS levels

$$\mathbf{N} = (N, N, N, N, N - p) \quad (6.12)$$

$$\mathbf{k} = \left(-\frac{1}{2}p + q_1 - q_2 + q_3, -\frac{3}{2}p + q_2 + q_4, p - q_3, p - q_1 - q_4, 0\right). \quad (6.13)$$

We can get rid of one of the q parameters by the redefinition

$$q_1 + q_4 = q'_1 \in [0, 2p], \quad q_2 + q_4 = q'_2 \in [0, 3p], \quad (6.14)$$

so that the bare CS levels become

$$\mathbf{k} = \left(-\frac{1}{2}p + q'_1 - q'_2 + q_3, -\frac{3}{2}p + q'_2, p - q_3, p - q'_1, 0\right). \quad (6.15)$$

This is nothing but the quiver CS theory for M2-branes at $C(Y^{p, q'_1, q'_2, q_3}(dP_2))$ presented in section 5.4.2, that uses toric phase b of dP_2 .

Higgsing phase c of dP_3 to phase a of dP_2

Consider the theory for phase c of dP_3 with bare FI parameters $\xi_6 = -\xi_1 \equiv \xi > 0$, and the VEV $\langle X_{61} \rangle = \xi I_{N \times N}$ so that D-term equations are solved. Integrating out massive matter leads to a low energy CS quiver theory for phase a of dP_2 , with the brane tiling in figure 11, gauge ranks and bare CS levels

$$\mathbf{N} = (N, N, N, N, N - p) \quad (6.16)$$

$$\mathbf{k} = \left(\frac{1}{2}p - q_2 + q_3 - q_4, -\frac{1}{2}p - q_1 + q_2, p - q_3, -p + q_1 + q_4, 0\right). \quad (6.17)$$

As in the (Seiberg dual) previous section, we redefine

$$q_1 + q_4 = q'_1 \in [0, 2p], \quad q_2 + q_4 = q'_2 \in [0, 3p], \quad (6.18)$$

so that the bare CS levels become

$$\mathbf{k} = \left(\frac{1}{2}p - q'_2 + q_3, -\frac{1}{2}p - q'_1 + q'_2, p - q_3, -p + q'_1, 0\right). \quad (6.19)$$

This is nothing but the quiver CS theory of section 5.4.1 for M2-branes probing the real cone over $Y^{p, q'_1, q'_2, q_3}(dP_2)$, that uses toric phase a of dP_2 .

Higgsing phases a and b of dP_2 to dP_1

Consider the theory for phase a of dP_2 of section 5.4.1, with bare FI parameters $\xi_3 = -\xi_1 \equiv \xi > 0$, and the VEV $\langle X_{31} \rangle = \xi I_{N \times N}$ so that D-term equations are solved. Integrating out massive matter and relabelling gauge groups $(1/3, 2, 4, 5) \rightarrow (1, 3, 4, 2)$ leads to the CS quiver theory for $C(Y^{p, q_1, q_2}(dP_1))$ of section 5.3, with ranks and levels

$$\mathbf{N} = (N, N - p, N, N) \quad (6.20)$$

$$\mathbf{k} = \left(\frac{3p}{2} - q_2, 0, -\frac{p}{2} - q_1 + q_2, -p + q_1 \right) . \quad (6.21)$$

Similarly, one can consider as a starting point the (Seiberg dual) theory of section 5.4.2 in phase b of dP_2 . Following the same Higgsing one gets to a quiver for dP_1 , the Seiberg dual (for node 4) of the previous one. That is the same quiver theory up to relabelling and a CP transformation that reverses arrows and changes sign to CS levels.

Higgsing phase a of dP_2 to phase a of \mathbb{F}_0

Consider again the theory for phase a of dP_2 , now with bare FI parameters $\xi_1 = -\xi_2 \equiv \xi > 0$, and the VEV $\langle X_{12} \rangle = \xi I_{N \times N}$ so that D-term equations are solved. Integrating out massive matter and relabelling gauge groups $(1/2, 3, 4, 5) \rightarrow (3, 2, 4, 1)$ leads to the CS quiver theory for $C(Y^{p, q_3, q_1}(\mathbb{F}_0))$ in phase a of section 5.2.1, with ranks and levels

$$\mathbf{N} = (N - p, N, N, N) \quad (6.22)$$

$$\mathbf{k} = (0, p - q_3, q_3 - q_1, -p + q_1) . \quad (6.23)$$

Higgsing phase b of dP_2 to phase b of \mathbb{F}_0

We can follow the same Higgsing in the Seiberg dual quiver, in phase b of dP_2 , with bare FI parameters $\xi_1 = -\xi_2 \equiv \xi > 0$ and the VEV $\langle X_{12} \rangle = \xi I_{N \times N}$ solving D-term equations. Relabelling gauge groups $(1/2, 3, 4, 5) \rightarrow (3, 2, 4, 1)$ leads to the CS quiver theory for $C(Y^{p, q_3, q_1}(\mathbb{F}_0))$ in phase b of section 5.2.2, with ranks and levels

$$\mathbf{N} = (N - p, N, N, N) \quad (6.24)$$

$$\mathbf{k} = (0, p - q_3, -2p + q_1 + q_3, p - q_1) . \quad (6.25)$$

Higgsing the dP_1 quiver to the dP_0 quiver

Finally consider the theory for M2-branes at $C(Y^{p, q_1, q_2}(dP_1))$ of section 5.3, with bare FI parameters $\xi_3 = -\xi_4 \equiv \xi > 0$, and the D-flat VEV $\langle X_{34} \rangle = \xi I_{N \times N}$. The resulting low energy theory is the CS quiver theory for M2-branes at $C(Y^{p, q_2}(dP_0))$ of section 5.1, with the brane tiling of figure 7(b) and ranks and bare CS levels

$$\mathbf{N} = (N, N - p, N) \quad (6.26)$$

$$\mathbf{k} = \left(\frac{3}{2}p - q_2, 0, -\frac{3}{2}p + q_2 \right) . \quad (6.27)$$

Higgsing phase c of PdP_4 to phase c of PdP_{3b}

Consider the theory for phase c of PdP_4 of section 5.11, with bare FI parameters $\xi_7 = -\xi_1 \equiv \xi > 0$ and the VEV $\langle X_{71} \rangle = \xi I_{N \times N}$ that solves D-term equations. After integrating out massive matter, relabelling gauge groups $(1/7, 2, 3, 4, 5, 6) \rightarrow (5, 4, 6, 2, 1, 3)$ and redefining

$$q_2 = q'_1 + q'_3 \in [0, 2p], \quad q_1 + q_3 = q'_2 \in [0, 2p], \quad q_1 = q'_2 - q'_3 \in [0, 2p] \quad (6.28)$$

we get to the CS quiver theory for phase c of PdP_{3b} of section 5.8.1, the worldvolume theory on M2-branes probing $C(Y^p, q'_1, q'_2, q'_3(PdP_{3b}))$.

Higgsing phase c of PdP_4 to phase b of PdP_{3c}

Consider again the theory for phase c of PdP_4 of section 5.11, now with bare FI parameters $\xi_2 = -\xi_3 \equiv \xi > 0$ and the VEV $\langle X_{23} \rangle = \xi I_{N \times N}$ solving D-term equations. After integrating out massive matter, relabelling gauge groups $(1, 2/3, 4, 5, 6, 7) \rightarrow (1, 2, 3, 4, 5, 6)$ and redefining

$$q_2 = q'_1 \in [0, 2p], \quad q_3 = q'_2 \in [0, p], \quad (6.29)$$

we get to the CS quiver theory for phase b of PdP_{3c} of section 5.9.1, the worldvolume theory on M2-branes probing $C(Y^p, q'_1, q'_2(PdP_{3c}))$.

Higgsing phase c of PdP_{3b} to phases a and b of dP_2

Consider the theory for phase c of PdP_{3b} of section 5.8.1, with bare FI parameters $\xi_1 = -\xi_3 \equiv \xi > 0$ and the VEV $\langle X_{13} \rangle = \xi I_{N \times N}$ that solves D-term equations. After integrating out massive matter, relabelling gauge groups $(1/3, 2, 4, 5, 6) \rightarrow (1, 5, 2, 4, 3)$ and redefining

$$q_1 + q_3 = q'_1 \in [0, 2p], \quad q_1 + q_2 = q'_2 \in [0, 3p], \quad q_2 = q'_3 \in [0, 3p] \quad (6.30)$$

we get to the CP-conjugate of the CS quiver theory for phase a of dP_2 of section 5.4.1, which is the worldvolume theory on M2-branes probing $C(Y^p, q'_1, q'_2, q'_3(dP_2))$. This is nothing but the Seiberg dual of the CS theory for phase b of dP_2 of section 5.4.2, as can be seen by dualising on the new node 3 and relabelling some nodes.

Similarly we can turn on bare FI parameters $\xi_5 = -\xi_1 \equiv \xi > 0$ in the theory for phase c of PdP_{3b} : the D-term equations are solved if we turn on the VEV $\langle X_{51} \rangle = \xi I_{N \times N}$. After integrating out massive matter, relabelling gauge groups $(1/5, 2, 3, 4, 6) \rightarrow (2, 5, 4, 1, 3)$ and redefining

$$q_1 + q_3 = q'_1 \in [0, 2p], \quad q_1 + 2q_3 = q'_2 \in [0, 3p], \quad q_2 = q'_3 \in [0, 3p] \quad (6.31)$$

we get to the CP-transform of the CS quiver theory for phase b of dP_2 of section 5.4.1, the worldvolume theory of M2-branes probing $C(Y^p, q'_1, q'_2, q'_3(dP_2))$. This is again dual to the CS theory for phase a of dP_2 of section 5.4.1, as can be seen by dualising on the new node 3 and relabelling some nodes.

Higgsing phase c of PdP_{3b} to PdP_2

Consider again the theory for phase c of PdP_{3b} of section 5.8.1, with bare FI parameters $\xi_4 = -\xi_6 \equiv \xi > 0$ and the VEV $\langle X_{46} \rangle = \xi I_{N \times N}$ that solves D-term equations. After integrating out massive matter, relabelling gauge groups $(1, 2, 3, 4/6, 5) \rightarrow (3, 5, 2, 4, 1)$ and redefining

$$q_1 + 2q_3 = q'_1 \in [0, 3p], \quad q_1 + q_3 = q'_2 \in [0, 2p] \quad (6.32)$$

we get the CS quiver theory for PdP_2 of section 5.7, the worldvolume theory on M2-branes probing $C(Y^{p, q'_1, q'_2}(PdP_2))$.

Higgsing PdP_2 to dP_1

Consider the theory for PdP_2 of section 5.7, with bare FI parameters $\xi_1 = -\xi_3 \equiv \xi > 0$ and VEV $\langle X_{13} \rangle = \xi I_{N \times N}$. Integrating out massive matter and relabelling gauge groups $(1/3, 2, 4, 5) \rightarrow (1, 4, 3, 2)$ leads to the low energy CS quiver theory for N M2-branes probing $Y^{p, q_2, q_1}(dP_1)$, see section 5.3.

Higgsing PdP_2 to $W\mathbb{C}\mathbb{P}^2_{[1,1,2]}$

Consider again the PdP_2 theory, now with bare FI parameters $\xi_3 = -\xi_4 \equiv \xi > 0$ and VEV $\langle X_{34} \rangle = \xi I_{N \times N}$. Relabelling gauge groups $(1, 2, 3/4, 5) \rightarrow (1, 3, 2, 4)$, the low energy theory is the CS quiver theory for N M2-branes probing $Y^{p, q_2}(W\mathbb{C}\mathbb{P}^2_{[1,1,2]})$ of section 5.6.

7. Adding torsion G_4 flux: The $Y^{p, q}(\mathbb{F}_0)$ case

All of our $Y^{p, q}(B_4)$ geometries are associated to rather large families of M-theory background, corresponding to turning on G_4 torsion flux in $H^4(Y^{p, q}, \mathbb{Z})$. We leave a completely general analysis of the field theories dual to the $Y^{p, q}(B_4)$ background with any value of the torsion for future work. In the following we work out in some detail the next simplest example after the $dP_0 = \mathbb{C}\mathbb{P}^2$ case worked out in detail in [14], which is $B_4 = \mathbb{F}_0 = \mathbb{C}\mathbb{P}^1 \times \mathbb{C}\mathbb{P}^1$. The AdS/CFT correspondence for the $Y^{p, q_1, q_2}(\mathbb{C}\mathbb{P}^1 \times \mathbb{C}\mathbb{P}^1)$ geometries has been studied in [27, 31]. For simplicity we will also set $q_1 = q_2$ in most of the following.

In [31] a Chern-Simons quiver with ranks $\mathbf{N} = (N, N, N, N)$ based on the (phase a) \mathbb{F}_0 quiver was proposed which describes half of the $Y^{p, q_1, q_2}(\mathbb{F}_0)$ geometries. In section 7.3 below we will derive this theory from our formalism, showing that it corresponds to non-zero G_4 torsion and explaining from θ -stability why it cannot cover the whole $Y^{p, q_1, q_2}(\mathbb{F}_0)$ family.

Our toric conventions for the $Y^{p, q_1, q_2}(\mathbb{F}_0)$ geometry were introduced in section 5.2. In the basis $\{\mathcal{C}_1, \mathcal{C}_2\} = \{D_3, D_4\}$ of toric divisors of \mathbb{F}_0 , the H^4 torsion group (A.23) is

$$\mathbb{Z}^3 / \langle v_0, v_1, v_2 \rangle, \quad v_0 = (2q_1 + 2q_2, q_2, q_1), \quad v_1 = (q_1, p, 0), \quad v_2 = (q_2, 0, p), \quad (7.1)$$

while the flux and source vectors (A.46) are given by

$$\begin{aligned}\mathcal{Q}_{\text{flux},-} &= (-n_0 \mid -q_2, -q_1 \mid 0), \\ \mathcal{Q}_{\text{flux},+} &= (-n_0 + 2n_1 + 2n_2 \mid -q_2 + 2p, -q_1 + 2p \mid 0), \\ \mathcal{Q}_{\text{source}} &= (-p \mid n_2, n_1 \mid N).\end{aligned}\tag{7.2}$$

Remark that there is no Freed-Witten anomaly. It will be convenient to consider a different (non-toric) basis for the 2-cycles of \mathbb{F}_0 :

$$\mathcal{C}'_1 = \mathcal{C}_1 + \mathcal{C}_2, \quad \mathcal{C}'_2 = \mathcal{C}_2.\tag{7.3}$$

In this basis, we have $v'_0 = (2q_1 + 2q_2, q_1 + q_2, q_1)$, $v'_1 = (q_1, p, 0)$, $v'_2 = (-q_1 + q_2, 0, p)$. In following we set $q_1 = q_2 \equiv q$. In that case, the torsion group is determined by the periodicity vectors

$$v'_0 = (4q, 2q, q), \quad v'_1 = (q, p, 0), \quad v'_2 = (0, 0, p).\tag{7.4}$$

These periodicities are realised by large gauge transformations of the B-field in type IIA. The B-fields periods are

$$b_0 = \frac{pn_0 - qn}{2q(2p - q)}, \quad b_1^{+'} = \frac{n}{p} - \frac{2q}{p}b_0, \quad b_2^{+'} = b_2^+ = \frac{n_2}{p} - \frac{q}{p}b_0,\tag{7.5}$$

where we defined $n \equiv n_1 + n_2$. Another important period is

$$\tilde{b} \equiv b_2^+ - b_1^{+'} = b_2^- - b_1^- = \frac{2n_2 - n}{p}.\tag{7.6}$$

The periodicities v'_0, v'_α are related to the shift of the B-periods as

$$\begin{aligned}\delta(n_0, n, n_2) = v'_0 &: \delta(b_0, b_1^{+'}, b_2^{+'}, \tilde{b}) = (1, 0, 0, 0), \\ \delta(n_0, n, n_2) = v'_1 &: \delta(b_0, b_1^{+'}, b_2^{+'}, \tilde{b}) = (0, 1, 0, -1), \\ \delta(n_0, n, n_2) = v'_2 &: \delta(b_0, b_1^{+'}, b_2^{+'}, \tilde{b}) = (0, 0, 1, 2).\end{aligned}\tag{7.7}$$

The central charge of a D4-brane on any 2-cycle \mathcal{C} is given exactly by

$$Z(D4_{\mathcal{C}}) = t_{\mathcal{C}} = b_{\mathcal{C}} + i\chi_{\mathcal{C}},\tag{7.8}$$

and in particular its real part is the corresponding B-field period. Of particular interest are the ‘‘non-anomalous’’ D4-branes wrapped on $\tilde{\mathcal{C}} \equiv \mathcal{C}_2 - \mathcal{C}_1$. We denote by $D4_i^{NA}$ the brane wrapped on $\tilde{\mathcal{C}}$ with l units of worldvolume flux, and by $\overline{D4}_{-l+1}^{NA}$ the brane wrapped with opposite orientation with $-l + 1$ units of worldvolume flux. In term of Chern characters on \mathbb{F}_0 ,

$$ch(D4_i^{NA}) = (0, -1, 1, l), \quad ch(\overline{D4}_{-l+1}^{NA}) = (0, 1, -1, -l + 1).\tag{7.9}$$

From the central charge, we find the inverse gauge couplings

$$g^{-2}(D4_i^{NA}) = \tilde{b} + l, \quad g^{-2}(\overline{D4}_{-l+1}^{NA}) = -\tilde{b} - l + 1.\tag{7.10}$$

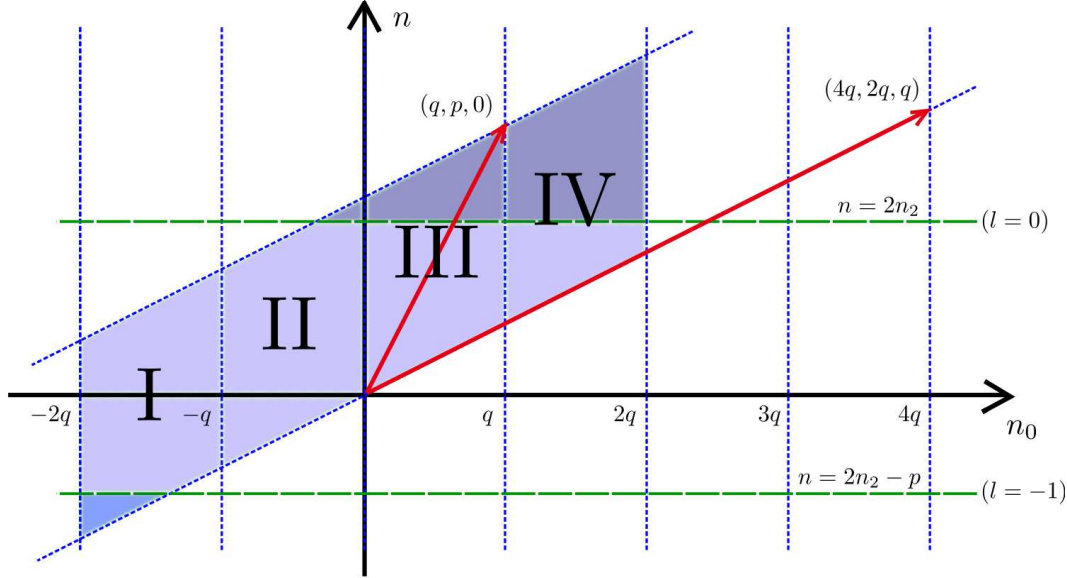


Figure 26: The (n_0, n) plane for $Y^{p,q}(\mathbb{F}_0)$, at some arbitrary value for n_2 . The red vectors are the periodicities $v'_0 = (4q, 2q, q)$ and $v'_1 = (q, p, 0)$ projected on the plane. The last periodicity $v'_2 = (0, 0, p)$ goes perpendicular to that plane. The walls of the first kind are shown in blue and the walls of the second kind (Seiberg duality walls) in green. The shaded area covers the fundamental domain once, and is subdivided into four windows $I - IV$ delimited by walls of the first kind.

We will see shortly that the states (7.9) occur in the quiver spectrum: they correspond to \mathcal{Q} representations of positive dimension. When $\tilde{b} \in \mathbb{Z}$, one of the gauge couplings (7.10) diverges, and we should change the basis of fractional branes accordingly, as we will explain momentarily. The locus $g^{-2} = 0$ defines a wall of the second kind, or Seiberg duality wall [73, 74]. In term of (n_0, n, n_2) , this occurs at

$$n = 2n_2 + lp, \quad \forall l \in \mathbb{Z}. \quad (7.11)$$

We call the locus (7.11) for a given l the “Seiberg duality wall of level l ”. Crossing the wall corresponds to doing *two* simultaneous Seiberg dualities on two different quiver nodes. The relevant Seiberg dualities for Chern-Simons quivers have been elucidated in [32, 33].

In addition, we also have the marginal stability walls — or walls of the first kind — for the fractional branes, which have been thoroughly discussed in this paper. Changing the value of the torsion flux (n_0, n, n_2) , we can cross the two kinds of walls; this is shown for instance in Figure 26.

7.1 Theories covering the full torsion group

Let us consider the toric quiver for $\mathcal{O}_{\mathbb{F}_0}(K)$ in phase a, and let us start with type IIA background fluxes near the torsionless point $(n_0, n, n_2) = (0, 0, 0)$. We saw in section 5.2.1 that we could use either dictionary $Q^\vee[\{p_5\}, \{0, -1\}]$ or $Q^\vee[\{p_8\}, \{0, 0\}]$ at the

torsionless point. Using first the dictionaries $Q_-^\vee = Q_+^\vee = Q^\vee[\{p_8\}, \{0, 0\}]$ with generic torsion, we find that

$$\begin{aligned}\boldsymbol{\theta}_- &= (n_0, q - n_0, -n_0, -q + n_0), \\ \boldsymbol{\theta}_+ &= (2n - n_0, 2p - q - 2n + n_0, -2n + n_0, -2p + q + 2n - n_0).\end{aligned}\tag{7.12}$$

Looking at the inequalities (5.25) defining the open string Kahler chamber $\{p_8\}$, one finds that this choice of dictionaries Q_\pm^\vee is consistent for

$$0 \leq n_0 \leq q, \quad 0 \leq 2n - n_0 \leq 2p - q.\tag{7.13}$$

This corresponds to the window III shown in Figure 26. Leaving window III towards window II, we see that $\boldsymbol{\theta}_+$ in (7.13) stays in the Kähler chamber $\{p_8\}$, while $\boldsymbol{\theta}_-$ crosses the wall to the Kähler chamber $\{p_5\}$. The correct LVM is obtained by checking consistency of the new pair of dictionaries, or equivalently by requiring that the theories glue along the wall $n_0 = 0$ between windows III and II. Crossing the walls to the successive windows, we find that we need to use the dictionaries:

$$\begin{aligned}\text{window } I : & \quad Q_-^\vee = Q^\vee[\{p_6\}, \{-1, -1\}], & \quad Q_+^\vee = Q^\vee[\{p_8\}, \{0, 0\}], \\ \text{window } II : & \quad Q_-^\vee = Q^\vee[\{p_5\}, \{0, -1\}], & \quad Q_+^\vee = Q^\vee[\{p_8\}, \{0, 0\}], \\ \text{window } III : & \quad Q_-^\vee = Q^\vee[\{p_8\}, \{0, 0\}], & \quad Q_+^\vee = Q^\vee[\{p_8\}, \{0, 0\}], \\ \text{window } IV : & \quad Q_-^\vee = Q^\vee[\{p_7\}, \{1, 0\}], & \quad Q_+^\vee = Q^\vee[\{p_8\}, \{0, 0\}],\end{aligned}\tag{7.14}$$

The field theories for these four windows are given in Table 1. The four dictionaries appearing in (7.14) are given explicitly by

$$\begin{aligned}Q_{(0)}^\vee[\{p_6\}, \{-1, -1\}] &= \begin{pmatrix} -1 & 0 & -2 & 0 \\ 1 & 0 & 1 & 0 \\ 1 & 1 & 1 & 1 \\ -1 & -1 & 0 & 0 \end{pmatrix}, & \quad Q_{(0)}^\vee[\{p_5\}, \{0, -1\}] &= \begin{pmatrix} 1 & 0 & 0 & 0 \\ 1 & 0 & 1 & 0 \\ -1 & 1 & -1 & 1 \\ -1 & -1 & 0 & 0 \end{pmatrix}, \\ Q_{(0)}^\vee[\{p_8\}, \{0, 0\}] &= \begin{pmatrix} 1 & 0 & 0 & 0 \\ -1 & 0 & 1 & 0 \\ -1 & 1 & -1 & 1 \\ 1 & -1 & 0 & 0 \end{pmatrix}, & \quad Q_{(0)}^\vee[\{p_7\}, \{1, 0\}] &= \begin{pmatrix} -1 & 2 & 0 & 0 \\ -1 & 0 & 1 & 0 \\ 1 & -1 & -1 & 1 \\ 1 & -1 & 0 & 0 \end{pmatrix}.\end{aligned}\tag{7.15}$$

So far we did not take into account the presence of the walls of the second kind (Seiberg duality walls) at $n = 2n_2 + lp$, $l \in \mathbb{Z}$. The four dictionaries (7.15) have in common that

$$ch(\mathbf{E}_1^\vee + \mathbf{E}_3^\vee) = (0, 1, -1, 1), \quad ch(\mathbf{E}_2^\vee + \mathbf{E}_4^\vee) = (0, -1, 1, 0).\tag{7.16}$$

Therefore $\mathbf{E}_1^\vee + \mathbf{E}_3^\vee$ is the D4-brane $\overline{D4}_1^{NA}$, and $\mathbf{E}_2^\vee + \mathbf{E}_4^\vee$ is the D4-brane $D4_0^{NA}$, in the notation of (7.9). Requiring that these two states have real gauge coupling, we find that

$$-p \leq n - 2n_2 \leq 0,\tag{7.17}$$

corresponding to being between the Seiberg dualities walls (7.11) of levels $l = -1$ and $l = 0$. The subscript (0) in (7.15) is to remind us that these dictionaries are valid only in the range (7.17). If the real part of $Z(\mathbf{E}_1^\vee + \mathbf{E}_3^\vee)$ goes negative, we should perform a double Seiberg duality on nodes 1 and 3, corresponding to crossing a wall (7.11) at level $l = -1$. Similarly, if $\text{Re } Z(\mathbf{E}_2^\vee + \mathbf{E}_4^\vee) = 0$ we are crossing the Seiberg duality wall of level $l = 0$, and we perform a double duality on nodes 2 and 4.

$$\text{Conditions :} \quad -2q \leq n_0 \leq -q , \quad 0 \leq 2n - n_0 \leq 2p - q$$

$$I : \left\{ \begin{array}{l} \mathbf{N} = (N + n - n_0 - p, N + n - n_0 - n_2 - q, N, N - n_2) \\ \mathbf{k} = (n + q, -n + p - q, -n - q, n - p + q) \end{array} \right.$$

$$\text{Conditions :} \quad -q \leq n_0 \leq 0 , \quad 0 \leq 2n - n_0 \leq 2p - q$$

$$II : \left\{ \begin{array}{l} \mathbf{N} = (N + n - n_0 - p, N + n - n_2, N, N - n_2) \\ \mathbf{k} = (n - n_0, -n + p - q, n_0 - n, n - p + q) \end{array} \right.$$

$$\text{Conditions :} \quad 0 \leq n_0 \leq q , \quad 0 \leq 2n - n_0 \leq 2p - q$$

$$III : \left\{ \begin{array}{l} \mathbf{N} = (N + n - p, N + n - n_2, N, N - n_2) \\ \mathbf{k} = (n - n_0, -n + n_0 + p - q, n_0 - n, n - n_0 - p + q) \end{array} \right.$$

$$\text{Conditions :} \quad q \leq n_0 \leq 2q , \quad 0 \leq 2n - n_0 \leq 2p - q$$

$$IV : \left\{ \begin{array}{l} \mathbf{N} = (N + n - p, N + n - n_2, N, N + n_0 - n_2 - q) \\ \mathbf{k} = (n - q, -n + n_0 + p - q, q - n, n - n_0 - p + q) \end{array} \right.$$

Table 1: Theories for F_0 covering the torsion domain. As explained in the text, these theories are valid only between the Seiberg duality walls of level $l = -1$ and $l = 0$, which means for $2n_2 - p \leq n \leq 2n_2$.

7.1.1 Crossing the Seiberg duality walls: mutated dictionaries

Consider for instance crossing the wall $l = 0$. We should perform a 3d Seiberg duality on node 2 and 4. The new dictionaries are determined by mutations as explained in [33]. For instance, in window I — first line of (7.14) —, we have

$$\begin{aligned} \theta_{2-} &= n_0 + q \leq 0, & \theta_{4-} &= -n_0 - q \geq 0, \\ \theta_{2+} &= -2n + n_0 + 2p - q \geq 0, & \theta_{4+} &= 2n - n_0 - 2p + q \leq 0. \end{aligned} \tag{7.18}$$

Starting with node 2, we should perform a left mutation on Q_-^\vee and a right mutation on Q_+^\vee . This gives us a Chern-Simons theory based on the quiver of phase b^{25} , whose $\theta_{4\pm}$ parameters are still the same as in (7.18). Therefore we proceed with a duality on node 4, corresponding to a right mutation at $r_0 < 0$ and a left mutation at $r_0 > 0$. The resulting quiver is in phase a again, but with the arrows reversed. We reverse to our original conventions by relabelling the nodes $(1, 2, 3, 4) \rightarrow (1, 4, 3, 2)$. With these mutations and relabelling, the new dictionaries we should use beyond the wall $l = 0$

²⁵With different conventions for labelling the notes with respect to section 5.2.2.

(and up to the wall $l = 1$) are

$$\begin{aligned} Q_{(1)}^\vee[\{p_6\}, \{-1, -1\}] &= \begin{pmatrix} -1 & -2 & 0 & 0 \\ 1 & 1 & 0 & 0 \\ 1 & 1 & 1 & 1 \\ -1 & 0 & -1 & 0 \end{pmatrix}, & Q_{(1)}^\vee[\{p_5\}, \{0, -1\}] &= \begin{pmatrix} 1 & 0 & 0 & 0 \\ 1 & 1 & 0 & 0 \\ -1 & -1 & 1 & 1 \\ -1 & 0 & -1 & 0 \end{pmatrix}, \\ Q_{(1)}^\vee[\{p_8\}, \{0, 0\}] &= \begin{pmatrix} 1 & 0 & 0 & 0 \\ -1 & 1 & 0 & 0 \\ -1 & -1 & 1 & 1 \\ 1 & 0 & -1 & 0 \end{pmatrix}, & Q_{(1)}^\vee[\{p_7\}, \{1, 0\}] &= \begin{pmatrix} -1 & 0 & 2 & 0 \\ -1 & 1 & 0 & 0 \\ 1 & -1 & -1 & 1 \\ 1 & 0 & -1 & 0 \end{pmatrix}. \end{aligned} \quad (7.19)$$

The walls of the first kinds remain unchanged in this new basis. The dictionaries (7.19) are valid for $2n_2 \leq n \leq 2n_2 + p$.

A similar analysis can be performed at the Seiberg duality wall of level $l = -1$. The resulting dictionaries after mutation on nodes 1 and 3 (and relabelling of the nodes $(1, 2, 3, 4) \rightarrow (3, 2, 1, 4)$) are

$$\begin{aligned} Q_{(-1)}^\vee[\{p_6\}, \{-1, -1\}] &= \begin{pmatrix} -1 & -1 & -1 & -1 \\ 1 & 0 & 1 & 0 \\ 1 & 0 & 2 & 0 \\ -1 & 1 & -2 & 2 \end{pmatrix}, & Q_{(-1)}^\vee[\{p_5\}, \{0, -1\}] &= \begin{pmatrix} 1 & -1 & 1 & -1 \\ 1 & 0 & 1 & 0 \\ -1 & 0 & 0 & 0 \\ -1 & 1 & -2 & 2 \end{pmatrix}, \\ Q_{(-1)}^\vee[\{p_8\}, \{0, 0\}] &= \begin{pmatrix} 1 & -1 & 1 & -1 \\ -1 & 2 & -1 & 2 \\ -1 & 0 & 0 & 0 \\ 1 & -1 & 0 & 0 \end{pmatrix}, & Q_{(-1)}^\vee[\{p_7\}, \{1, 0\}] &= \begin{pmatrix} -1 & 1 & 1 & -1 \\ -1 & 2 & -1 & 2 \\ 1 & -2 & 0 & 0 \\ 1 & -1 & 0 & 0 \end{pmatrix}. \end{aligned} \quad (7.20)$$

They are valid for $2n_2 - 2p \leq n \leq 2n_2 - p$.

We can easily generalise these results to any wall (7.11). At the Seiberg duality wall of level l , the corresponding mutation acts on dictionaries according to

$$Q_{l+1}^\vee = Q_l^\vee M_l, \quad \text{with} \quad M_l = \begin{pmatrix} 1 & l & -l & -l^2 \\ 0 & 0 & 1 & l \\ 0 & 1 & 0 & -l \\ 0 & 0 & 0 & 1 \end{pmatrix}, \quad (7.21)$$

while the walls of the first kind remain unchanged. Remark that $M_l^{-1} = M_l$ and therefore we can cross the wall in the opposite direction with $Q_l^\vee = Q_{l+1}^\vee M_l$. The dictionaries Q_l^\vee are valid for

$$(l-1)p \leq n - 2n_2 \leq lp. \quad (7.22)$$

Since the ranks and Chern-Simons levels are given by $\mathbf{N} = Q^{\vee T-1} \mathbf{Q}_{\text{source}}$ and $\mathbf{k} = Q^\vee \mathbf{Q}_{\text{flux}}$, we can account for the mutation (7.21) by a fictitious change of the type IIA parameters $\mathbf{Q}_{\text{source}} \rightarrow M_l^T \mathbf{Q}_{\text{source}}$ and $\mathbf{Q}_{\text{flux}} \rightarrow M_l \mathbf{Q}_{\text{flux}}$. We thus find that crossing a wall of level l amounts to changing the IIA parameters according to²⁶

$$n_2 \rightarrow n - n_2 - lp, \quad N \rightarrow N + l(2n_2 - n + lp), \quad (7.23)$$

keeping q , p , n_0 and n fixed. These rules make it obvious that the field theories change continuously as we cross the wall at $n = 2n_2 + lp$. They are reminiscent of the rules for non-chiral Seiberg dualities obtained from Hanany-Witten setups in [66]. We should insist,

²⁶The simplicity of these rules comes from the fact that we chose $q_1 = q_2 = q$, which implies that only \mathbf{N} changes as we cross the wall, while \mathbf{k} is invariant.

however, that this change of the IIA parameters is fictitious: The parameters of the background geometry stay what they are, while what changes are the dictionaries Q^\vee , and therefore the field theory parameters (\mathbf{N}, \mathbf{k}) . The rules (7.23) are just a convenient summary of the effect of these Seiberg dualities on the Chern-Simons quivers. Hence the field theories for $0 \leq n - 2n_2 \leq p$ are found from the field theories of Table 1 by replacing $n_2 \rightarrow n - n_2$, $N \rightarrow N$, and so on and so forth to attain any of the regions (7.22), as long as we are still inside the walls of the first kind delimiting the regions $I - IV$ in Figure 26.

7.2 Periodicities and Seiberg duality

As we perform a shift of (n_0, n, n_2) by any of the periodicity vectors (7.4), the field theory should stay invariant, up to a shift of N expected from the corresponding shift (A.41) of the D2-brane Page charge. For the case at hand, (A.41) gives

$$\begin{aligned} \delta(n_0, n, n_2) = v'_0 & : \delta N = -n_0 - 2q, \\ \delta(n_0, n, n_2) = v'_1 & : \delta N = -n_2, \\ \delta(n_0, n, n_2) = v'_2 & : \delta N = 2n_2 - n + p. \end{aligned} \tag{7.24}$$

We should check these type IIA expectations against the field theories we derived above.

First of all, we can check that the v'_0 periodicity is realised explicitly in Table 1: the theories on the left boundary of window I are the same as the theories on the right boundary of window IV , without any shift of N (this agrees with the first line of (7.24), since we start at $n_0 = -2q$).

From (7.7), it is apparent that a shift by v'_1 necessitates the crossing of one Seiberg duality wall in the negative direction ($\delta\tilde{b} = -1$) while a shift by v'_2 implies a crossing of two such walls in the positive direction ($\delta\tilde{b} = 2$).²⁷ Consider first the v'_1 periodicity. Starting with any theory of Table 1 on the bottom of the fundamental domain in Fig.26 (hence such that we are between the Seiberg duality walls $l = -1$ and $l = 0$), we can go to the upper boundary of the fundamental domain with a $v'_1 = (q, p, 0)$ shift, crossing the wall $l = 0$ in the process. Using the rules (7.23) for Seiberg duality, we can check that these two CS quivers are the same, up to a shift $\delta N = -n_2$ which agrees with the expectation (7.24).

Finally, let us consider the periodicity $v'_2 = (0, 0, p)$, which shifts n_2 by p . According to the rules (7.23) for Seiberg duality, crossing two successive Seiberg duality walls shifts n_2 according to

$$n_2 \quad \rightarrow \quad n - n_2 - lp \quad \rightarrow \quad n - (n - n_2 - (l - 1)p) - lp = n_2 - p. \tag{7.25}$$

This effective shift of n_2 from Seiberg dualities cancels the shifts from v'_2 . The shift $\delta N = 2n_2 - n + p$ expected from (7.24) is also recovered from (7.23).

²⁷Remark that v'_0 does *not* cross any Seiberg duality wall, unlike what is suggested by a naive reading of Fig.26, because $v'_0 = (4q, 2q, q)$ also goes in the n_2 direction perpendicular to the (n_0, n) plane shown in that figure.

We thus found that the periodicities of the torsion group $H_4(Y^{p,q}(\mathbb{F}_0))$ are reproduced by the field theories we derived, providing a non-trivial consistency check on their correctness.

7.3 Remark on $Y^{p,q_1,q_2}(\mathbb{F}_0)$ and quiver with equal ranks

For general q_1, q_2 , the structure of walls of the first and second kind is more complicated than for the $q_1 = q_2$ case of Figure 26, and we will not present a full analysis here. Nevertheless we can make some preliminary remarks allowing us to check the conjecture of [31] concerning some Chern-Simons quiver describing those geometries. The theory proposed in [31] is a Chern-Simons quiver with equal ranks, like in most of the heuristic proposals in the literature. We stress that from the string theory point of view there is nothing special about having equal ranks: it just corresponds to some particular value of the torsion flux.

Consider first the $q_1 = q_2$ theories of Table 1. We can find a theory with ranks $\mathbf{N} = (N, N, N, N)$ in window IV if we choose $n = n_2 = p$ and $n_0 = p + q$. However, requiring that this theory actually sits in window IV we must also set $q = p$. This results in a theory with

$$\mathbf{N} = (N, N, N, N), \quad \mathbf{k} = (0, p, 0, -p), \quad (7.26)$$

which moreover sits on the Seiberg duality wall $l = -1$. The corresponding geometry is $Y^{p,p,p}(\mathbb{F}_0) = Q^{1,1,1}/\mathbb{Z}_p$, and the theory (7.26) was first proposed in [11] for that geometry.²⁸ Similarly, there is a theory at $n = n_2 = 0$ and $n_0 = -p$, with $q = p$, sitting in window II , corresponding to $\mathbf{k} = (-p, 0, p, 0)$.

A third possibility from Table 1 is the equal rank theory in Window I , which again occurs only if $q = p$, at torsion flux $n = n_0 + p$ and $n_2 = 0$. The field theory is

$$\mathbf{N} = (N, N, N, N), \quad \mathbf{k} = (2p + n_0, -p - n_0, -2p - n_0, p + n_0), \quad (7.27)$$

for $-2p \leq n_0 \leq -p$. This theory again describes $Q^{1,1,1}/\mathbb{Z}_p$. For $p = 2$, $n_0 = -3$, such that $\mathbf{k} = (1, 1, -1, -1)$, this theory was proposed in [6, 75] to describe $Q^{2,2,2} \cong Q^{1,1,1}/\mathbb{Z}_2$, and we have thus derived this proposal and shown how it fits in a larger family of CS quiver theories.

Consider next the $Y^{p,q_1,q_2}(\mathbb{F}_0)$ geometry. The various chambers are modified with respect to Fig.26 but there is still a generalization of window IV where the consistent dictionaries are $Q_-^\vee = Q^\vee[\{p_7\}, \{1, 0\}]$ and $Q_+^\vee = Q^\vee[\{p_8\}, \{0, 0\}]$. Using these dictionaries with the charges (7.2), we find the Chern-Simons quiver

$$\begin{aligned} \mathbf{N} &= (N + n_1 + n_2 - p, N + n_1, N, N + n_0 - n_2 - q_2), \\ \mathbf{k} &= (n - q_2, -n + n_0 + p - q_1, q_1 - n, n - n_0 - p + q_2). \end{aligned} \quad (7.28)$$

²⁸We see that, ironically, the type IIA derivation first proposed in that same paper [11] was imprecisely applied to this $Q^{1,1,1}$ case, which needed the formalism of the present paper to be fully understood.

This includes a theory with equal ranks, for the choice of fluxes $(n_0, n_1, n_2) = (p + q_2, 0, p)$. With this choice, we have the theory

$$\mathbf{N} = (N, N, N, N), \quad \mathbf{k} = (p - q_2, p - q_1 + q_2, q_1 - p, -p), \quad (7.29)$$

which is the theory conjectured in [31]. Moreover, θ -stability for this theory constraints the values of the Chern-Simons levels, and we find that the string theory derivation is consistent only if

$$p \leq q_1 \leq 2p, \quad 0 \leq q_2 \leq p. \quad (7.30)$$

This explains why only in those ranges does the quiver theory (7.29) reproduce the cone $C(Y^{p, q_1, q_2}(\mathbb{F}_0))$ as its Abelian moduli space [31]. Remark that the theory (7.29) is not CP invariant, which is explained by the fact that it is dual to an M-theory background with non-zero torsion flux (M-theory parity acts as $(n_0, n_1, n_2) \rightarrow -(n_0, n_1, n_2)$ on our D4 Page charges); the special case (7.26) is CP invariant and the M-theory parity action $(n_0, n_1, n_2) = (2p, 0, p) \rightarrow (-2p, 0, -p)$ corresponds to a periodicity of Γ .

8. Conclusion and outlook

We provided a type IIA string theory derivation of Chern-Simons quiver gauge theories describing the low energy dynamics of M2-branes on the CY_4 cone over the seven-manifold $Y^{p, \mathbf{q}}(B_4)$, for any of the 16 toric Fano varieties B_4 .

While we focused on the type IIA description, either in term of branes or in term of the CS quiver, we only briefly commented on how the CS gauge theory probes the full CY_4 geometry in M-theory. We recalled the conjecture that the quantum chiral ring of the CS theory encodes the coordinate ring of the CY_4 , but we still lack a first principle approach to deal with the chiral ring of the IR SCFT. We believe that the conjecture (4.17) deserves further study, and we hope that the link we stressed to the GIT description of quiver moduli spaces can be fruitful in this respect.

There are a number of further directions for research one could follow. First of all, we can allow for D6-branes along noncompact toric divisors in some $\mathcal{O}_{B_4}(K)$ fibres in type IIA, still keeping the GLSM of \tilde{Y} geometric over the whole \mathbb{R} base so that the reduction to type IIA is understood. It would be interesting to pursue this generalisation and combine the results of this paper with the flavouring procedure of [13], allowing for even more general toric CY_4 geometries in term of CS quivers with fundamental matter.

Secondly, we mostly focused on the case of zero G_4 torsion flux in $Y^{p, \mathbf{q}}$. The case of general torsion has been solved for a special case in section 7 (and before that in [14] for $B_4 = \mathbb{CP}^2$), but remains challenging in general. To find the CS quiver theories dual to $Y^{p, \mathbf{q}}$ with any value of the torsion flux, one has to understand in general the interplay between the two kinds of walls in Kähler moduli space, and in its discretised version spanned by the type IIA quantised fluxes. The second kind of wall is a Seiberg

duality wall, and the relevant 3d Seiberg dualities have been understood in some detail only recently [32, 33].

More generally, it would be desirable to carry on the type IIA derivation to much more general cases, corresponding to generic toric CY_3 in type IIA. One of the main challenges to do so is also of general interest for D-brane physics: we would need a generalization of the dictionaries Q^\vee to any CY_3 . While the result of [52] reviewed in section 2.4 provides a tilting collection of line bundles \mathcal{E} for any crepant partial resolution of a toric CY_3 cone, it is not known in general how to define a “dual” collection \mathcal{E}^\vee corresponding to the fractional D-branes.

The final step to cover all toric CY_4 geometries would then involve generalising to cases where the $U(1)_M$ circle action degenerates to $U(1)_M/Z_h$ over certain loci and the CY_3 GLSM in type IIA is not in a geometric phase over the whole \mathbb{R} base. It was suggested that in such cases the M2-brane quiver contains non-Lagrangian sectors [12]. It would be interesting to pursue this proposal further.

Last but not least, the quiver-based approach we followed to study the “open string Kähler chambers” (delimited by marginal stability walls for fractional branes) in the Kähler moduli space of any toric CY_3 is of more general interest. For instance these methods might be applied to baryon counting problems in D-brane theories [76].

Acknowledgments

We thank Noppadol Mekareeya for collaboration at the beginning of this project, Francesco Benini for collaboration on earlier related work, and Jurgis Pasukonis for allowing us to use and develop his Mathematica package. CC is grateful to Ofer Aharony for interesting discussions. SC thanks Amihay Hanany and Rak-Kyeong Seong for sharing their database and results prior to publication, and Paola Cognigni for help with figures. CC is a Feinberg Postdoctoral Fellow at the Weizmann Institute of Science. The work of SC is supported by the STFC Consolidated Grant ST/J000353/1.

A. $Y^{p,q}(B_4)$ geometry and type IIA background

For any smooth toric CY_4 cone, there exist a Sasaki-Einstein metric on the seven dimensional base Y_7 of the cone [28] and a corresponding $AdS_4 \times Y_7$ background of M-theory. In the simplest cases when B_4 is $\mathbb{C}P^2$ or \mathbb{F}_0 , the $Y^{p,q}(B_4)$ metrics have been explicitly constructed in [26, 69, 68]. In this paper we are not explicitly interested in the metrics nor in the supergravity limit, but we do need to understand the topology of $Y^{p,q}$.

Following [26, 31], it is useful to realise the SE_7 geometry $Y^{p,q}(B_4)$ as a circle bundle over a six-manifold M_6 , which in turn is an S^2 bundle over the Fano variety B_4 . Such representation is physically sensible, because the circle fiber is the very M-theory circle we choose in section 3 to reduce to type IIA. Therefore M_6 is the manifold that appears transverse to AdS_4 in the IIA limit of the AdS_4/CFT_3 duality.

In the following subsection we discuss the topology of M_6 , which is intimately related to the CY_3 $\tilde{Y} = \mathcal{O}_{B_4}(K)$ we discussed in detail in section 2. In subsection A.2 we discuss the topology of $Y^{p,\mathbf{q}}$. In the remaining subsections we give more details on the IIA fluxes obtained from the reduction of M-theory on $AdS_4 \times Y^{p,\mathbf{q}}$ with non-zero torsion G_4 flux.

A.1 Topology of M_6

The manifold M_6 is defined as $Y^{p,\mathbf{q}}/U(1)_M$, where $Y^{p,\mathbf{q}}$ is the seven manifold at the base of the CY_4 cone, and the $U(1)_M$ action is the one discussed in section 3.3. In the following we infer the topology of M_6 from the GLSM of the CY fourfold, following closely section 5.3 of [77]. To discuss the conical CY_4 , it is convenient to rewrite (3.4) as a minimal GLSM²⁹ (using that $Q_{(s_0)}^\alpha = Q_0^\alpha + \mathcal{I}^{\alpha\beta} q_\beta$ and $Q_{(s_1)}^\alpha = -\mathcal{I}^{\alpha\beta} q_\beta$, as follows from (3.9) and (3.11)):

$$\begin{array}{c|cccccc} CY_4 & t_1 & \cdots & t_{m+2} & s_0 & s_p \\ \hline U(1)_\alpha & p Q_1^\alpha & \cdots & p Q_{m+2}^\alpha & p Q_0^\alpha + \tilde{q}^\alpha & -\tilde{q}^\alpha \\ \hline U(1)_M & 0 & \cdots & 0 & 1 & -1 \end{array} \quad (\text{A.1})$$

which only takes into account the external points of the toric diagram. The last line denotes the charges under the $U(1)_M$ of the M-theory circle, and we have defined $\tilde{q}^\alpha \equiv \mathcal{I}^{\alpha\beta} q_\beta$ for ease of notation. The coordinates (s_0, s_p) span the covering space \mathbb{C}^2 of the $\mathbb{C}^2/\mathbb{Z}_p$ fiber over B_4 . To see this, notice that the locus $s_0 = s_p = 0$ is an orbifold locus, left invariant by the subgroup $\mathbb{Z}_p \subset U(1)_\alpha, \forall U(1)_\alpha$. The action of the \mathbb{Z}_p on the fiber is

$$\mathbb{Z}_p : (s_0, s_p) \mapsto (\omega_p^{\tilde{q}^\alpha} s_0, \omega_p^{-\tilde{q}^\alpha} s_p). \quad (\text{A.2})$$

Hence, when all q^α are coprime with p we truly have a \mathbb{Z}_p action embedded in $U(1)_M$. This \mathbb{Z}_p acting on the fiber (s_0, s_p) is a residual gauge symmetry once we have gauge fixed the $U(1)_\alpha$ acting on $\{t_i\}$.

Topologically, the compact SE_7 $Y^{p,\mathbf{q}}$ is described by the equations

$$\begin{aligned} \sum_i Q_i^\alpha |t_i|^2 + (Q_0^\alpha p + \tilde{q}^\alpha) |s_0|^2 - \tilde{q}^\alpha |s_p|^2 &= 0, & \alpha = 1, \dots, m, \\ \sum_i |t_i|^2 + |s_0|^2 + |s_p|^2 &= L. \end{aligned} \quad (\text{A.3})$$

modulo the $U(1)^m$ gauge equivalence of the GLSM (A.1) – without the last line; L is real and positive, and otherwise arbitrary. The locus $s_0 = s_p = 0$ does not intersect the manifold $Y^{p,\mathbf{q}}$ cut out by (A.3); in fact the fixed point $s_0 = s_p = 0$ is the B_4 of vanishing size which lives at the tip of the CY_3 (and at $r_0 = 0$) in the $CY_3 \times \mathbb{R}$ description of section 3. Therefore \mathbb{Z}_p acts freely on $Y^{p,\mathbf{q}}$. We have a S^3/\mathbb{Z}_p bundle over B_4 , with S^3/\mathbb{Z}_p a Lens space. We want to quotient this Lens space by $U(1)_M$, to obtain a S^2 bundle over B_4 , called M_6 . To do that at the level of the GLSM description, we would have to

²⁹For simplicity we consider the case where p and q_α are coprime.

construct new coordinates invariant under $U(1)_M$. The only holomorphic choice, $s_0 s_p$, will not do, because such a coordinate can reach the origin $s_0 = s_p = 0$. Instead, since s_p and s_0 can never vanish together, we consider local patches on the S^3/\mathbb{Z}_p fiber, with either s_0 or s_p different from zero. Consider first the patch for which $s_0 \neq 0$. To go to the S^2 bundle, we introduce a coordinate

$$t^+ = \frac{s_p^*}{s_0}, \quad (\text{A.4})$$

which is invariant under $U(1)_M$. To summarise the remaining $U(1)_\alpha$ charges of the fields t_i and t^+ , we can write an auxiliary GLSM:

$$\frac{}{U(1)_\alpha} \left| \begin{array}{cccc} t_1 & \dots & t_{m+2} & t_0^+ \\ \hline Q_1^\alpha & \dots & Q_{m+2}^\alpha & -Q_0^\alpha \end{array} \right. \quad (\text{A.5})$$

This GLSM describes the anti-canonical bundle over B_4 , $\mathcal{O}_{B_4}(-K)$. In other words, the local patch $s_0 \neq 0$ on the fiber $S^3/U(1)_M \cong S^2$ is fibered over B_4 exactly like the line bundle $\mathcal{O}_{B_4}(-K)$. Similarly, on the patch $s_p \neq 0$ we define the coordinate

$$t^- = \frac{s_0}{s_p^*} \quad (\text{A.6})$$

In this case we have the canonical bundle $\mathcal{O}_{B_4}(K)$, with GLSM

$$\frac{}{U(1)_\alpha} \left| \begin{array}{cccc} t_1 & \dots & t_{m+2} & t_0^- \\ \hline Q_1^\alpha & \dots & Q_{m+2}^\alpha & Q_0^\alpha \end{array} \right. \quad (\text{A.7})$$

The two line bundles are patched together into a Riemann sphere, with $t^+ = 1/t^-$ on the overlap, giving us the sought-after M_6 manifold. The full $\mathbb{C}\mathbb{P}^1$ bundle is just the anti-canonical line bundle with the point at infinity on the \mathbb{C} fiber added. This can be written

$$M_6 \cong \mathbb{P}(\mathcal{O}_{B_4}(-K) \oplus \mathcal{O}_{B_4}). \quad (\text{A.8})$$

Equivalently, we could also write M_6 in term of the canonical bundle, $M_6 \cong \mathbb{P}(\mathcal{O}_{B_4}(K) \oplus \mathcal{O}_{B_4})$. We can describe both cases by the following GLSM's :

$$\begin{array}{c} M_6 \\ \mathcal{C}_+ \\ \mathcal{C}_0 \end{array} \left| \begin{array}{cccccc} t_1 & \dots & t_{m+2} & t_0^- & t_0^+ \\ \hline Q_1^\alpha & \dots & Q_{m+2}^\alpha & 0 & -Q_0^\alpha \\ 0 & \dots & 0 & 1 & 1 \end{array} \right. \quad \begin{array}{c} M_6 \\ \mathcal{C}_\alpha^- \\ \mathcal{C}_0 \end{array} \left| \begin{array}{cccccc} t_1 & \dots & t_{m+2} & t_0^- & t_0^+ \\ \hline Q_1^\alpha & \dots & Q_{m+2}^\alpha & Q_0^\alpha & 0 \\ 0 & \dots & 0 & 1 & 1 \end{array} \right. \quad (\text{A.9})$$

We should remark that the complex structure apparent in this toric description of M_6 is *not* inherited from the complex structure of the CY fourfold, due to the non-holomorphic relations (A.4) and (A.6). In fact, the physical metric on M_6 which preserves $\mathcal{N} = 2$ supersymmetry might not even be Kähler, in general. The toric description with its unphysical complex structure is however quite useful as a tool to describe the topology of M_6 .

Since M_6 is a sphere bundle over B_4 , $S^2 \rightarrow M_6 \rightarrow B_4$, one can compute its cohomology in term of the cohomology of B_4 through the Gysin sequence, and its homology by Poincaré duality. We find

$$\begin{array}{c|ccccccc} M_6 & H_0 & H_1 & H_2 & H_3 & H_4 & H_5 & H_6 \\ \hline & \mathbb{Z} & 0 & \mathbb{Z}^{m+1} & 0 & \mathbb{Z}^{m+1} & 0 & \mathbb{Z} \end{array} \quad (\text{A.10})$$

In particular, we have

$$H_2(M_6, \mathbb{Z}) \cong H_2(B_4, \mathbb{Z}) \oplus H_0(B_4, \mathbb{Z}), \quad H_4(M_6, \mathbb{Z}) \cong H_2(B_4, \mathbb{Z}) \oplus H_4(B_4, \mathbb{Z}). \quad (\text{A.11})$$

To be more concrete in the construction of $H_2(M_6)$ and $H_4(M_6)$ we need to specify how to embed cycles of B_4 in M_6 , that is we need to specify global sections of the S^2 bundle. The S^2 fiber is twisted along B_4 by the $U(1)$ which rotates its azimuthal angle. There are two fixed points of this $U(1)$ action, the north and the south pole of S^2 ($t^+ = 0$ and $t^- = 0$, respectively), which can be used to embed submanifolds of B_4 (and B_4 itself) in M_6 as global sections [27]. Let σ_N and σ_S denote the push-forward maps $B_4 \xrightarrow{\pi_*} M_6$ which fix the north pole or the south pole of the S^2 fiber, respectively. One can define nice representatives of the 2-cycles (A.11) by

$$-\mathcal{C}_0 = S^2, \quad \mathcal{C}_\alpha^+ = \sigma_N \mathcal{C}_\alpha, \quad \mathcal{C}_\alpha^- = \sigma_S \mathcal{C}_\alpha, \quad (\text{A.12})$$

where $-\mathcal{C}_0$ is the S^2 fiber over an arbitrary point on the base.³⁰ We anticipated these definitions in (A.9). All such 2-cycles are not independent: as a basis for H_2 we could pick $\{-\mathcal{C}_0, \mathcal{C}_\alpha^+\}$, but it will be convenient to work with the redundant set (A.12). Similarly we define the 4-cycles D_α and D^\pm :

$$S^2 \hookrightarrow D_\alpha \rightarrow \mathcal{C}_\alpha, \quad D^+ = \sigma_N B_4, \quad D^- = \sigma_S B_4, \quad (\text{A.13})$$

where D_α are restrictions of the S^2 -bundle to \mathcal{C}_α . The 4-cycles D^+ and D^- corresponds to the toric divisors $\{t^+ = 0\}$ and $\{t^- = 0\}$, while the 4-cycles D_α and the toric divisors $D_i = \{t_i = 0\}$ are related by

$$D_i = Q_i^\alpha (\mathcal{I}^{-1})_{\alpha\beta} D^\beta \quad (\text{A.14})$$

We can also invert this relation, meaning that we can take $D_\alpha = X_\alpha^i D_i$ for any X_α^i such that $X_\alpha^i Q_i^\beta = \mathcal{I}_\alpha^\beta$. The homology relations among the representatives (A.12)-(A.13) are

$$\begin{aligned} \mathcal{C}_\alpha^+ &= \mathcal{C}_\alpha^- - Q_0^\alpha \mathcal{C}_0, \\ D^+ &= D^- - Q_0^\alpha (\mathcal{I}^{-1})_{\alpha\beta} D^\beta, \end{aligned} \quad (\text{A.15})$$

as follows from (A.9). Moreover, using the toric description it is straightforward to compute the intersections among 2-cycles and 4-cycles:

$$\begin{array}{c|ccc|cc} & \mathcal{C}_0 & \mathcal{C}_\alpha^+ & \mathcal{C}_\alpha^- & D_\alpha & D^+ & D^- \\ \hline D_\beta & 0 & \mathcal{I}_{\alpha\beta} & \mathcal{I}_{\alpha\beta} & \mathcal{I}_{\alpha\beta} \mathcal{C}_0 & \mathcal{C}_\beta^+ & \mathcal{C}_\beta^- \\ D^+ & 1 & -Q_0^\alpha & 0 & \mathcal{C}_\alpha^+ & -Q_0^\rho (\mathcal{I}^{-1})_\rho^\sigma \mathcal{C}_\sigma^+ & 0 \\ D^- & 1 & 0 & Q_0^\alpha & \mathcal{C}_\alpha^- & 0 & Q_0^\rho (\mathcal{I}^{-1})_\rho^\sigma \mathcal{C}_\sigma^- \end{array} \quad (\text{A.16})$$

³⁰It will be convenient to take a minus sign in the definition $S^2 = -\mathcal{C}_0$, because the \mathcal{C}_0 as defined by (A.9) has an orientation opposite to the “natural” one, due to the complex conjugation in (A.4).

Equipped with the understanding of M_6 , we turn back to the Sasaki-Einstein seven-manifold which appears in M-theory.

A.2 Topology of $Y^{p,q}(B_4)$

Consider the seven-manifold $Y^{p,q}$ given by a circle fibration over M_6 :

$$S^1 \rightarrow Y^{p,q} \rightarrow M_6 . \quad (\text{A.17})$$

The circle bundle is fully characterised by its first Chern class $c_1 \in H^2(M_6, \mathbb{Z})$, which equals the type IIA RR 2-form flux in M_6 , or equivalently by the $m+1$ Chern numbers (p, q_α) . We can compute the cohomology of $Y^{p,q}$ from $H_*(M_6, \mathbb{Z})$ (A.10) and the Gysin sequence. One can show that

$$\pi_1(Y^{p,q}) = \mathbb{Z}_{\text{gcd}(p, q_1, \dots, q_m)} , \quad (\text{A.18})$$

so that $Y^{p,q}$ is simply connected if and only if the Chern numbers are co-prime. The homology $H_*(Y^{p,q}, \mathbb{Z})$ is

$$\begin{array}{c|cccccccc} Y^{p,q} & H_0 & H_1 & H_2 & H_3 & H_4 & H_5 & H_6 & H_7 \\ \hline & \mathbb{Z} & \mathbb{Z}_{\text{gcd}(p, q_\alpha)} & \mathbb{Z}^m & \Gamma & 0 & \mathbb{Z}^m \oplus \mathbb{Z}_{\text{gcd}(p, q_\alpha)} & 0 & \mathbb{Z} \end{array} , \quad (\text{A.19})$$

and similarly for cohomology by Poincaré duality. The most interesting group is

$$H^4(Y^{p,q}, \mathbb{Z}) \cong H_3(Y^{p,q}, \mathbb{Z}) \cong \Gamma , \quad (\text{A.20})$$

which we now explain. From the Gysin sequence one finds that

$$H^4(Y^{p,q}) \cong H^4(M_6)/\text{Im}(c_1) , \quad \text{with} \quad c_1 : H^2(M_6) \xrightarrow{\wedge c_1} H^4(M_6) . \quad (\text{A.21})$$

Let us consider $(-D^-, D_\alpha)$ as a basis of $H_4(M_6)$; in that case, the dual basis of $H^4(M_6)$ is given by $(-\mathcal{C}_0, (\mathcal{I}^{-1})^{\alpha\beta} \mathcal{C}_\beta^+)$. The image of the map c_1 in (A.21) is computed from (A.16):

$$\begin{aligned} c_1(-D^-) &= q_\alpha Q_0^\alpha \mathcal{C}_0 + q^\alpha \mathcal{C}_\alpha^+ \\ c_1(D_\alpha) &= -\mathcal{I}_{\alpha\beta} q^\beta \mathcal{C}_0 + p \mathcal{C}_\alpha^+ . \end{aligned} \quad (\text{A.22})$$

We find that Γ is the finite Abelian group

$$\Gamma = \mathbb{Z}^{m+1} / \langle v_0, v_1, \dots, v_m \rangle \quad (\text{A.23})$$

where the vectors $v = (v_0, v_\alpha)$ are read from (A.22):

$$v_0 = (-q_\gamma Q_0^\gamma, \mathcal{I}^{\beta\gamma} q_\gamma) , \quad v_\alpha = (q_\alpha, \delta_\alpha^\beta p) , \quad (\text{A.24})$$

and the index β parameterises the coordinates (but the first one) of the vectors. As a simple example, let us consider $Y^{p,q}(\mathbb{CP}^2)$. We have $m=1$, $\mathcal{I}=1$, $Q_0=-3$ and $F_2 = p D^+ - q D$, therefore

$$\Gamma = \mathbb{Z}^2 / \langle (3q, q), (q, p) \rangle , \quad (\text{A.25})$$

which was computed in [27] and explained from the field theory point of view in [14].

A.3 Type IIA background and the IIA dual of torsion flux

Given a Sasaki-Einstein metric on $Y^{p,q}(B_4)$, we have $\mathcal{N} = 2$ supersymmetric solution of 11d supergravity, given by

$$\begin{aligned} ds^2 &= R^2 \left(\frac{1}{4} ds^2(AdS_4) + ds^2(Y^{p,q\alpha}(B_4)) \right), \\ G_4 &= \frac{3}{8} R^3 d\text{vol}(AdS_4). \end{aligned} \quad (\text{A.26})$$

We have N units of M2-brane charge on $Y^{p,q}$, where N is related to the radius R according to:

$$\frac{1}{(2\pi l_p)^6} \int_{Y^{p,q}} *G_4 = N = \frac{6R^6}{(2\pi l_p)^6} \text{Vol}(Y^{p,q}). \quad (\text{A.27})$$

The manifold $Y^{p,q}$ has a fourth cohomology $H_3(Y^{p,q}, \mathbb{Z}) \cong \Gamma$ (A.23) which is purely torsion. A torsion G_4 flux does not affect the supergravity equations of motion, and we therefore have a distinct M-theory background for each element $[G_4] \in \Gamma$.

We are interested in the corresponding type IIA solutions $AdS_4 \times M_6$. The M_6 metric is of the type introduced in [26]. A nice account of this class of IIA reduction can be found in [78]. As we already stated, we are not interested in the metric nor in the supergravity limit in particular. For this reason we will only discuss the RR fluxes that are present on M_6 , as we go from the M-theory background (A.26) with generic $[G_4] \in \Gamma$ to the type IIA dual. The charges so-defined are conserved quantities of great use to derive the dual CS quiver gauge theory.

One can straightforwardly generalise the analysis of [14] (section 3.5) of the D-brane charges to any $Y^{p,q}(B_4)$. The D6-brane Page charges are directly related to the Chern numbers, according to

$$\begin{aligned} Q_{6;0} &\equiv \int_{-c_0} F_2 = -p, \\ Q_{6;\alpha-} &\equiv \int_{c_\alpha^-} F_2 = -\mathcal{I}^{\alpha\beta} q_\beta, & Q_{6;\alpha+} &\equiv \int_{c_\alpha^+} F_2 = -\mathcal{I}^{\alpha\beta} q_\beta - Q_0^\alpha p. \end{aligned} \quad (\text{A.28})$$

The D4-brane Page charges are the integral of $B_2 \wedge F_2$ over the 4-cycles (A.13). They are given by

$$\begin{aligned} Q_{4;-} &= - \int_{D^-} F_2 \wedge B_2 = n_0 - \frac{1}{2} q^\alpha \mathcal{I}_{\alpha\beta} s^\beta, \\ Q_{4;\alpha} &= \int_{D_\alpha} F_2 \wedge B_2 = n_\alpha - \frac{1}{2} p \mathcal{I}_{\alpha\beta} s^\beta, \\ Q_{4;+} &= - \int_{D^+} F_2 \wedge B_2 = Q_{4;-} + Q_0^\alpha (\mathcal{I}^{-1})_{\alpha\beta} Q_{4;\beta}. \end{aligned} \quad (\text{A.29})$$

with

$$(n_0, n_\alpha) \in \mathbb{Z}^{m+1} \quad (\text{A.30})$$

the integers parameterizing the torsion group Γ (A.23). The parameters s_α are the Freed-Witten anomaly parameters, which are 0 or 1 depending on whether the 4-cycle

D_α in M_6 is spin or only spin^c — see equation (A.36) below. Finally, the D2-brane Page charge is

$$Q_2 = N - \frac{p}{8} s_\alpha s_\beta \mathcal{I}^{\alpha\beta}. \quad (\text{A.31})$$

The quantization of the D4 Page charge results in a quantised flat background B-field. Defining the periods

$$b_0 \equiv \int_{-c_0} B_2, \quad b_\alpha^- \equiv \int_{\mathcal{C}_\alpha^-} B_2, \quad b_\alpha^+ \equiv \int_{\mathcal{C}_\alpha^+} B_2 = b_\alpha^- + Q_\alpha^0 b_0, \quad (\text{A.32})$$

we find

$$b_0 = \frac{-p n_0 + q^\alpha n_\alpha}{q_\alpha \mathcal{I}^{\alpha\beta} q_\beta + p Q_0^\alpha q_\alpha}, \quad b_\alpha^+ = -\mathcal{I}_{\alpha\beta} \frac{s^\beta}{2} + \frac{n_\alpha}{p} - \frac{\mathcal{I}^{\alpha\beta} q_\beta}{p} b_0. \quad (\text{A.33})$$

The periodicities (A.24) defining Γ are realised as the following large gauge transformations of the B-field:

$$\begin{aligned} \delta(n_0, n_\beta) = v_0 &\longleftrightarrow \delta(b_0, b_\beta^+) = (1, 0) \\ \delta(n_0, n_\beta) = v_\alpha &\longleftrightarrow \delta(b_0, b_\beta^+) = (0, \delta_{\beta\alpha}). \end{aligned} \quad (\text{A.34})$$

A.4 D6-branes and Freed-Witten anomaly

To obtain the F_2 fluxes and the corresponding Page D6-charges (A.28), we can wrap D6-branes on various 4-cycles of M_6 at some radial position in AdS_4 ³¹ where they are not stable, and let them fall inside. At a fixed radial position such a wrapped D6-brane acts as a domain wall between two regions with different RR flux.

When a 4-cycle is not spin but only spin^c , the wrapped D6-brane must carry some half-integer worldvolume flux to cancel the Freed-Witten anomaly [61]. This induces some extra background D4 Page charge, giving rise to the half-integer shifts in (A.29). It also induces the shift of the D2 Page charge in (A.31).

Let us consider the various 4-cycles (A.13) in M_6 . The topology of D^\pm is B_4 . We have

$$\int_{\mathcal{C}_\alpha} c_1(B_4) = -Q_0^\alpha, \quad (\text{A.35})$$

so that B_4 fails to be spin whenever some of the Q_0^α is odd. The other 4-cycles are D_α . These are S^2 bundles over \mathcal{C}_α ³², which are spin or spin^c depending on whether Q_0^α is odd or even. One can show that all these Freed-Witten anomalies can be cancelled by turning on the pull-back of a common bulk 2-form

$$F = \frac{1}{2} \sum_\alpha s^\alpha D_\alpha, \quad \text{with} \quad s_\alpha = (\mathcal{I}^{-1})_{\alpha\beta} Q_0^\beta \pmod{2}. \quad (\text{A.36})$$

³¹Or at some radial position in the cone $C(M_6)$, if we do not wish to consider the decoupling limit nor the supergravity limit, like in most of this paper.

³²In B_4 (or rather in \tilde{B}_4) all the \mathcal{C}_α are topologically 2-spheres as well. S^2 bundle over S^2 are classified by $\pi_1(SO(3)) = \mathbb{Z}_2$, so there are only two distinct topologies, trivial or not. In term of the description (A.8) we have $D_\alpha \cong \mathbb{P}(\mathcal{O}(Q_0^\alpha) \oplus \mathcal{O})$. When Q_0^α is odd the corresponding D_α is not spin (and it corresponds to the non-trivial topology).

on every D6-brane. Let us also remark that at the torsionless point $(n_0, n_\alpha) = (0, 0)$, we have a non-zero flat B -field

$$B_2 = -\frac{1}{2} \sum_\alpha s_\alpha D^\alpha, \quad (\text{A.37})$$

turned on whenever there is a Freed-Witten anomaly. This B -field induces the non-zero half-integer periods b_α^+ in (A.33), and it is such that the gauge invariant worldvolume flux $\mathcal{F} = B_2 + F$ on any probe D6-brane vanishes. That the B -field is non-zero even in the torsionless case was first argued for the ABJM theory in [66]; the present results generalise that understanding to our family of geometries. How this subtlety in charge quantization translates in the M-theory language is not well understood, to the best of our present knowledge.

A.5 Large gauge transformations and shift of the D2 Page charge

Under a large gauge transformation of the B -field, Page charges shift by integers [45, 79]. We have already seen this in (A.34) for the D4-brane Page charges: Large gauge transformations of B are in one to one correspondence with periodicities of the torsion group Γ in M-theory.

It is important to note that the D2-brane Page charges shifts as well along these periodicities. The D2 Page charge computed on M_6 is

$$Q_2 = \int_{M_6} \left(*F_4 - \frac{1}{2} B_2 \wedge B_2 \wedge F_2 \right). \quad (\text{A.38})$$

Remark that $Q_2 = Q_2^{\text{Maxwell}} + \tilde{Q}_2$, where we defined

$$\tilde{Q}_2 \equiv -\frac{1}{2} \int_{M_6} B_2 \wedge B_2 \wedge F_2. \quad (\text{A.39})$$

Computing \tilde{Q}_2 explicitly in term of (n_0, n_α) , we find

$$\tilde{Q}_2(n_0, n_\alpha) = -\frac{p}{8} s_\alpha \mathcal{I}^{\alpha\beta} s_\beta + \frac{n_\alpha s^\alpha}{2} - \frac{n_\alpha (\mathcal{I}^{-1})^{\alpha\beta} n_\beta}{2p} + \frac{(pn_0 - q^\alpha n_\alpha)^2}{2p(q_\alpha I^{\alpha\beta} q_\beta + pQ_0^\alpha q_\alpha)}. \quad (\text{A.40})$$

At the torsionless point we have³³ $Q_2^{\text{Maxwell}} = N$, while the Page charge is given by (A.31). As we move in the torsion group, the Page charge Q_2 is invariant, while the Maxwell charge varies accordingly. On the other hand, under a large gauge transformation (A.34) the Page charge Q_2 shifts according to

$$\delta_v Q_2 = \tilde{Q}_2(n_0 + \delta n_0, n_\alpha + \delta n_\alpha) - \tilde{Q}_2(n_0, n_\alpha), \quad (\text{A.41})$$

where $v = (\delta n_0, \delta n_\alpha)$ is any periodicity vector of Γ . One can show that the shift $\delta_v Q_2$ is always an integer.

³³There are further corrections from gravitational effects similarly to [80], but such contributions will not be studied in this work.

A.6 Fluxes and D-branes in $C(M_6)$

In the bulk of this paper we are not interested in M_6 *per se*, but rather in the cone $C(M_6) = CY_4/U(1)_M$ seen as a foliation of $\tilde{Y}_\pm \cong \mathcal{O}_{B_4}(K)$ along a line $\mathbb{R} \cong \{r_0\}$. We showed in section A.1 that M_6 and \tilde{Y} are closely related. The north pole (resp. south pole) of the S^2 fiber of M_6 is the exceptional locus B_4 of \tilde{Y}_+ at $r_0 > 0$ (resp. \tilde{Y}_- at $r_0 < 0$), and cycles living there can be compared. We have:

$$\begin{aligned} \mathcal{C}_\alpha^+ &= \mathcal{C}_\alpha \text{ at } r_0 > 0 & D^+ &= D_0 \text{ at } r_0 > 0 \\ \mathcal{C}_\alpha^- &= \mathcal{C}_\alpha \text{ at } r_0 < 0 & D^- &= D_0 \text{ at } r_0 < 0. \end{aligned} \tag{A.42}$$

These are the only cycles which are common to the CY_3 and M_6 ; for instance the divisors D_α , are different in the CY_3 and in M_6 despite having the same name: they are non-compact in the CY_3 and compact in M_6 .

The fluxes through \mathcal{C}_α^\pm and B_4 in \tilde{Y}_\pm are the same as measured on the corresponding cycles in M_6 . We collect them into two $(m+2)$ -covectors of charges

$$\mathbf{Q}_{\text{flux},\pm} \equiv (-Q_{4;\pm} \mid Q_{6;\alpha\pm} \mid 0). \tag{A.43}$$

The last entry is zero because we do not allow for D8-brane charge F_0 , thus allowing a M-theory uplift [81]; see [33] for a sketch of how to generalise the present formalism to the case of $F_0 \neq 0$.

On the other hand, the fluxes through the remaining 2- and 4- cycles \mathcal{C}_0 and D_α of M_6 correspond to explicit D-brane sources wrapped on the dual 4-cycles B_4 and $(\mathcal{I}^{-1})^{\alpha\beta}\mathcal{C}_\beta \subset B_4$ at $r_0 = 0$. For the (anti)D6-brane wrapped on B_4 this was shown in section 3.4. Similarly, the jump of the D4 Page charge across $r_0 = 0$ denotes explicit sources through the 2-cycles:

$$Q_{4;+} - Q_{4;-} = Q_0^\alpha (\mathcal{I}^{-1})_\beta^\alpha Q_{D4;\beta}. \tag{A.44}$$

In the presence of torsion flux $(n_0, n_\alpha) \in \Gamma$, we have $(\mathcal{I})^{\beta\alpha}n_\alpha$ D4-branes wrapped on \mathcal{C}_β at $r_0 = 0$. Remark that only the combination $Q_0^\alpha (\mathcal{I}^{-1})_{\alpha\beta}n^\beta$ appears in (A.44); the remaining $m-1$ choices n_α orthogonal to $(\mathcal{I}^{-1})_{\alpha\beta}Q_0^\beta$ are “non-anomalous” D4-branes. We collect the information about the D-brane sources in a covector of Page charges

$$\mathbf{Q}_{\text{source}} \equiv (Q_{6;0} \mid (\mathcal{I}^{-1})^{\alpha\beta}Q_{4;\beta} \mid Q_2). \tag{A.45}$$

In this notation, the results (A.28), (A.29) and (A.31) are summarised by

$$\begin{aligned} \mathbf{Q}_{\text{flux},-} &= (-n_0 + \frac{1}{2}s_\alpha q_\beta \mathcal{I}^{\alpha\beta} \mid -\mathcal{I}_{\alpha\beta}q^\beta \mid 0), \\ \mathbf{Q}_{\text{source}} &= (-p \mid (\mathcal{I}^{-1})^{\alpha\beta}n_\beta - \frac{1}{2}s_\alpha p \mid N - \frac{1}{8}s_\alpha s_\beta \mathcal{I}^{\alpha\beta}p). \end{aligned} \tag{A.46}$$

References

- [1] O. Aharony, O. Bergman, D. L. Jafferis, and J. Maldacena, “N=6 superconformal Chern-Simons-matter theories, M2-branes and their gravity duals,” *JHEP* **10** (2008) 091, [arXiv:0806.1218 \[hep-th\]](#).
- [2] J. M. Maldacena, “The Large N limit of superconformal field theories and supergravity,” *Adv.Theor.Math.Phys.* **2** (1998) 231–252, [arXiv:hep-th/9711200 \[hep-th\]](#).
- [3] B. S. Acharya, J. Figueroa-O’Farrill, C. Hull, and B. J. Spence, “Branes at conical singularities and holography,” *Adv.Theor.Math.Phys.* **2** (1999) 1249–1286, [arXiv:hep-th/9808014 \[hep-th\]](#).
- [4] D. L. Jafferis and A. Tomasiello, “A Simple class of N=3 gauge/gravity duals,” *JHEP* **0810** (2008) 101, [arXiv:0808.0864 \[hep-th\]](#).
- [5] D. Martelli and J. Sparks, “Moduli spaces of Chern-Simons quiver gauge theories and AdS(4)/CFT(3),” *Phys. Rev.* **D78** (2008) 126005, [arXiv:0808.0912 \[hep-th\]](#).
- [6] A. Hanany and A. Zaffaroni, “Tilings, Chern-Simons Theories and M2 Branes,” *JHEP* **0810** (2008) 111, [arXiv:0808.1244 \[hep-th\]](#).
- [7] S. Franco, A. Hanany, J. Park, and D. Rodriguez-Gomez, “Towards M2-brane Theories for Generic Toric Singularities,” *JHEP* **0812** (2008) 110, [arXiv:0809.3237 \[hep-th\]](#).
- [8] K. Ueda and M. Yamazaki, “Toric Calabi-Yau four-folds dual to Chern-Simons-matter theories,” *JHEP* **0812** (2008) 045, [arXiv:0808.3768 \[hep-th\]](#).
- [9] Y. Imamura and K. Kimura, “Quiver Chern-Simons theories and crystals,” *JHEP* **0810** (2008) 114, [arXiv:0808.4155 \[hep-th\]](#).
- [10] A. Hanany, D. Vegh, and A. Zaffaroni, “Brane Tilings and M2 Branes,” *JHEP* **0903** (2009) 012, [arXiv:0809.1440 \[hep-th\]](#).
- [11] M. Aganagic, “A Stringy Origin of M2 Brane Chern-Simons Theories,” [arXiv:0905.3415 \[hep-th\]](#).
- [12] D. L. Jafferis, “Quantum corrections to N=2 Chern-Simons theories with flavor and their AdS(4) duals,” [arXiv:0911.4324 \[hep-th\]](#).
- [13] F. Benini, C. Closset, and S. Cremonesi, “Chiral flavors and M2-branes at toric CY4 singularities,” *JHEP* **1002** (2010) 036, [arXiv:0911.4127 \[hep-th\]](#).
- [14] F. Benini, C. Closset, and S. Cremonesi, “Quantum moduli space of Chern-Simons quivers, wrapped D6-branes and AdS4/CFT3,” *JHEP* **1109** (2011) 005, [arXiv:1105.2299 \[hep-th\]](#).
- [15] D. Gang, C. Hwang, S. Kim, and J. Park, “Tests of AdS4/CFT3 correspondence for $\mathcal{N} = 2$ chiral-like theory,” [arXiv:1111.4529 \[hep-th\]](#).

- [16] D. L. Jafferis, “The Exact Superconformal R-Symmetry Extremizes Z,” [arXiv:1012.3210 \[hep-th\]](#).
- [17] N. Hama, K. Hosomichi, and S. Lee, “Notes on SUSY Gauge Theories on Three-Sphere,” *JHEP* **03** (2011) 127, [arXiv:1012.3512 \[hep-th\]](#).
- [18] Y. Imamura and S. Yokoyama, “Index for three dimensional superconformal field theories with general R-charge assignments,” *JHEP* **04** (2011) 007, [arXiv:1101.0557 \[hep-th\]](#).
- [19] S. Cheon, H. Kim, and N. Kim, “Calculating the partition function of N=2 Gauge theories on S^3 and AdS/CFT correspondence,” *JHEP* **1105** (2011) 134, [arXiv:1102.5565 \[hep-th\]](#).
- [20] D. Martelli and J. Sparks, “The large N limit of quiver matrix models and Sasaki-Einstein manifolds,” *Phys.Rev.* **D84** (2011) 046008, [arXiv:1102.5289 \[hep-th\]](#).
- [21] S. Cheon, D. Gang, S. Kim, and J. Park, “Refined test of AdS4/CFT3 correspondence for N=2,3 theories,” *JHEP* **1105** (2011) 027, [arXiv:1102.4273 \[hep-th\]](#).
- [22] D. L. Jafferis, I. R. Klebanov, S. S. Pufu, and B. R. Safdi, “Towards the F-Theorem: N=2 Field Theories on the Three-Sphere,” *JHEP* **1106** (2011) 102, [arXiv:1103.1181 \[hep-th\]](#).
- [23] A. Amariti, C. Klare, and M. Siani, “The Large N Limit of Toric Chern-Simons Matter Theories and Their Duals,” [arXiv:1111.1723 \[hep-th\]](#).
- [24] A. Hanany and K. D. Kennaway, “Dimer models and toric diagrams,” [arXiv:hep-th/0503149 \[hep-th\]](#).
- [25] S. Franco, A. Hanany, K. D. Kennaway, D. Vegh, and B. Wecht, “Brane dimers and quiver gauge theories,” *JHEP* **0601** (2006) 096, [arXiv:hep-th/0504110 \[hep-th\]](#).
- [26] J. P. Gauntlett, D. Martelli, J. F. Sparks, and D. Waldram, “A New infinite class of Sasaki-Einstein manifolds,” *Adv.Theor.Math.Phys.* **8** (2006) 987–1000, [arXiv:hep-th/0403038 \[hep-th\]](#).
- [27] D. Martelli and J. Sparks, “Notes on toric Sasaki-Einstein seven-manifolds and AdS(4) / CFT(3),” *JHEP* **0811** (2008) 016, [arXiv:0808.0904 \[hep-th\]](#).
- [28] A. Futaki, H. Ono, and G. Wang, “Transverse Kahler geometry of Sasaki manifolds and toric Sasaki-Einstein manifolds,” [arXiv:math/0607586 \[math-dg\]](#).
- [29] A. Hanany and R.-K. Seong, “Brane Tilings and Reflexive Polygons,” [arXiv:1201.2614 \[hep-th\]](#).
- [30] A. D. King, “Moduli of representations of finite-dimensional algebras,” *Quart. J. Math. Oxford Ser. (2), Vol. 45, No. 180.* (1994) .

- [31] A. Tomasiello and A. Zaffaroni, “Parameter spaces of massive IIA solutions,” *JHEP* **1104** (2011) 067, [arXiv:1010.4648 \[hep-th\]](#).
- [32] F. Benini, C. Closset, and S. Cremonesi, “Comments on 3d Seiberg-like dualities,” *JHEP* **1110** (2011) 075, [arXiv:1108.5373 \[hep-th\]](#).
- [33] C. Closset, “Seiberg duality for Chern-Simons quivers and D-brane mutations,” [arXiv:1201.2432 \[hep-th\]](#).
- [34] I. Wolfram Research, *Mathematica Edition: Version 7.0*. Wolfram Research, Inc., 2008.
- [35] J. Davey, A. Hanany, and J. Pasukonis, “On the Classification of Brane Tilings,” *JHEP* **1001** (2010) 078, [arXiv:0909.2868 \[hep-th\]](#).
- [36] M. R. Douglas and G. W. Moore, “D-branes, quivers, and ALE instantons,” [arXiv:hep-th/9603167 \[hep-th\]](#).
- [37] D.-E. Diaconescu, M. R. Douglas, and J. Gomis, “Fractional branes and wrapped branes,” *JHEP* **9802** (1998) 013, [arXiv:hep-th/9712230 \[hep-th\]](#).
- [38] A. E. Lawrence, N. Nekrasov, and C. Vafa, “On conformal field theories in four-dimensions,” *Nucl.Phys.* **B533** (1998) 199–209, [arXiv:hep-th/9803015 \[hep-th\]](#).
- [39] I. R. Klebanov and E. Witten, “Superconformal field theory on three-branes at a Calabi-Yau singularity,” *Nucl.Phys.* **B536** (1998) 199–218, [arXiv:hep-th/9807080 \[hep-th\]](#).
- [40] D. R. Morrison and M. Plesser, “Nonspherical horizons. 1.,” *Adv.Theor.Math.Phys.* **3** (1999) 1–81, [arXiv:hep-th/9810201 \[hep-th\]](#). Revised.
- [41] C. Beasley, B. R. Greene, C. Lazaroiu, and M. Plesser, “D3-branes on partial resolutions of Abelian quotient singularities of Calabi-Yau threefolds,” *Nucl.Phys.* **B566** (2000) 599–640, [arXiv:hep-th/9907186 \[hep-th\]](#).
- [42] B. Feng, A. Hanany, and Y.-H. He, “D-brane gauge theories from toric singularities and toric duality,” *Nucl.Phys.* **B595** (2001) 165–200, [arXiv:hep-th/0003085 \[hep-th\]](#).
- [43] B. Feng, S. Franco, A. Hanany, and Y.-H. He, “UnHiggsing the del Pezzo,” *JHEP* **0308** (2003) 058, [arXiv:hep-th/0209228 \[hep-th\]](#).
- [44] K. D. Kennaway, “Brane Tilings,” *Int. J. Mod. Phys.* **A22** (2007) 2977–3038, [arXiv:0706.1660 \[hep-th\]](#).
- [45] D. Marolf, “Chern-Simons terms and the three notions of charge,” [arXiv:hep-th/0006117](#).
- [46] A. Hanany and D. Vegh, “Quivers, tilings, branes and rhombi,” *JHEP* **10** (2007) 029, [arXiv:hep-th/0511063](#).

- [47] D. R. Gulotta, “Properly ordered dimers, R-charges, and an efficient inverse algorithm,” *JHEP* **0810** (2008) 014, [arXiv:0807.3012 \[hep-th\]](#).
- [48] S. Franco and D. Vegh, “Moduli spaces of gauge theories from dimer models: Proof of the correspondence,” *JHEP* **0611** (2006) 054, [arXiv:hep-th/0601063 \[hep-th\]](#).
- [49] M. A. Luty and W. Taylor, “Varieties of vacua in classical supersymmetric gauge theories,” *Phys. Rev.* **D53** (1996) 3399–3405, [arXiv:hep-th/9506098](#).
- [50] D. Martelli and J. Sparks, “Symmetry-breaking vacua and baryon condensates in AdS/CFT,” *Phys.Rev.* **D79** (2009) 065009, [arXiv:0804.3999 \[hep-th\]](#).
- [51] S. Mozgovoy, “Crepant resolutions and brane tilings I: Toric realization,” [arXiv:0908.3475 \[math.AG\]](#).
- [52] M. Bender and S. Mozgovoy, “Crepant resolutions and brane tilings II: Tilting bundles,” [arXiv:0909.2013 \[math.AG\]](#).
- [53] A. Hanany, C. P. Herzog, and D. Vegh, “Brane tilings and exceptional collections,” *JHEP* **0607** (2006) 001, [arXiv:hep-th/0602041 \[hep-th\]](#).
- [54] P. S. Aspinwall, “D-Branes on Toric Calabi-Yau Varieties,” [arXiv:0806.2612 \[hep-th\]](#).
- [55] D. Cox, J. Little, and H. Schenck, *Toric Varieties*. American Mathematical Society, 2011.
- [56] N. Carqueville and A. Quintero Velez, “Remarks on quiver gauge theories from open topological string theory,” *JHEP* **1003** (2010) 129, [arXiv:0912.4699 \[hep-th\]](#).
- [57] W. Stein *et al.*, *Sage Mathematics Software (Version 4.7.2)*. The Sage Development Team, 2011. <http://www.sagemath.org>.
- [58] R. Minasian and G. W. Moore, “K theory and Ramond-Ramond charge,” *JHEP* **9711** (1997) 002, [arXiv:hep-th/9710230 \[hep-th\]](#).
- [59] P. S. Aspinwall, “D-branes on Calabi-Yau manifolds,” [arXiv:hep-th/0403166 \[hep-th\]](#).
- [60] C. P. Herzog, “Seiberg duality is an exceptional mutation,” *JHEP* **0408** (2004) 064, [arXiv:hep-th/0405118 \[hep-th\]](#).
- [61] D. S. Freed and E. Witten, “Anomalies in string theory with D-branes,” [arXiv:hep-th/9907189 \[hep-th\]](#).
- [62] M. R. Douglas, B. Fiol, and C. Romelsberger, “Stability and BPS branes,” *JHEP* **0509** (2005) 006, [arXiv:hep-th/0002037 \[hep-th\]](#).
- [63] P. S. Aspinwall, “D-branes, Pi-stability and theta-stability,” [arXiv:hep-th/0407123 \[hep-th\]](#).

- [64] P. S. Aspinwall and I. V. Melnikov, “D-branes on vanishing del Pezzo surfaces,” *JHEP* **0412** (2004) 042, [arXiv:hep-th/0405134](#) [[hep-th](#)].
- [65] O. Aharony, O. Bergman, and D. L. Jafferis, “Fractional M2-branes,” *JHEP* **11** (2008) 043, [arXiv:0807.4924](#) [[hep-th](#)].
- [66] O. Aharony, A. Hashimoto, S. Hirano, and P. Ouyang, “D-brane Charges in Gravitational Duals of 2+1 Dimensional Gauge Theories and Duality Cascades,” *JHEP* **01** (2010) 072, [arXiv:0906.2390](#) [[hep-th](#)].
- [67] D. Gaiotto and D. L. Jafferis, “Notes on adding D6 branes wrapping RP^3 in $AdS(4) \times CP^3$,” [arXiv:0903.2175](#) [[hep-th](#)].
- [68] J. P. Gauntlett, D. Martelli, J. Sparks, and D. Waldram, “Supersymmetric AdS backgrounds in string and M-theory,” [arXiv:hep-th/0411194](#) [[hep-th](#)].
- [69] W. Chen, H. Lu, C. Pope, and J. F. Vazquez-Poritz, “A Note on Einstein Sasaki metrics in $D \geq 7$,” *Class.Quant.Grav.* **22** (2005) 3421–3430, [arXiv:hep-th/0411218](#) [[hep-th](#)].
- [70] O. Aharony, “IR duality in $d = 3$ $N = 2$ supersymmetric $USp(2N(c))$ and $U(N(c))$ gauge theories,” *Phys. Lett.* **B404** (1997) 71–76, [arXiv:hep-th/9703215](#).
- [71] S. Cremonesi, “Type IIB construction of flavoured ABJ(M) and fractional M2 branes,” *JHEP* **1101** (2011) 076, [arXiv:1007.4562](#) [[hep-th](#)].
- [72] S. Cremonesi, *work in progress*.
- [73] M. Kontsevich and Y. Soibelman, “Stability structures, motivic Donaldson-Thomas invariants and cluster transformations,” *ArXiv e-prints* (Nov., 2008) , [arXiv:0811.2435](#) [[math.AG](#)].
- [74] M. Aganagic and K. Schaeffer, “Wall Crossing, Quivers and Crystals,” [arXiv:1006.2113](#) [[hep-th](#)].
- [75] J. Davey, A. Hanany, N. Mekareeya, and G. Torri, “Phases of M2-brane Theories,” *JHEP* **0906** (2009) 025, [arXiv:0903.3234](#) [[hep-th](#)].
- [76] A. Butti, D. Forcella, and A. Zaffaroni, “Counting BPS baryonic operators in CFTs with Sasaki-Einstein duals,” *JHEP* **0706** (2007) 069, [arXiv:hep-th/0611229](#) [[hep-th](#)].
- [77] D. Martelli and J. Sparks, “Toric geometry, Sasaki-Einstein manifolds and a new infinite class of AdS/CFT duals,” *Commun.Math.Phys.* **262** (2006) 51–89, [arXiv:hep-th/0411238](#) [[hep-th](#)].
- [78] D. Martelli and J. Sparks, “ AdS_4/CFT_3 duals from M2-branes at hypersurface singularities and their deformations,” [arXiv:0909.2036](#) [[hep-th](#)].

- [79] F. Benini, F. Canoura, S. Cremonesi, C. Nunez, and A. V. Ramallo, “Backreacting Flavors in the Klebanov-Strassler Background,” *JHEP* **09** (2007) 109, [arXiv:0706.1238 \[hep-th\]](#).
- [80] O. Bergman and S. Hirano, “Anomalous radius shift in AdS(4)/CFT(3),” *JHEP* **0907** (2009) 016, [arXiv:0902.1743 \[hep-th\]](#).
- [81] O. Aharony, D. Jafferis, A. Tomasiello, and A. Zaffaroni, “Massive type IIA string theory cannot be strongly coupled,” *JHEP* **1011** (2010) 047, [arXiv:1007.2451 \[hep-th\]](#).